A SERIES OF STUDIES TO SUPPORT AND IMPROVE DPM SAMPLING IN UNDERGROUND MINES

Sarah Crawford Gaillard

Thesis submitted to the faculty of the Virginia Polytechnic Institute and State University
in partial fulfillment of the requirements for the degree of

Master of Science
In
Mining Engineering

Emily A. Sarver, Chair
Kray Luxbacher
Cigdem Keles

August 8, 2017
Blacksburg, VA

Keywords: Diesel Particulate Matter, DPM, Monitoring DPM, DPM Impactor, Particle Size Selector, Sharp-cut cyclone, Transmission Electron Microscope, Airtec, Elemental Carbon

A SERIES OF STUDIES TO SUPPORT AND IMPROVE DPM SAMPLING IN UNDERGROUND MINES

Sallie Crawford Gaillard

ACADEMIC ABSTRACT

Diesel particulate matter (DPM) is the solid portion of diesel exhaust, which occurs primarily in the submicron range. It is complex in nature, occuring in clusters and agglomerated chains, and with variable composition depending on engine operating conditions, fuel type, equipment maintenance, etc. DPM is an occupational health hazard that has been associated with lung cancer risks and other respiratory issues. Underground miners have some of the highest exposures to DPM, due to work in confined spaces with diesel powered equipment. Large-opening mines present particular concerns because sufficient ventilation is very challenging. In such environments, reliable DPM sampling and monitoring is critical to protecting miner health.

Though complex, DPM is made up primarily of elemental (EC) and organic carbon (OC), which can be summed to obtain total carbon (TC). The Mine Safety and Health Administration (MSHA) currently limits personal DPM exposures in metal/non-metal mines to 160 $\mu g/m^3$ TC on an 8-hour time weighted average. To demonstrate compliance, exposures are monitored by collecting filter samples, which are sent to an outside lab and analyzed using the NIOSH 5040 Standard Method. To support real-time results, and thus more timely decision making, the Airtec handheld DPM monitor was developed. It measures EC, which is generally well correlated with TC, using a laser absorption technique as DPM accumulates on a filter sample. Though intended as a personal monitor, the Airtec has application as an engineering tool. A field study is reported here which demonstrated the usefulness of the Airtec in tracking temporal and spatial trends in DPM. An approach to sensitizing the monitor to allow "spot checking" was also demonstrated.

Since DPM in mine environments generally occurs with other airborne particulates, namely dust generated during the mining process, DPM sampling must be done with consideration for analytical interferences. A common approach to dealing with mineral dust interferences is to use size selectors in the sampling train to separate DPM from dust; these devices are generally effective because DPM and dust largely occur in different size ranges. An impactor-type device (DPMI) is currently the industry standard for DPM sampling, but it is designed as a consumable device. Particularly for continuous monitoring applications, the sharp cut cyclone (SCC) has been suggested as a favorable alternative. In another field study reported here, the effect of aging (i.e., loading as an artifact of sampling) on the DPMI and SCC was investigated. Results suggest the effective cut size of the DPMI will be reduced much more rapidly than that of the SCC with aging – though even in a relatively high dust, high DPM environment, the DPMI performs adequately.

In a third field study, the possibility of attachment between DPM and respirable dust particles was investigated. Such a phenomenon may have implications for both reliable sampling and health outcomes. Data collected by transmission electron microscope (TEM) on samples collected in the study mine showed that DPM-dust attachment does indeed occur. Moreover, the study results suggest that respirable particulate sampling – as opposed to submicron sampling, which is currently used – may be favorable for ensuring that oversized DPM is not excluded from samples. This strategy may require additional sample preparation to minimize dust interferences, but methods have been previously developed and were demonstrated here.

A SERIES OF STUDIES TO SUPPORT AND IMPROVE DPM SAMPLING IN UNDERGROUND MINES

Sallie Crawford Gaillard

GENERAL AUDIENCE ABSTRACT

Diesel particulate matter (DPM) is the solid portion of diesel exhaust, which occurs primarily in the submicron range (i.e., less than one micron). It generally forms as agglomerated chains or clusters. The size and shape is dependent on the engine operating conditions, fuel type, equipment maintenance, etc. DPM is an occupational health hazard that has been associated with lung cancer risks and other respiratory issues. Underground miners have some of the highest exposures to DPM, due to work in confined spaces with diesel powered equipment. In such environments, reliable DPM sampling and monitoring is critical to protecting miner health.

Though complex, DPM is made up primarily of elemental (EC) and organic carbon (OC), which can be summed to obtain total carbon (TC). Exposure to DPM, as regulated by the Mine Safety and Health Administration (MSHA) is monitored by collecting filter samples, which are analyzed using the NIOSH 5040 Standard Method. To support real-time results, and thus more timely decision making, the Airtec handheld DPM monitor was developed. Though intended as a personal monitor, the Airtec has application as an engineering tool. A field study is reported here which demonstrated the usefulness of the Airtec in tracking changes of DPM in specific locations as well as over time. An approach to sensitizing the monitor to allow “spot checking” or making very quick assesments in a location was also demonstrated.

DPM in mine environments generally occurs with other airborne particulates, namely dust generated during the mining process. Sampling must be completed to avoid these interferences by sampling DPM only. Since DPM and dust typically occur in different size ranges, size selectors in the sampling train are used to separate DPM from dust. An impactor-type device (DPMI) is currently the industry standard for DPM sampling, but it is designed as a one time use item. Particularly for continuous monitoring applications, the sharp cut cyclone (SCC) has been suggested as a favorable alternative. In another field study reported here, the effect of aging (i.e., multiple monitorings using the same size selector) on the DPMI and SCC was investigated. Results suggest the effective cut size of the DPMI will be reduced much more rapidly than that of the SCC with aging – though even in a relatively high dust, high DPM environment, the DPMI performs adequately.

In a third field study, the possibility of attachment between DPM and respirable dust particles was investigated. Such a phenomenon may have implications for both reliable sampling and health outcomes. Using microscopy, samples collected in the study mine showed that DPM-dust attachment does indeed occur. Moreover, the study results suggest that respirable particulate sampling – as opposed to submicron sampling, which is currently used – may be favorable for ensuring that oversized DPM is not excluded from samples. This strategy may require additional sample preparation to minmize dust interferences, but methods have been previously developed and were demonstrated here.

ACKNOWLEDGEMENTS

There are many people in my life that have helped me get where I am today. A starting point will be a struggle, but first I would like to thank my parents.

Mom, you have never given up on me even though it was a struggle to just get me through high school, but look where I am now! You have always seen the potential in me and always encouraged my direction even though it may have been hard to watch. I know you are proud of me and that I finally owned up to the potenial you always new I had. Growing up, I always new you were a force to be reckonded with at home and in your career. I couldn't tell you how many times a collegue of yours told me how impressive you are. I thank you for instilling in me the dedication and passion you have in your own life and career. Dad, I thank you for giving me the ability to approach tasks in innovative ways. You created a perfect example of "work smarter, not harder" in me. I get my workhorse attitude from you and I am sure my past and future employers appreciate that. Thank you for your support and the countless times you sang me "You are my sunshine". To my sisters Emily and Julia, thank you for being there whenever I needed you. I couldn't have achieved what I have with out such an amazing family support system.

To my advisor, Dr. Emily Sarver, thank you for supporting me and being an influential person in my life. Your drive, passion and dedication is for lack of a better term, impressive. Other influential people that saw my potential and helped me in gaining the experience I have today are Dr. Robert Mensah-Biney, Dr. Rudolph Olson, Tom Newman, Kirsten Lovan, Alex Neidermeier and Joseph Jamison. One more thank you to my Holden Hall boys Scott, Will, Ben and Kent. My time in Blacksburg would have been boring without you all! I will be forever grateful for these individuals either knowingly or not giving me their time, advice, guidence and just plain old looking out for me.

My research would also not be complete with out the help of everyone on Dr. Sarvers research team, those at CDC/NIOSH Office of Mine Safety and Health Research (OMSHR) for funding my thesis work under contract No. 200-2014-59646. I would especially like to thank Dr. Emanuele Cauda, Jim Noll and Shawn Vanderslice of OMSHR for their hard work in sample prep and analysis and answering all my questions! A special thank you to all the mine personnel who were nothing but helpful and most enjoyable to be around. Certainly made my trips to the mine memorable! Last but not least, I would like to thank my committee members, Dr. Kray Luxbaucher and Dr. Cigdem Keles.

Thank you again to all who have been a part of my journey.

TABLE OF CONTENTS

LIST OF FIGURES

LIST OF TABLES

PREFACE

This thesis presents three field studies related to diesel particulate matter (DPM) sampling and monitoring in underground mines. Each study is reported in a separate chapter. All were conducted in the same large-opening stone mine, which has partnered with Virginia Tech to provide access to an active operation for DPM research. This research is being conducted as part of a larger project funded by CDC/NIOSH (contract No. 200-2014-59646). The work described in Chapter 1 was performed by the Virginia Tech research team, and this chapter was published as a peer-reviewed technical paper in Mining Engineering. It is reproduced here with permission from the publisher (the Society for Mining, Metallurgy and Exploration). The studies reported in Chapters 2 and 3 were designed and conducted in collaboration with Dr. Emanuele Cauda of NIOSH's Office for Mine Safety and Health Research. Dr. Cauda is a co-author on these chapters.

In Chapter 1, the FLIR Airtec monitor was used to evaluate temporal changes in DPM in different locations of the mine. The Airtec is a near real-time instrument, which was developed by NIOSH and later commercialized as personal DPM monitor. Thus, its primary application is in alerting individuals to their cumulative exposure during a current work shift. However, the Airtec can also be used as an engineering tool to track DPM in particular locations or related to particular activities or operational changes. This is demonstrated in Chapter 1 by showing diurnal to seasonal patterns in DPM in the study mine. A method of sensitizing the Airtec to allow "spot checking" of DPM (i.e., within minutes) is also presented. Chapter 1 has been published.

In Chapter 2, the effects of aging as an artifact of DPM sampling on size selector devices is investigated. Size selectors are commonly used for DPM sampling in mines in order separate relatively large mineral dust particles from the relatively small DPM. Impactor size selectors are the current industry standard for this purpose, but sharp-cut cyclones have also been suggested. The former physically traps the oversized dust particles to remove them from the DPM sample and is therefore susceptible to loading (or "aging"), whereas the latter separates particles by splitting the sample stream and should be minimally influenced by aging. However, neither device type has been thoroughly field tested in this regard. The field study presented here tested these devices side-by-side to determine their performance with gradual aging (versus new/clean devices), and the influence on effective particle cut size was specifically investigated.

In Chapter 3, the possibility of attachment between DPM and respirable dust in the mine atmosphere is investigated. Such a phenomenon is of interest with respect to DPM sampling. Since sampling in mines typically uses a size selector, any DPM that is effectively oversized due to attachment with relatively large dust particles may be excluded from a sample. Though little published literature on the topic exists, attached particulates could have important health implications too. For the field study reported here, samples of particulates in three size ranges (submicron, respirable, total airborne) were collected in three different locations of the mine to determine where the DPM effectively occurs. Additionally, samples of airborne particulates were collected with a small electrostatic precipitator for analysis by electron microscopy, such that instances of DPM-dust attachment might be observed if this is indeed happening. The electrostatic precipitator was used in order to preserve the state of particulates as they occurred in the mine atmosphere (i.e., either attached to one another or not).

Chapter 1. Area monitoring and spot-checking for diesel particulate matter in an underground mine

S. Gaillard, E. McCullough, E. Sarver

Virginia Tech, Department of Mining and Minerals Engineering, Blacksburg, VA, 24060, USA

This paper was originally published in Mining Engineering, Vol. 68, No. 12, 2016, pp. 57-62.

Abstract

Diesel particulate matter (DPM) has been regulated by the U.S. Mine Safety and Health Administration since 2002 in underground metal and nonmetal mines. To demonstrate regulatory compliance, DPM samples must be collected and later analyzed by the U.S. National Institute for Occupational Safety and Health (NIOSH) 5040 standard method, but the FLIR Airtec DPM monitor can serve as a complementary engineering tool. The monitor is a handheld instrument that offers near-real-time measurements of elemental carbon (EC), which is a primary constituent of DPM. As part of an ongoing field study, the monitor was used to survey EC in an underground stone mine. This effort was aimed at determining spatial and temporal DPM variations in several key locations. The results of prolonged area monitoring—that is, lasting several hours — revealed that DPM concentrations were diluted substantially as air moved away from the primary production zone, but that concentrations could vary quite a bit in a single location from day to day and between seasons. DPM concentrations were generally lower in winter than in summer, which is consistent with increased natural ventilation airflows during winter. Using a modified sampling cassette, an attempt was also made to sensitize the Airtec monitor to allow for "spot-checking" of EC concentrations — that is, measurements made in several minutes. Preliminary field data showed that the sensitive cassette performed well in terms of providing accurate data that could be useful for rapid assessment of DPM.

1. Introduction

Diesel particulate matter (DPM) is the solid fraction of the exhaust emissions from a diesel engine. It largely consists of elemental carbon (EC) and organic carbon (OC) (Birch, 2003). The World Health Organization International Agency for Research on Cancer classified diesel exhaust, including DPM, as a carcinogen (World Health Organization, 2012). It is believed to cause and/or exacerbate respiratory illness upon inhalation, deposition and retention in lung tissue. Because DPM exists in both the micro- and nanoparticulate ranges, it can bypass typical autoimmune defense mechanisms that keep larger particles out of the respiratory system (Ristovski et al., 2012).

Compared with workers in other occupations involving frequent use of diesel-powered equipment, such as dock workers and truck drivers, underground miners are exposed to relatively high DPM concentrations because they work in enclosed environments (Noll and Janisko, 2013; Noll, Janisko and Mischler, 2013). A variety of engineering and administrative controls have been devised to reduce DPM exposures in mines, and increased airflow is often a key

component. In largeopening mines, which are most common in the metal and nonmetal sector, DPM abatement through increased ventilation can be quite challenging because moving and controlling large air volumes is difficult (Grau et al., 2002; Grau and Krog, 2009). Dynamic ventilation conditions often result in variable and unpredictable DPM concentrations over space and time.

The U.S. Mine Safety and Health Administration (MSHA) has regulated DPM exposure in metal and nonmetal mines since 2002. Its final rule limits personal exposure to total carbon (TC), which is the sum of EC and OC, to an eight-hour time-weighted average of 160 $\mu g/m^3$ (U.S. Mine Safety and Health Administration, 2006). To demonstrate compliance, operators must use the U.S. National Institute for Occupational Safety and Health (NIOSH) 5040 Method for the analysis of collected DPM samples (Birch, 2003). However, the handheld Airtec DPM monitor (FLIR Systems Inc., Nashua, NH) was developed as a way to provide near-real-time measurements of EC for tracking personal DPM exposures over a work shift (Janisko and Noll, 2010; Noll et al., 2014). The monitor works by capturing DPM on a filter and successively measuring laser extinction as the dark EC particles accumulate. The laser extinction is directly correlated to EC, but the monitor is also programmed to display TC as a time-weighted average (Takiff and Aiken, 2010). For this, an assumed TC to EC ratio of 1.3 is used, as discussed in Janisko and Noll (2008). Based on comparative analysis with NIOSH 5040 Method results, NIOSH confirmed the instrument meets or exceeds its accuracy criteria across a range of EC concentrations expected in mining environments (Noll and Janisko, 2013; Noll, Janisko and Mischler, 2013).

In addition to monitoring personal DPM exposures, the monitor can be used for area monitoring (Janisko and Noll, 2010; Takiff and Aiken, 2010; Noll et al, 2005; McCullough, Rojas-Mendoza and Sarver, 2015). By operating the instrument in a given location for a prolonged period, an understanding of the temporal variation, such as over a shift or over multiple shifts if monitoring on consecutive days, in DPM concentrations can be gained. Such monitoring in multiple locations can further provide valuable information regarding spatial variation in DPM within a mine (Janisko and Noll, 2010; Noll and Janisko, 2007). In the case that a quick assessment is needed, for example, as part of an occasional survey across different mine locations, the monitor might also be used for "spot-checking." However, this application will require sensitization of the instrument in most instances, as the desired time horizon for measurement is much shorter than that for which the monitor was developed — for example, 10 minutes versus 10 hours. To measure over shorter time periods, the monitor must be able to detect relatively smaller changes in EC deposition on the filter.

In this paper, the utility of the Airtec for area monitoring is demonstrated based on data collected in an underground stone mine. Results are presented from prolonged monitoring across multiple mine locations on multiple days, and in opposite seasons. Additionally, the monitor is discussed along with resulting spot-checking data.

2. Site and experimental details

2.1 Study mine and monitoring locations.

All data were collected in an underground stone mine with a diesel fleet consisting of about 40 pieces of equipment, including haul trucks, drills, loaders, auxiliary equipment and light-duty vehicles. The mine operates five days a week with two shifts per day. It is considered a large-opening mine, and air velocities are generally very low, less than 0.5 m/s (100 ft/min) in some locations, as is often observed in such operations (Grau et al., 2002; Grau and Krog, 2009). One fan is located on the surface forcing fresh air into the mine at a pressure of about 95 kPa (950 mbar), and the main ramp into the mine serves as another air intake, using natural ventilation. There is also a large auxiliary fan near the production zone and several booster fans, and ventilation tubing and curtains are further used to direct airflow in priority areas. Air exits the mine through a single exhaust.

DPM is the only airborne occupational health hazard known to be of real concern in the study mine. Concentrations of respirable dust, including silica, are quite low, and blast fumes dissipate overnight between shifts. Six distinct locations were selected for this study based on their proximity to activities or airways of interest (Table 1.1). Figure 1.1 illustrates the relative positions of the locations within the mine, with arrows indicating airflow direction.

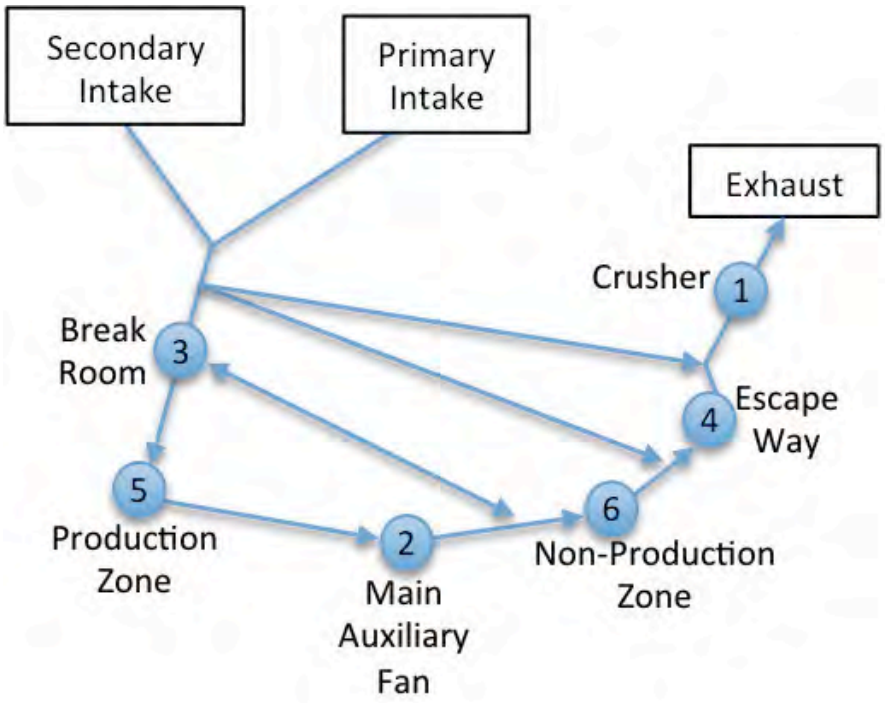

Figure 1.1 Schematic of relative position of all monitoring locations in the study mine.

Table 1.1 Description of monitoring locations in the study mine.

Location	Description
1	Near main mine exhaust and underground crusher operation, moderate traffic (production and non-production equipment/vehicles).
2	Immediately upstream of main auxiliary fan.
3	Outside of portable break room, workers drive to this location for breaks.
4	Escape route far downstream from production zones.
5	Near primary production zone.
6	No production, centrally-located, moderate traffic.

2.2 Equipment and data collection.

In late July through mid- August 2015, the Airtec was used for prolonged DPM monitoring, with EC concentration measured over time, and spotchecking, with rapid assessments of EC concentration. In December 2015, additional prolonged monitoring was conducted. An Anemosonic UA6 ultrasonic anemometer (TSI, Shoreview, MN; discontinued) or PMA-2008 vane anemometer (Mine and Process Service, Inc., Kewanee, IL) was used during some spot checks to determine the air speed near the monitoring equipment.

Three Airtec monitors, each calibrated to the standard flow rate of 1.7 L/min, were used with the standard cyclone and impactor, which remove large, non-DPM particles (Noll et al., 2005). The monitor displays data as a five-minute rolling average for either EC or time-weighted average TC concentration, such that it does not display nonzero values until at least minute 6. The sample collection rate of each monitor was set to either one data point or five data points per minute, meaning that a new five-minute average value was displayed every minute or every five minutes, respectively.

For prolonged area monitoring, the monitors were operated with standard cassettes and sample filters, 37 mm in diameter, designed to allow continuous DPM monitoring over an entire work shift, with the main target parameter being time-weighted average TC concentration, which is consistent with evaluating compliance with personal exposure limits. Due to the limits of the optical sensor in the Airtec, this means that when operating the Airtec to monitor a fixed location it may take a relatively long time before enough EC accumulates on the sample filter for the instrument to begin reading stable values. In order to collect spot-check data with the Airtec, it therefore needs to be sensitized.

As a possible approach, NIOSH developed a sensitive cassette that effectively reduces the exposed filter area to a circle about 10 mm in diameter, such that apparent EC collection and thus laser extinction happen relatively quickly. All spot-check data in the study mine were collected using the sensitive cassette, and a preliminary experiment was conducted to compare results from standard and sensitive cassettes.

3. Results and discussion

3.1 Prolonged area monitoring of EC concentrations.

During the summer and winter of 2015, 11 and 23 prolonged monitoring data sets were collected, respectively (Fig. 1.2). The tests were started at roughly the same time of day, near the beginning of a regular work shift, and continued for at least 300 minutes, with data reported only between 0 and 300 minutes to be consistent between all tests. In locations where multiple prolonged tests were conducted, each was on a different day. In all cases, the Airtec was positioned at approximately head height, or 1.8 m (6 ft), and care was taken to monitor about the same point in each location from day to day, either near the center of the tunnel cross section or about 0.6 m (2 ft) off the rib in locations with traffic.

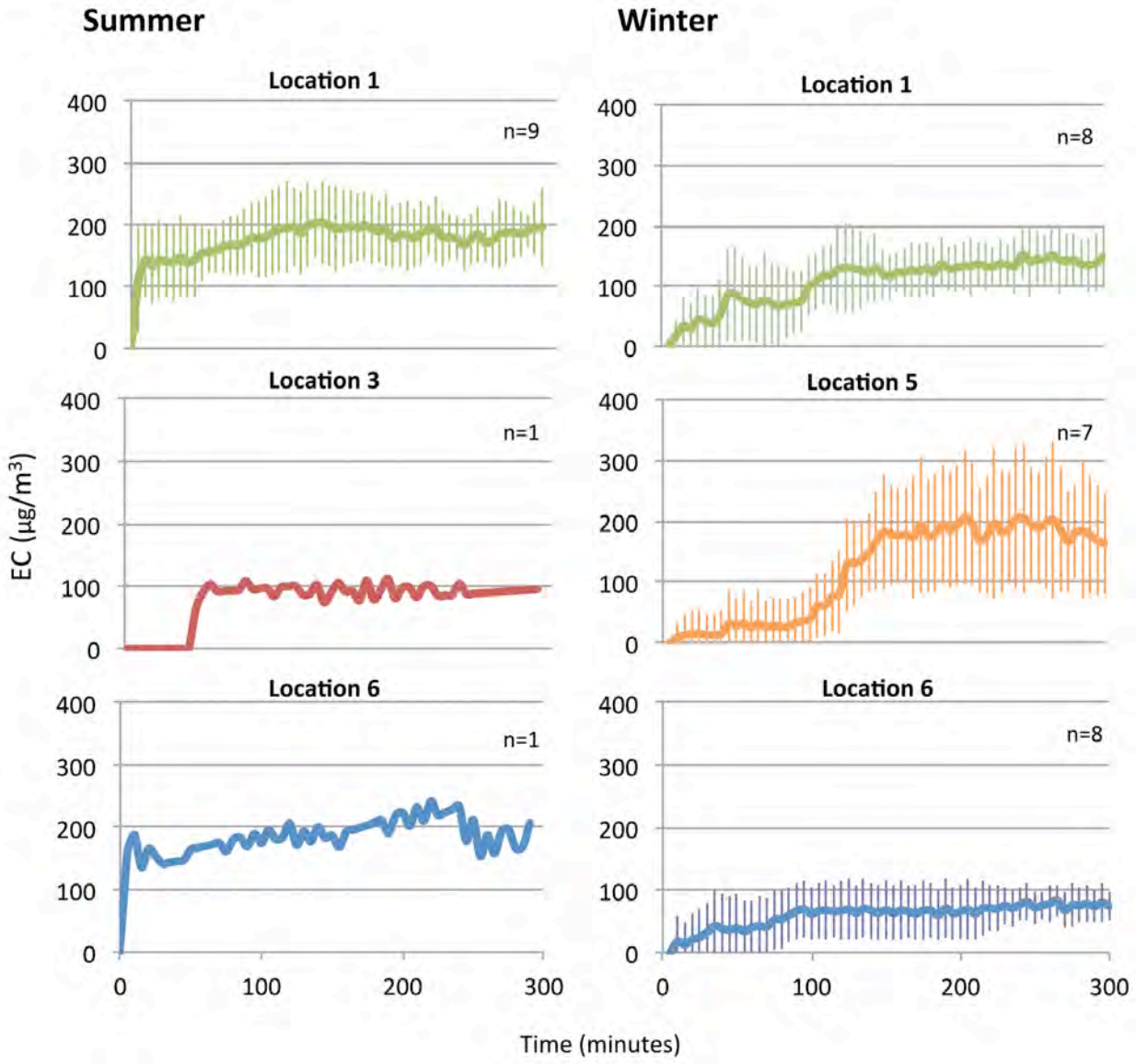

Figure 1.2 Prolonged monitoring results from summer and winter. For locations where multiple data sets were collected in the same season, n values are given and results are shown as an average with error bars representing the standard deviation.

Though the data collected for this study are somewhat limited, several key observations can be made from Fig. 1.2. First, as may be expected, DPM concentrations, using EC as a proxy, appear to vary both spatially and temporally in the mine. During the summer, locations 1 and 6, which are both along the main exhaust route from the mine, had higher EC concentrations than location 3, which is along the intake airways but is likely affected by some recirculating airflow that picks up DPM near production. From the winter monitoring data, it is clear that location 5, just outby from the main production zone, had the highest DPM concentrations recorded in that season. The DPM appears to be substantially diluted by the time it reaches locations 6 and 1.

Furthermore, DPM concentrations in the study mine seem to vary with season, which is consistent with the wellestablished understanding of ventilation in large-opening mines (Grau et al., 2002; Grau and Krog, 2009). Comparing summer versus winter data in locations 1 and 6, EC concentrations are clearly lower in the winter, despite no significant known changes in production or ventilation controls. According to monthly airspeed measurements taken by mine personnel in the main exhaust tunnel, where the cross section is small enough to perform a proper traverse, airflows were on the order of 92 m^3/s (195,000 cfm) during the summer tests and 109 m^3/s (230,000 cfm) during the winter tests.

Finally, Fig. 1.2 also suggests that DPM concentrations can be quite variable within a particular location in the mine. Some variation is likely due to accumulation of emissions with progression of the work shift, and this is demonstrated clearly in the winter data from location 5, but variability between days is also possible.

Figure 1.3 shows three consecutive weeks of prolonged monitoring data from location 1 from the summer and winter. This location may be expected to have relatively stable DPM concentrations over a work shift as it is located furthest from the primary emissions in the production zone. In the summer, EC values generally tended to increase over the workweek and then drop over the weekend, when there was no production. This may indicate that during summer workweeks DPM was accumulating in the mine faster than it could be exhausted overnight. In the winter, however, the trend of rising EC concentrations over the workweek was generally not observed, though the week 3 data do show an increase from Monday to Wednesday. So, while accumulation of DPM from one day to the next in a given location may explain some variation in prolonged monitoring data, there are surely many other factors at play, including dynamic ventilation conditions. As shown below, air speed measurements made for this study indicated that flows can change dramatically, even over relatively short time horizons such as days.

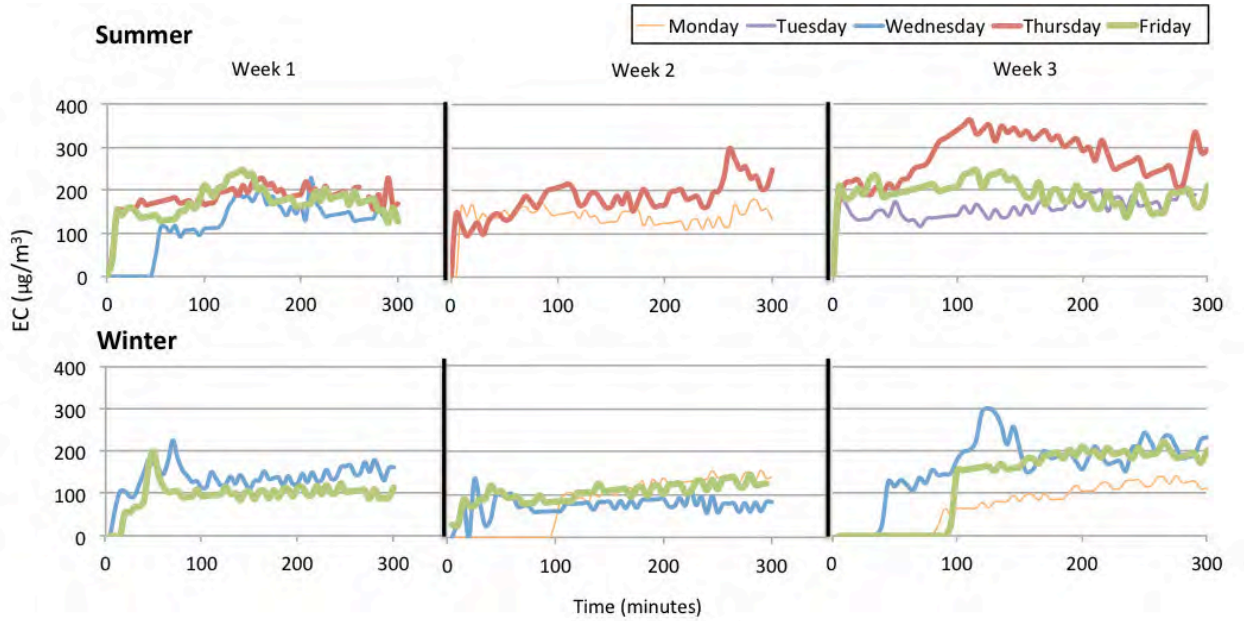

Figure 1.3 Results of prolonged monitoring at location 1 by weekday from summer and winter. In both seasons, data were collected on multiple days during three consecutive weeks.

3.2 Spot-checking of EC concentrations.

To confirm that the sensitive cassettes produced reliable EC concentration data, a series of basic tests were conducted briefly in the study mine. First, two Airtecs both using the sensitive cassettes were compared side by side. Then, the sensitive cassettes were compared against the standard cassettes. Locations and test times were chosen such that a range of EC concentrations could be sampled, but concentrations were expected to be stable during sampling due to the relative distance between the sampling locations and DPM emissions sources, and anecdotal experience of mine personnel and the research team. In nine side-by-side tests using sensitive cassettes, the absolute difference between the monitors was 13.4 ± 9.5 percent. However, in two of the tests with relatively high differences, 31 and 16 percent, the initial optical sensor value of one Airtec was observed to be very low, only about half that of a typical initial value. This can happen if the exposed filter area on the sensitive cassette is slightly misaligned with the laser and optical sensor, and may have influenced the quality of data collected. Excepting those two tests, the average difference between the monitor was 10.3 ± 7.2 percent. This is well within the range of possible spatial variability, which has been reported to be up to 20 percent (Vinson, Volkwein and McWilliams, 2007).

To compare EC values measured with the sensitive versus the standard cassettes, eight comparison tests were conducted (Fig. 1.4). For seven tests, a single monitor was used to first collect data on a standard filter, and then it was immediately used to collect data in the same location on a sensitive filter. The total lag time in these tests between the end of the standard cassette data and the data plateau for the sensitive cassette was relatively short, only the 2-3 minutes required to change the cassette and then the time required for the sensitive cassette data to reach plateau, 6-15 minutes. Thus, it is expected that any changes in DPM concentration in the sampling location were minor and should not substantially affect the sensitive and standard cassette comparisons. In test 5, two calibrated monitors were run side by side, one with each

filter type. Because the sensitive cassette uses a smaller filter area than the standard cassette, Airtec data from the former must be corrected. In Fig. 1.4, all sensitive cassette data had been corrected by dividing the EC concentrations by 13.3, the standard-to sensitive filter area ratio.

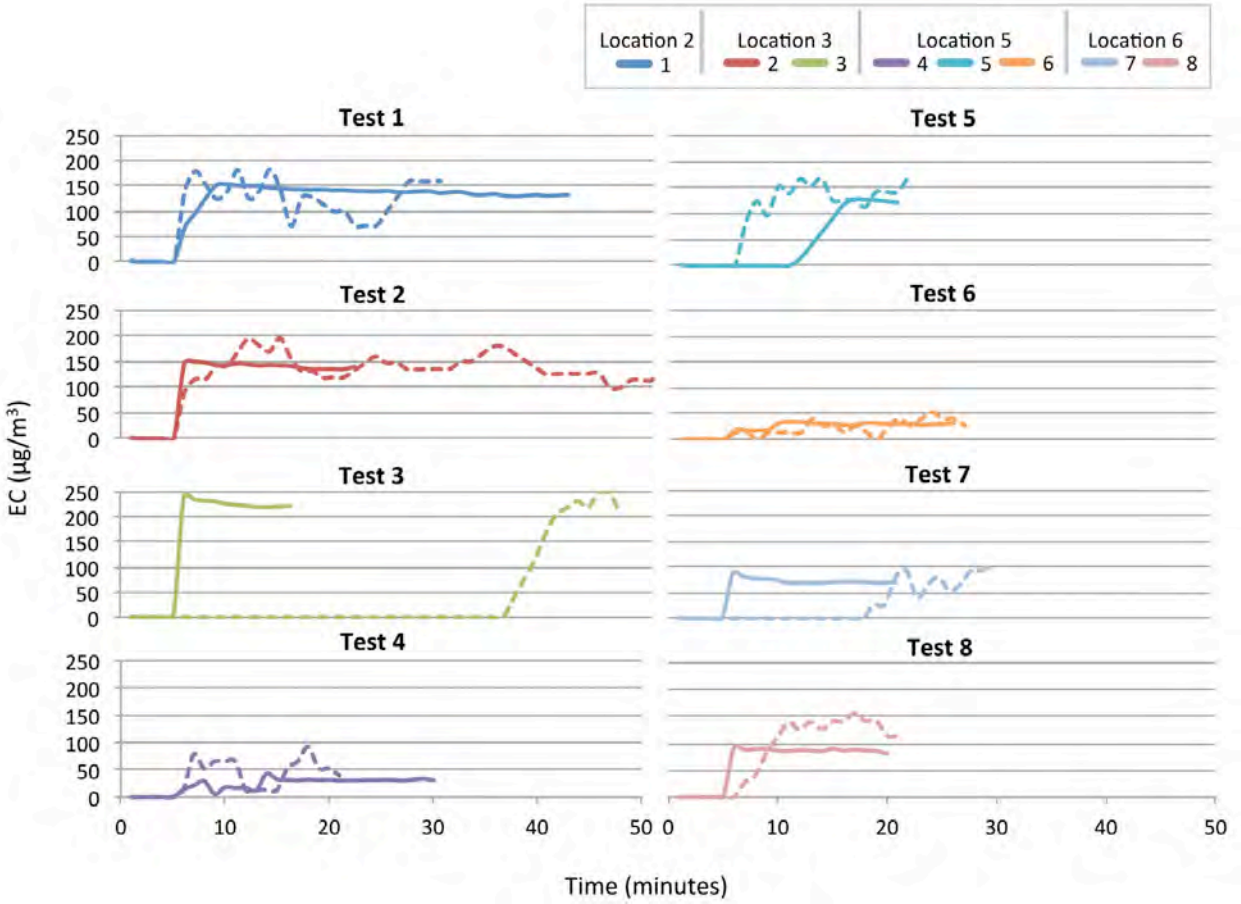

Figure 1.4 EC concentrations measured in eight comparison tests using standard (dashed lines) and sensitive (solid lines) cassettes. The x-axis represents the relative data collection time for a given cassette, with all data starting at 1 minute. In test 5, the cassettes were tested simultaneously using two Airtec monitors running side by side. In all other tests, the cassettes were tested in back-to-back runs using a single monitor, and data from both runs were overlaid to allow comparison of EC values and time-to-data plateau.

The need to sensitize the Airtec for spot-checking is well illustrated in Fig. 1.4. While the sensitive cassette data tended to plateau relatively quickly and remain stable, the standard cassette data took longer to plateau, if at all. By comparing the apparent EC concentrations where data plateaued, or fluctuations at least dampened, the sensitive and standard cassette data generally tended to correlate well. In five of the eight comparison tests — tests 1, 2, 3, 5 and 7 — the observed ratio of the apparent EC concentration from the standard cassette to the uncorrected value from the sensitive cassette was 13.5 ± 0.5. This is very close to the expected 13.3 value, suggesting that the sensitive cassettes are indeed performing as intended. In tests 4 and 6, it appears that the standard cassette data did not have a chance to reach plateau within the test period, possibly because the EC concentrations in the test area were too low. This highlights a

primary advantage of using the sensitive cassette for short-term measurements. In test 8, the initial optical sensor value on the sensitive cassette run was observed to be very low. All spot-check data shown here had been corrected by the 13.3 factor.

Another important observation from Fig. 1.4 is that, while data from the sensitive cassettes tended to plateau quickly, the time to the first nonzero values can vary. Based on observations in additional follow-up tests, not shown, this also seems to be related to the initial optical sensory value of the Airtec, which can be influenced by the initial condition of the filter when the instrument begins collecting data. Slightly used filters, such as from a prior spot-check, generally tended to produce data plateaus more quickly, beginning on minute 6, than new filters, which took up to 10 minutes or, rarely, more. With this knowledge, only spot-checking data where a plateau was observed or inferred are reported below.

To demonstrate the utility of spot-check surveying with the Airtec, data were collected at head height in all six locations in the study mine during the summer of 2015. Air speed measurements were also recorded during some of the spot-checks (Fig. 1.5). In each location, spot-checks were performed on multiple days, during the middle of the workshift at least two hours after the shift began and at least two hours before it ended. Some of the spot-check data shown in Fig. 1.5 are from tests where the initial optical sensor value was relatively low, but based on our experience to date, data collected under such conditions are expected to vary by only up to about 30 percent versus data collected with a typical initial optical sensor value, with no bias between the two conditions or the specific instruments. Thus, the large variations in reported spot-check data are believed to be real.

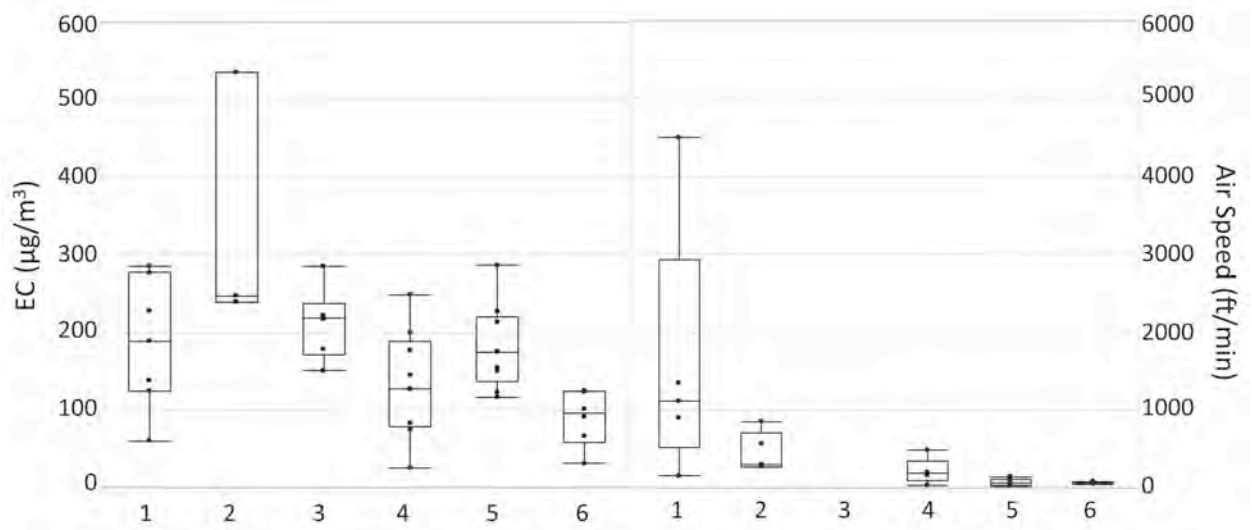

Figure 1.5 Spot-check and air-speed data collected at head height in all mine locations. Air speeds were measured only twice in location 6 and not measured at all in location 3.

In general, the spot-check surveys confirmed that spatial and temporal DPM variations can be significant in the study mine. Consistent with observations from prolonged monitoring, locations 1 and 5, near the exhaust and production zone, tended to have relatively high EC concentrations that were variable from day to day. This was also the case for location 4, along the main air route

between production and the mine exhaust, and, somewhat surprisingly, location 3. Based on the single prolonged monitoring data set from that location, it was expected to have relatively low EC concentration, but spot-checking revealed that the concentration can be fairly high. Because spot-checking was done mid-shift, it is possible that traffic to and from the break room near location 3 caused large but temporary fluctuations in DPM. Also somewhat unexpected are the spot-check results from location 6, which suggest relatively low EC concentrations in contrast to the prolonged monitoring results. The spot-checking results from location 2, near the auxiliary fan, were the most variable. This may be related to movement of concentrated DPM pockets by the fan. While only a limited amount of air speed data was collected during this study, it illustrates the dynamic ventilation conditions in the study mine.

Spot-check tests were additionally conducted in locations 2, 4 and 5 to compare measured EC concentrations at head versus cab height, or 4.9 m (16 ft), with 14 comparisons made (Table 1.2). For these tests, a spot-check was done at head height and another was done immediately afterwards at cab height at the same point in the tunnel. Generally, little difference is seen between DPM concentrations within this vertical distance and no real trend in the relative difference between the measurement heights. In 10 of the tests, the absolute difference was less than 10 percent, which is the expected average error in side-by-side spot-check measurements as reported above.

Table 1.2 Results of spot-check tests conducted at head versus cab height.

Test	Spot-checked EC concentration ($\mu g/m^3$)		Difference (%)
	Head height	Cab height	
1	240	227	5.4
2	239	239	0.1
3	256	232	9.9
4	83	72	14.5
5	177	173	2.3
6	75	88	-15.9
7	145	148	-2.3
8	214	195	9.4
9	134	189	-34.3
10	192	197	-2.7
11	286	265	7.7
12	117	115	1.9
13	161	199	-21.2
14	176	190	-7.6

4. Conclusions

While the NIOSH 5040 Method is required for demonstrating compliance with DPM exposure limits in underground metal and nonmetal mines, the FLIR Airtec DPM monitor is a useful engineering tool that provides the ability to evaluate DPM concentrations in near real time. Using its standard operating parameters and sampling cassettes, it can be used not only to track personal exposures but also to conduct area monitoring. In this work, the area-monitoring

application of the monitor was demonstrated in an underground stone mine. The monitor was also studied for a spot-checking application to allow rapid EC measurements. Use of a sensitive cassette, which reduces the exposed filter area, proved to be a simple and effective way to sensitize the monitor for this purpose. In general, the results from both prolonged area monitoring and spot-checking indicate that EC, and thus DPM, concentrations can vary significantly in both space and time within the study mine.

Beyond use in occupational health programs, the Airtec or similar environmental monitoring technologies may also contribute to the improved understanding of mine ventilation systems, particularly in large-opening mines, which are challenged when it comes to airflow modeling and analysis. Such technologies could further provide insights into the fates of airborne particulates as they travel from their sources.

5. Acknowledgments

The authors thank NIOSH for funding this work under CDC/NIOSH contract number 200-2014 59646 and especially James Noll and Shawn Vanderslice for their guidance. Sincere appreciation is also extended to all personnel at the study mine who have so willingly cooperated on and supported this work, and to Lucas Rojas Mendoza for assisting with data collection. Finally, thanks to Jamie Cohen, Steven Hyde and others at FLIR Systems Inc. for Airtec applications assistance.

6. References

Birch, M.E., 2003, "Monitoring of diesel particulate exhaust in the workplace," *NIOSH Manual of Analytical Methods*, 4th Edition, U.S. National Institute for Occupational Safety and Health.

Grau, R., and Krog, R., 2009, "Ventilating large opening mines," *Journal of the Mine Ventilation Society of South Africa*, Vol. 62, No. 1, pp. 8-14.

Grau, R., Mucho, T., Robertson, S., Smith, A., and Garcia, F., 2002, "Practical techniques to improve the air quality in underground stone mines," *Proceedings of the 9th U.S./North American Mine Ventilation Symposium*, pp. 123-129.

Janisko, S., and Noll, J.D., 2008, "Near real time monitoring of diesel particulate matter in underground mines," *Proceedings of the 12th U.S./North American Mine Ventilation Symposium*, pp. 509-513.

Janisko, S., and Noll, J.D., 2010. "Field evaluation of diesel particulate matter using portable elemental carbon monitors," *Proceedings of the 13th U.S./North American Mine Ventilation Symposium*, pp. 47-52.

McCullough, E., Rojas-Mendoza, L., and Sarver, E., 2015, "DPM monitoring in underground metal/nonmetal mines," *Proceedings of the 15th North American Mine Ventilation Symposium*, pp. 325-330.

Noll, J., Cecala, A., Organiscak, J., and Janisko, S., 2014, "Real-time DPM monitoring: NIOSH develops a new tool for assessing and controlling exposure," *Engineering & Mining Journal*, pp. 78-81.

Noll, J., and Janisko, S., 2007, "Using laser absorption techniques to monitor diesel particulate matter exposure in underground stone mines. *Proceedings of SPIE*, Vol. 6759, pp. 67590P-67590P11. http://dx.doi.org/10.1117/12.737790.

Noll, J.D., and Janisko, S., 2013, "Evaluation of a wearable monitor for measuring real-time diesel particulate matter concentrations in several underground mines," *Journal of Occupational & Environmental Hygiene*, Vol. 10, pp. 716-722. http://dx.doi.org/10.1080/15459624.2013.821575.

Noll, J., Janisko, S. and Mischler, S.E., 2013, "Real-time diesel particulate monitor for underground mines," *Analytical Methods*, Vol. 5, No. 12, pp. 2954-2963. http://dx.doi.org/10.1039/c3ay40083b.

Noll, J.D., Timko, R.J., McWilliams, L., Hall, P., and Haney, R., 2005, "Sampling results of the improved SKC diesel particulate matter cassette," *Journal of Occupational and Environmental Hygiene*, Vol. 2, pp. 29-37. http://dx.doi.org/10.1080/15459620590900320.

Ristovski, Z.D., Miljevic, B., Surawski, N.C., Morawska, L., Fong, K.M, Goh, F., and Yang, I.A., 2012, "Respiratory health effects of diesel particulate matter," *Respirology*, Vol. 17, No. 2, pp. 201-212. http://dx.doi.org/10.1111/j.1440-1843.2011.02109.x.

Takiff, L., and Aiken, G., 2010, "A real-time, wearable elemental carbon monitor for use in underground mines," *13th U.S. North American Mine Ventilation Symposium*, pp. 137-141.
U.S. Mine Safety and Health Administration, 2006, "Diesel Particulate Matter Exposure of Underground Metal and Nonmetal Miners; Final Rule," *Federal Register*, Vol. 71, No. 96, pp. 28924.

Vinson, R., Volkwein, J. and McWilliams, L., 2007, "Determining the spatial variability of personal sampler inlet locations," *Journal of Occupational and Environmental Hygiene*, Vol. 4, No. 9, pp. 708–714. http://dx.doi.org/10.1080/15459620701540618.

World Health Organization International Agency for Research on Cancer, 2012, "IARC: Diesel engine exhaust carcinogenic".

Chapter 2. Impact of aging on performance of impactor and sharp-cut cyclone size selectors for DPM sampling

Sallie Gaillard[a], Emily Sarver[a*], Emanuele Cauda[b]

[a] *Virginia Tech, Department of Mining and Minerals Engineering, Blacksburg, VA 24060, USA*
[b] *CDC/NIOSH Office of Mine Safety and Health Research (OMSHR), Pittsburgh, PA 15236, USA*

.

Abstract

Diesel particulate matter (DPM) is an occupational health hazard in underground mines. It generally occurs in the submicron range, and is often present in the mine atmosphere with significant concentrations of dust particles that tend to occur in the supramicron range. Since dust can interfere with analytical methods to measure DPM, it is often removed from a sample stream using impactor-type size selector (DPMI). Because the DPMI physically removes oversized particles from the stream, its performance may be gradually reduced with aging. Sharp cut cyclones (SCCs) represent an alternative size selector for DPM sampling applications, with a major advantage being that, by design, they should not be susceptible to rapid aging. This paper presents results of a field study designed to compare the performance of aged versus new/clean DPMIs and SCCs in an underground mine. DPMI aging resulted in clogging of the device, and eventually a reduction of its effective particle cut size – though, when sample flow rate was maintained, DPM sample mass collection was not affected until significant aging had occurred. Under the conditions present for this study, effects of SCC aging were observed to be minimal by the end of the study period.

1. Introduction

Sub-micron particles are increasingly recognized as significant respiratory health hazards (Cantrell & Watts, 1997; Kenny, et al., 2000; Ristovski, et al., 2012). Diesel particulate matter (DPM) represents a major source of submicron particles in both environmental and occupational environments (Kittleson, 1998; Abdul-Khalek et al., 1998). Due to their work around large equipment in confined spaces, underground miners have some of the highest exposures to DPM (EPA, 2002; Grau et al., 2004). DPM largely consists of solid elemental carbon (EC), commonly known as “soot”, and organic carbon (OC) that may be sorbed to EC particles (Kittleson, 1998; Abdul-Khalek et al., 1998). EC and OC can be measured by thermal-optical methods such as the NIOSH 5040 Standard Method (Birch, 2016), and their sum is referred to as total carbon (TC). While the complex nature of DPM does not allow for its direct measurement, both TC and EC have been accepted as suitable surrogates for monitoring occupational exposures to DPM (Noll et al., 2007 and Birch, 2016).

In the US, personal DPM exposures in underground metal/non-metal mines are regulated on a TC basis; in 2008, the 8-hour time-weighted average limit was set at 160 $\mu g/m^3$ TC (MSHA, 2008). To measure exposures, personal samples are collected using a small air

pump to draw DPM onto a quartz fiber filter, which is subsequently analyzed using the 5040 Method. To avoid analytical interference from mineral dust, an "impactor" is often placed just upstream of the filter. This device uses an impaction substrate, which serves as a particle size selector. It removes larger particles (i.e., mostly mineral dust) from the flow and allows smaller particles (i.e., mostly DPM) to pass to the filter (Cantrell and Rubow, 1992). Since the larger particles are physically trapped in the impactor, it gradually becomes loaded and should eventually be replaced. Effects of this loading or "aging" on sample results have only been studied in a laboratory setting to date (Cauda et al., 2014).

The SKC jeweled DPM impactor (SKC, Inc., Eighty Four, PA, USA), referred to as the DPMI herein, is the current industry standard for DPM monitoring (Birch, 2016). At the required flow rate for compliance sampling (1.7 LPM), the DPMI has a cut size of about 0.8 μm. Particularly in dusty environments, use of a small cyclone upstream of the impactor is also common practice. The 10-mm Dorr-Oliver (DO) cyclone provides a first cut of very large particles (i.e., d_{50} of about 4.5 μm, and d_{90} of about 3 μm at 1.7 LPM), which could cause rapid clogging of the impactor or substantial interference with 5040 Method or similar analysis. Nevertheless, the DPMI is intended as a single use device for collecting DPM samples for such analysis (SKC, 2003).

In addition to collecting filter samples for subsequent analysis, DPM can be monitored in near real-time by the handheld Airtec DPM monitor (FLIR Systems, Inc. Nashua, NH). The Airtec works by drawing in mine air at 1.7 LPM through a DO cyclone and DPMI, then particles less than 0.8 μm are deposited onto a filter in a cassette located inside the Airtec housing (Noll et al, 2013; Noll & Janisko, 2013). The instrument continually measures EC accumulation on that filter using a laser extinction principle whereby changes in laser absorption are correlated to EC mass in the sampling environment (Takiff and Aiken, 2010). In this application, FLIR recommends that the DPMI be replaced after three internal cassette changes (FLIR, 2011).

As an alternative to the consumable DPMI, sharp-cut cyclones (SCCs) have also been considered for DPM sampling applications (Cauda et al., 2014). The SCC is named for its sharp separation curve. Unlike traditional cyclones, which exhibit a gradual separation curve, the SCC is highly efficient – meaning it rejects nearly all particles larger than its "cut size" and passes nearly all smaller particles (Kenny et al., 2000). SCCs have been successfully used in ambient air sampling applications and may perform better than impactors in high dust concentrations (Kenny and Gussman, 2000). For mining applications, controlled laboratory studies have shown that they can perform comparably to impactors with respect to cut size and effective separation of mineral dust from DPM (Kenny et al., 2000; Cauda et al., 2014), although long-term performance of SCCs in mine settings has not been specifically investigated. Given that the SCC is designed for continual use, perhaps with periodic cleaning, it seems an obvious choice for some particular applications such as in continuous DPM monitoring systems (Barrett et al., 2017, Pritchard et al., 2016).

Use of size selectors for particulate sampling is premised on the notion that their performance does not appreciably change over the time period of use. That is, a necessary assumption is that as these devices age they function consistently (i.e., maintain the desired cut size) and do

not interfere with critical sampling conditions (e.g., flow rate) or results (e.g., collection of a particular constituent of interest). For DPM sampling, however, practical investigations are scarce. In order to determine how gradual loading as an artifact of sample collection can affect the performance of DPMI and SCC devices, a preliminary field study was conducted. The general approach was to incrementally compare total sample mass collected with devices as they aged versus the sample mass collected with new/clean devices. Additionally, the impact of aging on effective cut size of the tested devices was investigated.

2. Methods

2.1 Study site

This study was conducted in a large-opening underground stone mine. The mine employs an all-diesel production fleet with about 40 pieces of equipment (e.g., haul trucks, loaders), plus passenger and utility vehicles. While all production equipment has some version of a diesel particulate matter filter, either by the manufacturer or aftermarket, DPM remains an occupational health concern. Like other large opening mines (Grau et al., 2004), the study mine is influenced by natural ventilation, which generally causes lower air flows in the summer than in the winter (Gaillard et al., 2016). This leads to slower clearing of contaminants and thus overall higher levels of DPM in the summer. For forced ventilation, the mine uses two main fans – one blower fan installed on the surface and an exhausting fan in the main exhaust tunnel. There are a number of additional auxiliary and booster fans to target priority areas underground.

The particular sampling location for this study was near the primary crusher, which is also adjacent to the main mine exhaust. These circumstances generally mean that both dust and DPM concentrations are relatively high here compared to other locations in the mine. Sampling occurred on twelve separate days between August and November 2016, each time during about the first five hours of a regular production shift.

2.2 Sample collection

In this study, three different sampling trains were used as shown in Figure 2.1 below. The first train consisted of an Escort ELF personal sampling pump (Zefon International Inc., Ocala, FL) equipped with a SCC 0.695 (BGI by Mesa Labs, Butler, NJ) and a two-piece filter cassette with two pre-burned quartz filters (i.e., primary and secondary) and a cellulose pad. The DPM sample is collected onto the primary filter, and the secondary can be used for correcting OC results (Birch, 2016). The filters were analyzed by the NIOSH 5040 Method, further explained below (see sample thermograms in Appendix A). The second train also used an ELF pump equipped with a DO cyclone and DPMI cassette. This cassette contains both the DPMI and sample filters (i.e., the primary and secondary quartz filters), which were again analyzed by the 5040 Method. The third train was an Airtec monitor equipped with a DO cyclone and DPMI. In this case, the standard FLIR DPMI cassette did not contain sample filters; the DPM was collected on the Airtec's standard filter in its internal cassette, such that EC mass accumulation was determined by the instrument.

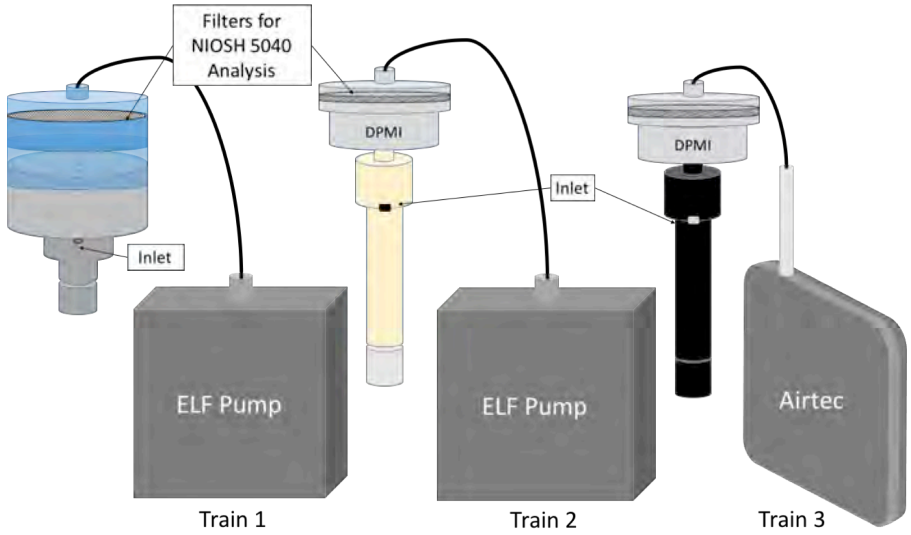

Figure 2.1 Three sampling trains used in the field study.

Flow rates for the Airtecs and ELF pumps with DPMIs were set to 1.7 LPM, which should produce a DPMI cut size of about 0.8 µm. The ELF pumps with SCCs were set to 2.2 LPM in order to produce a similar cut size (Cauda et al., 2014). This assured that EC mass measurements from all sampling trains could be directly compared (after adjusting for sampling flow rate). The flow rate of each pump was measured before and after the 5-hour sampling period using a Defender 510 Primary Air Flow Calibrator (Mesa Laboratories Co., Lakewood, CO). It should be noted that the SCC was not tested with the Airtec because this would have required increasing the flow rate from the standard 1.7 LPM to 2.2 LPM, which is outside of the recommended operating range.

The study design was such that four units of each sampling train were used simultaneously in all 12 sampling periods (Table 2.1). For the first sampling period, all size selectors were new/clean at the beginning of the period, and all had been aged by 5 hours at the end of the period. In the next sampling period, two of the SCCs from Train 1 were cleaned, and two of the DPMIs from Trains 2 and 3 were replaced and their corresponding DO cyclones were cleaned. These devices were designated as “clean.” The other SCCs were not cleaned and the other DPMIs were not replaced (and corresponding DO cyclones were not cleaned). These devices were designated as “dirty”, and had been aged for 10 hours at the end of the second sampling period. The same protocol was followed for all subsequent sampling periods, such that the dirty devices were never replaced or cleaned – and they had been aged for a total of 60 hours at the end of the sampling campaign. While sets of dirty DPMIs and DOCs remained paired for the entire sampling campaign, use of specific ELF pumps and Airtecs with each size selector train (i.e., DPMI/DO cyclone or SCC) was randomized. However, the same four Airtecs and eight ELF pumps were utilized for the entire study.

Table 2.1 Schedule for aging (dirty) or replacement/cleaning (clean) of size selectors with study progression.

SCC or DPMI replicate	Total aging time (hr) of size selector for sampling period (beginning – end)		
	Day 1	Day 2…	…Day 12
1 – new/clean	0-5	0-5	0-5
2 – new/clean	0-5	0-5	0-5
3 – dirty	0-5	5-10	55-60
4 – dirty	0-5	5-10	55-60

To clean the SCCs and DO cyclones, they were taken apart and placed in a mild soap solution. The parts were allowed to sit for about 5 minutes, gently agitated, and then rinsed and patted dry. To fully dry the parts before reassembling, they were placed under a fume hood with the fan on at least overnight. In all instances, the DPM collection filters were new for each sampling unit. For Train 1, new filters were used for every sample (i.e., since the SCC is separate from the filter cassette). In Train 2 and 3, for clean DPMIs, the entire cassette was replaced such that the DPMI and filters were new. For dirty DPMIs, new filters were placed into the original cassette before each sampling period. This was done by carefully opening the cassette to replace the filters and then resealing them. For Train 3, new Airtec internal cassettes and filters were used for every sample.

During sample collection, the inlets of all sampling units were positioned side-by-side (i.e., with no more than a few inches between them) and oriented in approximately the same direction to minimize spatial variability in results. All pumps were switched on and off at approximately the same time (i.e., within a few seconds of one another).

To get an idea of the dust concentrations in the sampling location, an Optical Particle Sizer (OPS) Model 3330 (TSI Inc., Shoreview, MN) was used to monitor particle number concentrations during the last six sampling periods (i.e., days 7-12). The OPS counts particles in 16 size bins between 0.3 and 10 μm. Assuming that virtually all DPM is less than 0.8 μm and that virtually all mineral dust is greater than 0.8 μm, the OPS data can be used to assess the relative concentrations of these two particle types, which should be split by the SCC (Table 2.1). Further, at 1.7 LPM, nearly all dust smaller than 3 μm should pass through the DO cyclone (i.e., d_{90} of 3 μm) such that it must be removed by the DPMI; with increasing dust size, fewer and fewer particles should pass through the cyclone (i.e., d_{50} of 4.5 μm and d_{10} of 6 μm).

Table 2.2 Particle concentrations (#/cc) in the range of 0.3 to 10 μm measured by OPS. Particles less than 0.8 μm are assumed to be DPM, and those greater than 0.8 μm are assumed to be mineral dust. Nearly all dust particles less than about 3 μm should be collected in a DPMI when using a DO cyclone upstream. Virtually all dust should be rejected from the sample stream by a SCC.

Day	DPM (#/cc)	Dust (#/cc)		Total Dust (#/cc)
		(~90% collected by DPMI)	(~50% collected by DPMI)	
	0.3 – 0.809 μm	0.809 – 3.014 μm	3.752 – 4.672 μm	0.809 – 10 μm
Day 7	2760.58	44.49	5.47	53.65
Day 8	2285.77	102.01	15.29	128.24
Day 9	2601.42	74.73	9.28	90.23
Day 10	625.96	71.14	9.37	87.02
Day 11	1231.11	63.79	8.26	77.74
Day 12	1608.45	69.64	7.49	81.86

2.3 Sample analysis

All filter samples collected in Trains 1 and 2 (ELF pumps) were prepared (i.e., by removing a 1.5 cm^2 punch sub-sample) and analyzed by the 5040 Method. A Sunset Laboratory Inc. Lab OC-EC Aerosol Analyzer (Tigard, OR) was used at the diesel research laboratories at NIOSH's Office of Mine Safety and Health Research (OMSHR) campus in Pittsburgh, PA. Since the quantity of interest in this study was EC mass collected, only the results of the primary filters (i.e., the top filter in the sampling cassette) are reported here. The 5040 analyzer outputs EC results on a mass per filter area basis ($\mu g/cm^2$). This was converted to an EC mass per filter value for each sample using the total filter area (i.e., 8.5 cm^2), and also an EC concentration in the sampling environment ($\mu g/m^3$) using the sampling time and measured flow rate (i.e., average of pre- and post-sampling flows).

Filter samples collected in Train 3 were analyzed by the Airtec, which has been calibrated to 5040 EC measurements. The instrument's method of analysis has been described in detail elsewhere (Noll and Janisko, 2007; Takiff and Aiken, 2010), but essentially it uses the voltage decay of its optical sensor to determine mass accumulation of EC over a given period of time. Using its internal algorithm, which assumes a standard flow rate, the Airtec converts the EC mass to an environmental concentration value that is displayed on the screen. However, in this study, the Airtec EC mass (and concentration) values were corrected for the measured flow rates.

2.4 Penetration efficiency of size selectors

Following the sampling campaign, the penetration efficiency of new and aged (5 and 60 hours) DPMIs and SCCs was also determined. This was done in a calm air chamber on the NIOSH-OMSHR Pittsburgh campus, using a similar strategy as that described by Cauda et al. (2014). In brief, spherical particles of standard sizes (i.e., 400, 500, 600 and 800 nm; Nanosphere ™ solutions purchased from Thermo Scientific, Waltham, MA) were sampled through the size selector devices. Particle concentrations in the air that passed through the devices were measured, as were concentrations in the chamber itself (i.e., measured using a

DO cyclone only). The difference between these two measurements can be used to assess what the size selector is removing. The particle concentrations were measured using an Aerodynamic Particle Size (APS) Model 3321 analyzer (0.5 to 20 μm; TSI Inc., Shoreview, MN) and a Scanning Mobility Particle Spectrometer (SMPS) Model 3080 (0.01 to 0.6 μm; TSI Inc., Shoreview, MN). These two instruments ensured that the entire size range of interest could be covered.

Figure 2.2 shows a schematic of the experimental apparatus used for penetration efficiency tests. To aerosolize the particle suspension in the chamber, multiple drops of each nanosphere size standards were placed into a nebulizer jar (BGI Collison Nebulizer, Mesa Labs, 10 Park Place, Butler, NJ) with about 15 mL of deionized water. The air and particle suspension were piped to the top of the chamber which was under negative pressure. To limit the moisture level inside the chamber, silica beads were placed on a grate located just below the top access port of the chamber. Before testing with size selectors was commenced, the chamber was allowed to fill and particle concentrations stabilized as confirmed by the APS and SMPS.

The penetration efficiency testing in the chamber was conducted at the same flow rates as sampling (i.e., 1.7 LPM for the DPMIs and 2.2 LPM for the SCCs) in order to ensure that results could be compared to the expected 0.8 μm cut size for a new/clean device. For each test, alternating measurements were made between the number concentrations of particles passing through a DO cyclone only (i.e., background) and passing through the DO cyclone and size selector of interest (SS). The sequence of measurements for one experiment was: 1) DO cyclone , 2) SS, 3) DO cyclone , 4) SS, 5) DO cyclone where the APS took 20 samples for 20 seconds each and the SMPS took 3 samples for 135 seconds each. For each sequence, the average particle number concentration of each size channel was determined. Then the two SS sequences were divided by the average of the background (DO cyclone) before and after each SS sequence. The two SS average values were then averaged together to get one particle number concentration value. This procedure was repeated twice for each size selector tested. The final average of these two replicate tests are reported here. The d_{50} penetration (i.e., cut size) of each SS was determined upon plotting penetration versus particle size.

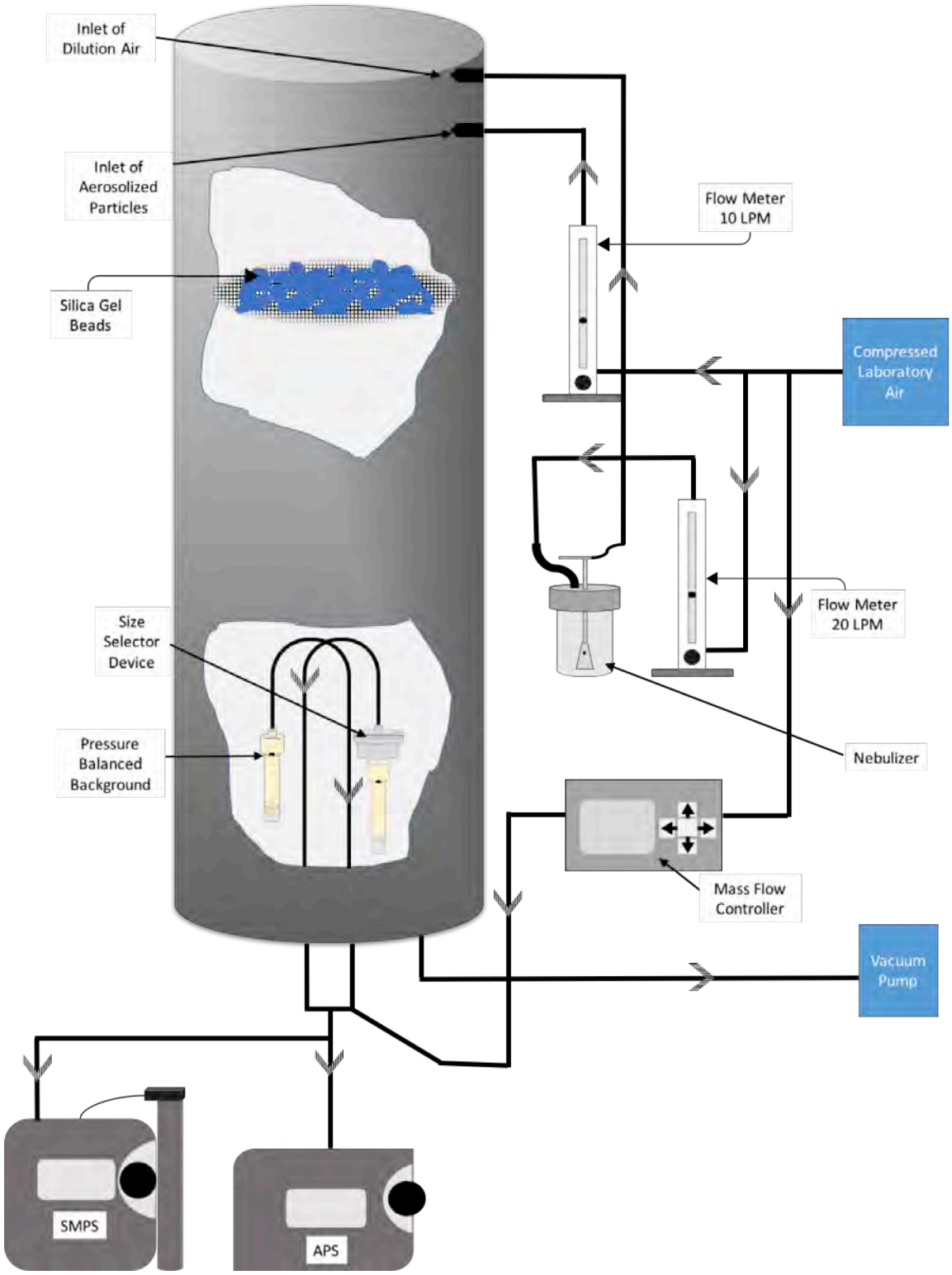

Figure 2.2 Schematic of experimental setup for size selector penetration efficiency tests (adapted from Cauda et al., 2014).

3. Results and discussion

Since the Airtec displays EC concentration data in near real-time (i.e., as a 5-minute rolling average), it could be used to make inferences about the relative performance of the aging versus new DPMIs throughout the study. Figure 2.3 shows time series data from the Airtec units for each of the 12 sampling periods, which has been corrected using the measured flow rate of a given sampling unit (i.e., the raw Airtec output assumes a 1.7 LPM flow rate); uncorrected data are shown in Figure A.1, Appendix A. While all four Airtec units track fairly well together during the initial sampling periods, those with dirty DPMIs eventually start to diverge from those with clean DPMIs. This observation suggests that the aging DPMIs not only limited the total volume of air being sampled, but also reduced the effective particle cut size. Beginning on Day 4, the units with dirty DPMIs began to register flow errors. These errors are registered when the Airtec senses a flow restriction, as might be expected with a DPMI that is becoming physically clogged, and the errors were registered more frequently as the study progressed. Notably, the Airtecs with clean DPMIs never registered flow errors during the study.

The overall effect of DPMI aging on sample EC mass is illustrated well in Figure 2.4, which shows total mass per filter for each sampling unit and sampling period. Note that the Airtec results have been corrected for flow in the figure, and the SCC results have been normalized (i.e., to correspond with the 1.7 LPM flow rate used by the DPMIs such that total mass values can be directly compared). Both the Airtec and ELF pumps were affected, as evidenced by the difference between the clean and dirty DPMI results on the later days of the study. A clear divergence is seen on day 9 for the Airtecs (i.e., both dirty results are lower than both clean results), and on day 8 for the ELF pumps. Photographs comparing aged DPMIs at 0, 5 and 45 hours (i.e., end of days 1 and 8) are shown in Figure 2.5. Distinct buildup of dark material around the four airflow channels is visible, as is more subtle coloring around the outer portions of the 45-hr aged DPMI. While some dust buildup was visible on the 45-hr aged SCC, even after 60 hours no real influence could be observed on sample mass accumulation (Figure 2.5).

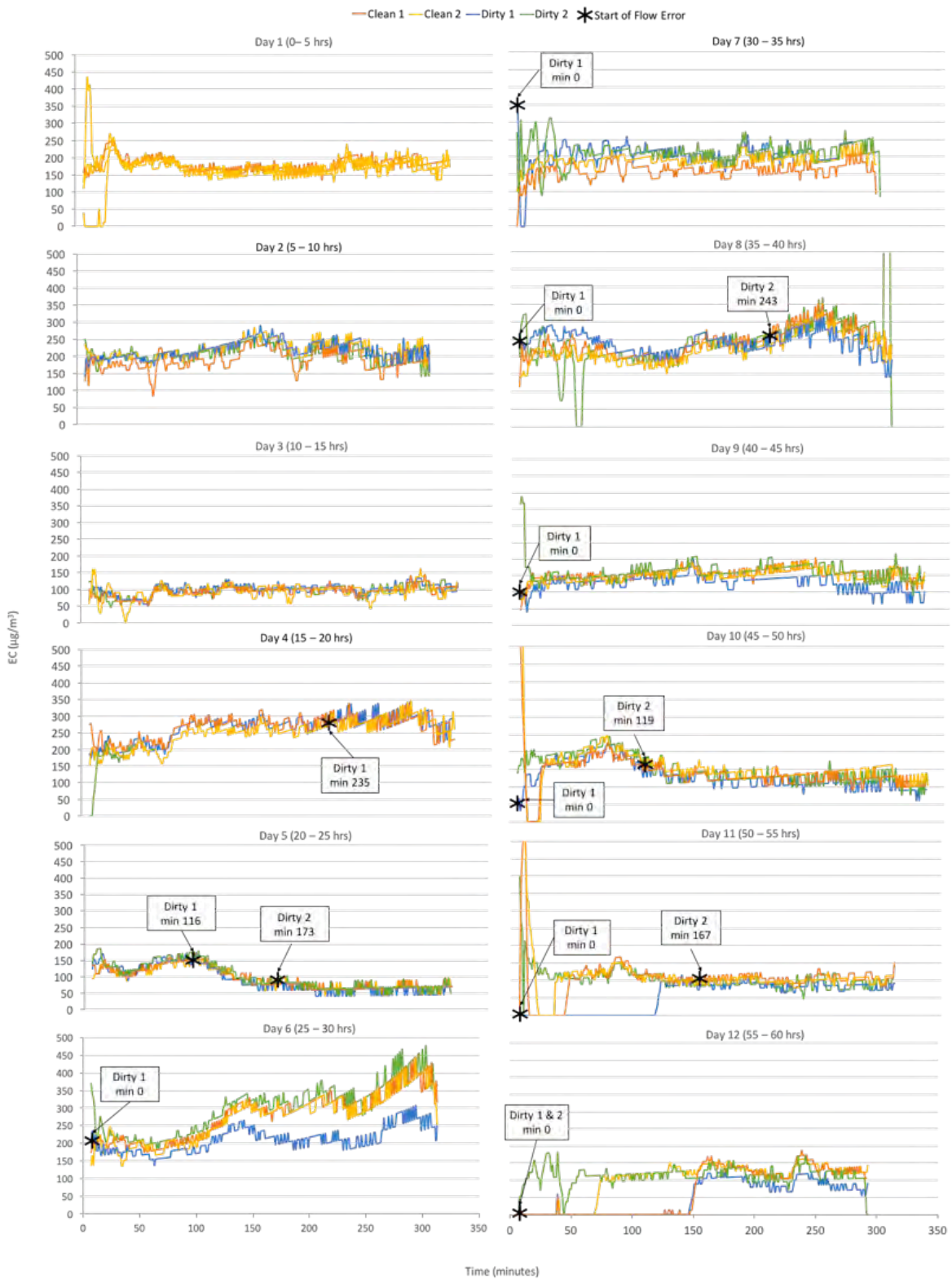

Figure 2.3 Time series data showing mass EC concentration values (as 5 minute rolling average) measured by the Airtecs. The mass concentrations are corrected to a standard flow rate of 1.7 LPM. Times when flow errors were registered on the Airtecs using dirty DPMIs are denoted on each plot.

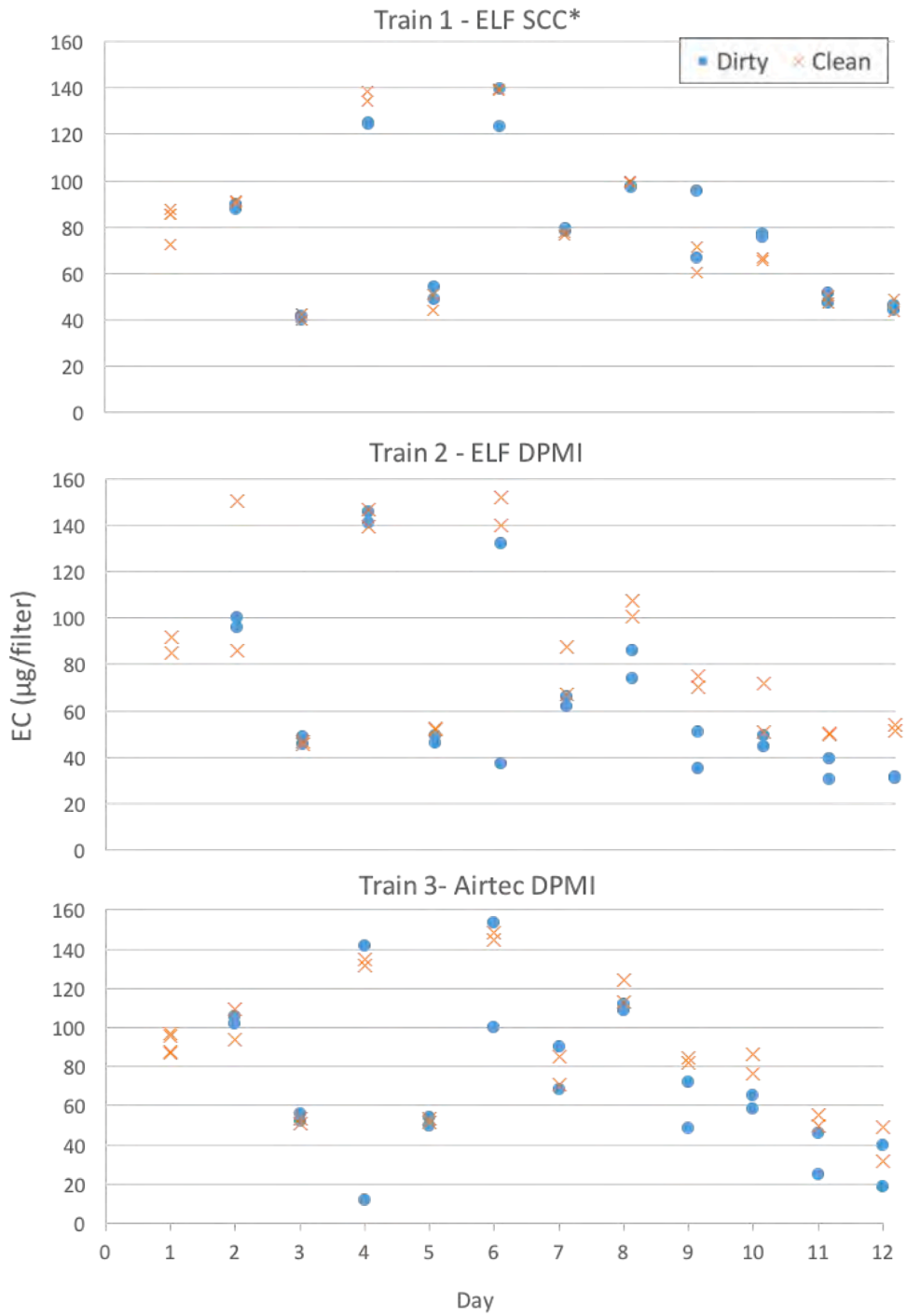

Figure 2.4 EC mass accumulation on sample filters. Filters from Trains 1 and 2 were analyzed by the 5040 Method. (Results from Train 1 were normalized to the 1.7 LPM flow rate used in Trains 2 and 3.) EC mass on filters in Train 3 was determined by the Airtec reading, which has been corrected here for measured flow rate.

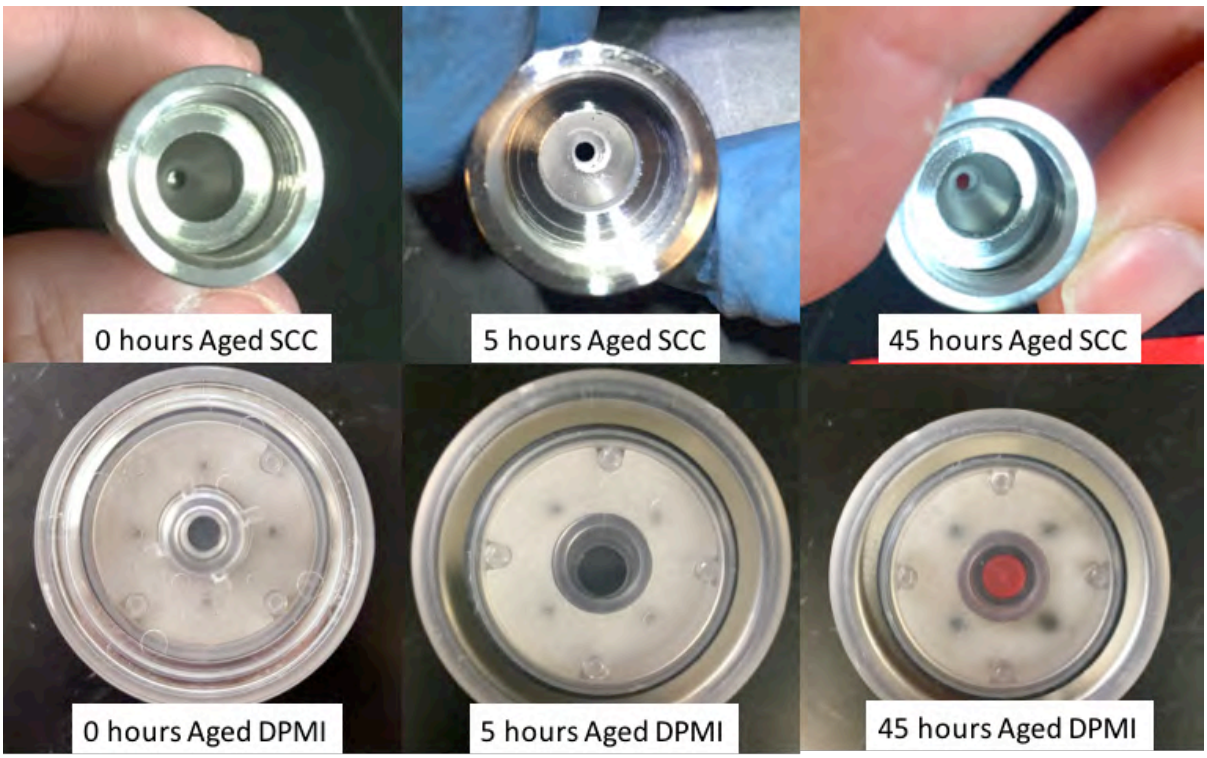

Figure 2.5 New and aged SCCs (top) and DPMIs (bottom) at 5 and 45 total hours of sampling using ELF pumps.

To better understand the effects of the DPMI aging, the measured flow rates of the Airtecs and ELF pumps should also be examined (Figure 2.6). While the Airtec does not have a stated acceptable error tolerance for flow rate, 5% is specified by MSHA for sampling with the ELF pump (MSHA, 2014). Using a 5% tolerance (shown by the dashed lines in Figure 2.6), the flow rates of Airtecs with dirty DPMIs began significantly decreasing from their set value of 1.7 LPM on day 4, and the problem became increasingly worse with further aging. This observation is consistent with the aforementioned flow errors associated with use of the dirty DPMIs, and it confirms that aging physically restricts flow through the device. The dust monitoring data (Table 2.2) also provides some indication about potential for particle loading in the DPMI. While data was only collected on days 7-12, the days with the lowest observed dust concentrations (days 7 and 8) correlated with smaller deviations from the set flow rate for the Airtecs using dirty DPMIs.

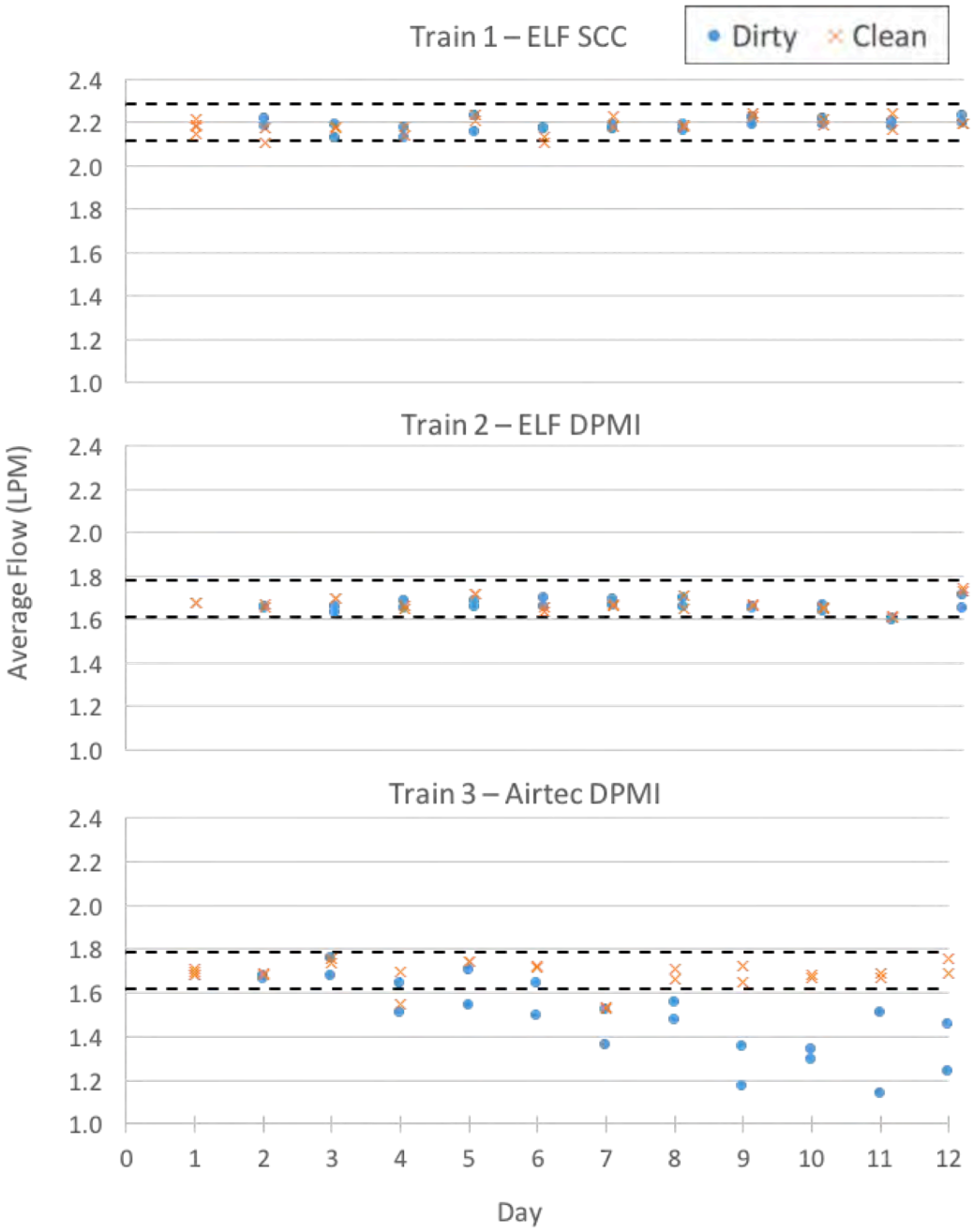

Figure 2.6 Average flow rate of ELF pumps and Airtecs pre- and post-sample collection for each sampling period. The dashed lines represent a 5% error tolerance around the set flow rates (i.e., 1.7 LPM).

Unlike the Airtecs, the ELF pumps are designed to automatically adjust to achieve their set flow, as demonstrated in Figure 2.6. This means that a higher total volume of air was sampled through the aged DPMIs using the ELF pumps than when using the Airtecs. All else equal, this would be expected to yield higher EC mass on those ELF pump samples than on the Airtec samples – though such a comparison here is confounded by the fundamental difference in analytical methods for the Airtec and 5040 samples, which might produce results that vary by 20% (Noll and Janisko, 2007; Takiff and Aiken, 2010). Indeed, even

differences between Airtec and ELF samples collected with clean DPMIs are observed (Figure 2.4).

As suggested earlier, beyond restricting flow, the physical loading of the DPMI with continued sampling was also expected to reduce its effective cut size. Figure 2.7 shows the results of the penetration efficiency tests, which confirmed this hypothesis. While a minor reduction is noted for the 5-hour aged DPMIs (and SCCs), the change is dramatic for the 60-hour DPMIs. The two devices aged with the Airtecs showed an average d_{50} cut size of about 0.36 µm; and those aged with the ELF pumps showed an average of 0.39 µm. Taken together with the observation that, despite maintaining their set flow rate, the ELF pumps with aged DPMIs collected less EC than those with clean DPMIs, this implies DPM in the study mine must include a sizeable mass fraction that is greater than about 0.39 µm. Based on the results from the SCC testing, however, it seems that the fraction of very large DPM agglomerates is negligible. The average d_{50} of the 60-hour aged SCCs was only 0.70 µm – and the aged and clean SCCs generally produced the same EC mass accumulation results.

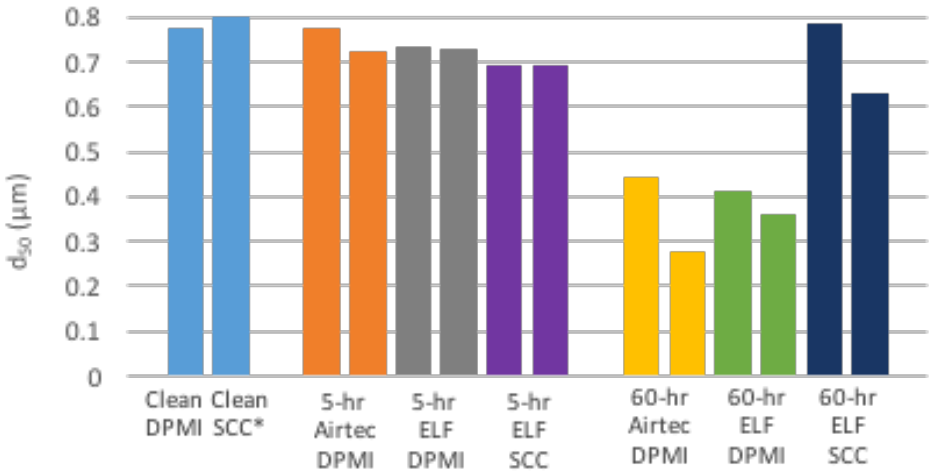

Figure 2.7 Penetration efficiencies of the Airtec DPMIs and ELF DPMIs and SCCs after 5 and 60 hours of aging. The clean SCC is reported as having a cut size of about 0.8 µm at a flow of 2.2 LPM (Cauda et al., 2014).

4. Conclusions

The results of this study offer several important insights into the performance of impactor and SCC size selectors for DPM sampling. In general, the DPMI can undergo substantial aging without much effect on DPM sample mass collected – even in a relatively high DPM environment. This is because, while aging means that the DPMI is becoming physically clogged, its effective cut size is reduced gradually and most DPM actually occurs far below the initial cut size (i.e., 0.8 µm).

Two key caveats to the above conclusion must be noted however. First, due to the clogging effect of particles being loaded into the DPMI, sampling pumps should either automatically adjust to maintain a desired flow rate, or pump flow rate should be carefully monitored to allow accurate determination of DPM concentration in the sampled environment. In the latter

instance, if the flow rate deviates significantly from the desired value, the cut size of the DPMI, by design, could be changed. Second, the severity of DPMI aging will surely be related to not only the relative DPM concentration in the sampled environment, but also the dust concentration. In dustier environments, the DPMI will age more rapidly. This underscores the need to use a DO cyclone upstream of the DPMI, as is often recommended and was done here.

With respect to the SCC, the data reported here indicate that aging of this device is indeed very slow. Moreover, it produced similar results to new DPMIs. As such, it may be a favorable alternative to impactor-type size selectors for DPM sampling – particularly for continuous monitoring applications. In that case and depending on the DPM and dust conditions in the sampled environment, a routine program might be developed to periodically clean the SCC in order to maintain its performance.

5. Acknowledgements

The authors would like to thank CDC/NIOSH (Contract Number: 200-2014-59646) for funding the work. Sincere thanks also to Shawn Vanderslice of NIOSH for sample analysis, Chelsea Barrett for helping with equipment setup, and all the personnel at the study mine for their interest and support.

6. References

Abdul-Khalek, I.S., Kittelson, D.B., Graskow, B.R., Wei, Q. and Brear, F. (1998). Diesel Exhaust Particle Size: Measurement Issues and Trends. *SAE Technical Paper Series*.

Barrett, C., Gaillard, S., Sarver, E. (2017). Demonstration of continuous monitors for tracking DPM trends over prolonged periods in an underground mine. *Proceedings of the 16th North American Mine Ventilation Symposium, Golden, CO, June 17-22, 2017*. (Society for Mining, Metallurgy, and Exploration, Littleton, CO).

Birch, M. E. (2016). Monitoring of Diesel Particulate Exhaust in the Workplace. *NIOSH Manual of Analytical Methods (NMAM)*, 5th Edition.

Cantrell, Bruce K. and Watts, Winthrop F. Jr. (1997). Diesel Exhaust Review Aerosol: Review of Occupational Exposure. *Applied Occupational and Environmental Hygiene*, 12:12, 1019-1027.

Cantrell, Bruce K. and Rubow, Kenneth L. (1992) Diesel Exhaust Aerosol Measurements in Underground Metal and Nonmetal Mines. *Diesels in underground mines: measurement and control of particulate emissions proceedings*. Bureau of Mines Information and Technology Transfer Seminar, Minneapolis, MN, September 29-30.

Cauda, Emanuele, Sheehan, Maura, Gussman, Robert, Kenny, Lee; and Volkwein, Jon. (2014). An Evaluation of Sharp Cut Cyclones for Sampling Diesel Particulate Matter Aerosol

in the Presence of Respirable Dust. *Annals of Occupational Hygiene*, Vol 58., No. 8, 995-1005.

FLIR Systems. (2011). Airtec Diesel Particulate Monitor. *Operations Manual*, Rev. 9.

Gaillard, S., McCullough, E., Sarver, E., (2016). Area Monitoring and Spot-checking for DPM in an Underground Mine. *Mining Engineering*, Vol. 68, No. 12, pg. 57-62.

Grau, R.H., III., Robertson, S.B., Mucho, T.P., Garcia, F., Smith, A.C. (2004). NIOSH Ventilation Research addressing Diesel Emissions and other Air Quality Issues in Nonmetal Mines. *Transactions 2004* 316: 149-158. Littleton, CO: Society for Mining, Metallurgy, and Exploration, Inc.

Haney, Robert A. (2000). Sampling and Inferences For Diesel Particulate Matter in Underground Metal and Nonmetal Mines. Retrieved from http://www.msha.gov/S&HINFO/TECHRPT/diesel/haneyimvc7.pdf

International Agency for Research on Cancer (IARC). (2012). *IARC: Diesel Engine Exhaust Carcinogenic* [Press Release]. Retrieved from https://www.iarc.fr/en/media-centre/pr/2012/pdfs/pr213_E.pdf.

Kenny L.C., Gussman, R.A. (2000). A direct approach to the design of cyclones for aerosol-monitoring applications. *Journal of Aerosol Science*. 31:12, 1407-1420.

Kenny, L.C., Gussman, R., Meyer, M. (2000). Development of a Sharp-Cut Cyclone for Ambient Aerosol Monitoring Applications. *Aerosol Science and Technology*. 32:4, 338-358, DOI:10.1080/02786820033669.

Kimbal, Kyle C., Pahler, Leon, Larson, Rodney, VanDerslice, Jim (2012). Monitoring Diesel Particulate Matter and Calculating Diesel Particulate Densities Using Grimm Model 1.109 Real-Time Aerosol Monitors in Underground Mines., 9:6, 353-361.

Kittelson, D. (1998). Engines and nanoparticles: A review. *Journal of Aerosol Science*, 29(5-6), 575-588.

National Institute of Occupational Safety and Health (NIOSH). (2016). Limestone. *NIOSH Pocket Guide to Chemical Hazards.* Retrieved from: https://www.cdc.gov/niosh/npg/npgd0369.html.

National Institute of Occupational Safety and Health (NIOSH). (2012). Occupational Cancer Carcinogen List. Retrieved from http://www.cdc.gov/niosh/topics/cancer/npotocca.html. Accessed October 23, 2016.

Noll, J.D., Bugarski, A.D., Patts, L.D., Mischler, S.E. and McWilliams, L. (2007). Relationship between elemental carbon, total carbon, and diesel particulate matter in several underground Metal/Non-metal mines. *Environmental Science & Technology*, 41(3), 710-716. doi:10.1021/es061556a

Noll, J.D., Janisko, S. (2013). Evaluation of a wearable monitor for measuring real-time diesel particulate matter concentrations in several underground mines. *Journal of Occupational & Environmental Hygiene*, 10:12, 712-722.

Noll J.D., Janisko S., Mischler SE. (2013). Real-time diesel particulate monitor for underground mines. *Analytical Methods*; 5(12), 2954–63.

Noll, J. D., Timko, R. J., McWilliams, L., Hall, P., & Haney, R. (2005). Sampling results of the improved SKC diesel particulate matter cassette. *Journal of Occupational and Environmental Hygiene*, 2(1), 29-37. doi:10.1080/15459620590900320

Noll, J., Janisko, S. (2007). Using laser absorption techniques to monitor diesel particulate matter exposure in underground stone mines. *Proceedings of SPIE, Smart Biomedical and Physiological Sensor Technology V*, 6759(1) doi:10.1117/12.737790

Pritchard, C., Hill, J., Volkwein, J., Miller, A. (2016). Reduction in diesel particulate matter through advanced filtration and monitoring techniques. *Proceedings of 2016 SME Annual Conference and Expo, February 21-24, 2016, Phoenix, Arizona*. (Society for Mining, Metallurgy, and Exploration, Littleton, CO).

Ristovski, Z. D., Miljevic, B., Surawski, N. C., Morawska, L., Fong, K. M., Goh, F., & Yang, I. A. (2012). Respiratory health effects of diesel particulate matter. *Respirology*. 17(2), 201-212. doi:10.1111/j.1440-1843.2011.02109.x.

SKC. (2003). DPM Cassette with Impactor Cat. No. 225-317. *Operating Instructions*, Rev 1703. Retrieved from: http://www.skcinc.com/catalog/pdf/instructions/40081.pdf.

Takiff, L. and Aiken, G. (2010). A real-time, wearable elemental carbon monitor for use in underground mines. *13th United States/North American Mine Ventilation Symposium.*

U.S. Department of Labor Mine Safety and Health Administration (MSHA). (2008). Diesel Particulate Matter Exposure of Underground Metal and Nonmetal Miners. Rules and Regulations, Federal Register 30 CFR Part 57. Vol. 73, No. 98, pp. 29058-29060. Retrieved from: https://arlweb.msha.gov/REGS/FEDREG/NOTICES/2008Misc/E8-11329.asp

U.S. Department of Labor Mine Safety and Health Administration (MSHA). (2014). *Sampling Pumps and Airflow Calibrations*. Metal/Nonmetal Health Inspections Process Procedures Handbook Series, Ch. 4.

U.S. Environmental Protection Agency (EPA). (2002). Health Assessment Document for Diesel Engine Exhaust, National Center for Environmental Assessment, Washington, DC, for the Office of Transportation and Air Quality; EPA/600/ 8–90/057F. Retrieved from https://cfpub.epa.gov/si/si_public_file_download.cfm?p_download_id=36319.

Chapter 3. A field study on the possible attachment of DPM and respirable dust in mining environments

Sallie Gaillard[a], Emily Sarver[a*], Emanuele Cauda[b]

[a] *Virginia Tech, Department of Mining and Minerals Engineering, Blacksburg, VA 24060, USA*
[b] *CDC/NIOSH Office of Mine Safety and Health Research (OMSHR), Pittsburgh, PA 15236, USA*

Abstract

Diesel particulate matter (DPM) and mineral dusts are often present together in mine environments. DPM is generally considered to occur in the submicron range, whereas dust particles generated in the mine are often supramicron. To avoid analytical interferences when measuring DPM surrogates (i.e., elemental or total carbon, EC or TC), size selectors are frequently used to separate sub- and supramicron particles. This approach has previously been shown to exclude a fraction of the DPM from the sample. The excluded DPM may itself be oversized, but another possibility is that submicron DPM attaches to respirable dust in the mine atmosphere. To gain insights into the possible attachment between DPM and dust, a field study was conducted in an underground stone mine. Submicron, respirable and total airborne particulate samples were collected in three locations to determine the EC and TC concentrations by the NIOSH 5040 Standard Method, and carbonate interferences were addressed by acidification of the samples prior to analysis. Additionally, airborne particulates were collected onto grids for analysis by transmission electron microscope (TEM) in order identify specific instances of DPM-dust attachment. A low-flow sampler with an electrostatic precipitator was used for this purpose to maximize the possibility of collecting particles as they occurred in the mine atmosphere, rather than forcing them together as an artifact of sampling.

1. Introduction

Diesel particulate matter (DPM) is a significant occupational health hazard for underground mine workers (Cantrell and Rubow, 1992; Cantrell and Watts, 1997; Burgarski et al., 2011). DPM is largely comprised of elemental (EC) and organic carbon (OC), which have been observed to occur in a relatively constant ratio in mine settings (Kittelson, 1998; Abduhl-Khalek, 1998; Noll et at., 2007). For this reason, EC and total carbon (TC, taken as the sum of EC and OC) have been established as suitable surrogates for monitoring DPM (MSHA, 2008). In metal and non-metal mines in the US, MSHA regulates a personal exposure limit of 160 $\mu g/m^3$ of TC on an 8-hr time-weighted average basis (MSHA, 2008). To measure TC, filter samples are collected and analyzed by the NIOSH 5040 standard method (MSHA, 2008; Birch, 2016). This is a thermal-optical method that includes a series of temperature ramps in first a helium atmosphere and then an oxygen atmosphere to drive off the OC and then EC, respectively; any EC created from thermal decomposition of OC can be corrected by tracking laser transmittance (i.e., color) changes on the sample filter during analysis (Birch, 2016).

Mine atmospheres generally have significant airborne dust concentrations, which can interfere with the 5040 analysis (Haney, 2000; Noll et al., 2005; Noll et al., 2013; Vermeulen et al., 2010). Mineral dusts with carbonate content can be thermally decomposed in the OC measurement step of the 5040 method, effectively increasing the TC result. Mineral dusts with refractory minerals may also affect the optical measurements during the analysis (Haney, 2000; Birch, 2016). To address the problem of carbonate interference, the carbonate carbon can be removed from the sample by acidification prior to 5040 analysis, or it can be removed analytically from the 5040 result (Birch, 2016) – though these approaches have not been practically favored. Another approach, and one which applies to all dust types, is use of a particle size selector during sampling. Devices such as the DPM impactor (DPMI; SKC, Eighty Four, PA) are designed to remove larger particles from the sample stream such that only particles smaller than the device's cut size (i.e., 0.8 μm at a flow rate of 1.7 LPM) are deposited on the sample filter. This approach thus takes advantage of the size difference that generally exists between DPM, which is mostly in the submicron range, and dust, which is mostly in the supramicron range (Cantrell and Rubow, 1991; Cantrell and Watts, 1997; Haney, 2000; Noll et al., 2005).

There is of course no perfect cut size to completely segregate one particle type from the other. It is well established that DPM occurs in two primary modes: the nuclei mode includes nano-sized (i.e., less than 50 nm) particles of semi-volatile organic compounds, and the accumulation mode includes spherical soot particles that agglomerate together in globs and chains, often with adsorbed organics (Kittelson, 1998; Abduhl-Khalek, 1998; Cantrell and Watts, 1992; Bukowiecki et al., 2002; Pietikainen, 2009). The nuclei mode represents about 90% of DPM by particle number, while the accumulation mode accounts for most of the DPM mass (Kittelson, 1998; Abduhl-Khalek, 1998). Only a small fraction of DPM particles (i.e., 5-20% by mass) are larger than about 1 μm, and these are formed by continued agglomeration under conditions allowing relatively long residence times with high particle concentrations (Cantrell and Watts, 1992 Bukowiecki et al., 2002; Chou et at., 2003). On the other hand, dust generated in many mine environments tends to be mostly greater than about 1 μm (Cantrell and Watts, 1997).

Considering these general size ranges, the size selector approach to DPM sampling has proven to be quite efficient in limiting mineral dust interferences in 5040 analysis (Haney, 2000; Noll et al., 2005; Noll et al., 2013). However, there is a potential to miss some of the DPM. Anecdotally, this is evident in the gradual blackening appearance of a DPMI with use, or the collection of black particulates in the grit pot of a cyclone size selector. Inadvertent DPM removal when using a size selector can happen if the device by virtue of its design actually removes some DPM, if the DPM itself is larger than the selector's cut size, or if the DPM is effectively larger than the cut size because it is attached to larger particles. Removal of DPM in the size selector may be an issue, for example, in cases where an impactor is used excessively. As the impactor begins to load with particulates, including DPM, the effect becomes increasingly worse because the impactor's cut size is gradually reduced (see Chapter 2; Cauda et al., 2014a). Moreover, in cases where tubing must be used between the size selector and filter cassette (e.g., in real-time monitoring instruments like the FLIR Airtec), the tubing can also remove some DPM. Nonconductive tubing is often recommended to minimize this problem (Noll et al, 2013).

The case of oversized DPM has also been considered (Cantrell and Rubow, 1991; Haney, 2000; Vermeulen et al., 2010). Vermeulen et al. (2010) conducted extensive work in seven non-metal mines to collect submicron (i.e., using an impactor), respirable (i.e., using a Dorr-Oliver cyclone, to remove all particles greater than 10 μm and yield a d_{50} cut size of about 3.5 μm), and total particulates (i.e., using an open-face cassette). Their results showed that respirable and total EC were generally similar, but submicron EC was consistently less than respirable EC. Specifically, submicron EC was 77% of respirable EC, on average, though this fraction varied between 54-84%. These results indicate that some DPM is practically missed by typical sampling procedures, and are consistent with others where a similar experimental approach (i.e., measurements using different sampling trains) was used in the lab or the field (e.g., Haney, 2000; Noll et al., 2005).

Although exclusion of oversized DPM during sampling has commonly been attributed to the size of the DPM itself, attachment of DPM and dust could also be a contributing factor. In a lab study aimed at measuring airborne DPM in the presence of mineral dust particles, Noll et al. (2013) suggested that coagulation (i.e., attachment) between DPM and dust might cause less DPM to be collected on sample filters when using an impactor than when not using it. To specifically investigate this possibility of mixed aerosol exposures, Cauda et al. (2014b) conducted some lab tests in a calm air chamber containing DPM and mineral dust concentrations that may be typical of a mine environment. They used a small electrostatic precipitator (ESPnano; DASH Connector Technology, Spokane, WA) to collect samples of the airborne particles. The precipitator creates an electric field that charges the particles and simultaneously deposits them onto a collection plate. This allows determination of whether particles may interact in the ambient air; if particles deposit together, they likely occurred together in the air, rather than being forced together during sampling (Miller et al., 2010). Based on microscopy analysis, Cauda et al. concluded that some DPM and dust particles were indeed coagulating in the chamber.

Mixed aerosols in general, and the attachment of DPM and dust in particular, have not been widely investigated. Beyond the possibility for underestimation of DPM by typical sampling procedures, there may be unique health implications. For example, while some mine dusts (e.g., limestone) are generally regarded as minor respiratory irritants (NIOSH, 2016), the synergistic or antagonistic effects of DPM and dust co-exposures or DPM-laden dust exposures are not known. Indeed, only a few studies exist that specifically examine co-exposures to mine particulates (e.g., Karagianes et al., 1981).

The purpose of this field study was to explore the possibility of DPM and dust attachment in an operating stone mine. The experimental design combined two types of sampling and analysis: collection of submicron, respirable and total particulates for 5040 analysis to determine effective size fractions of DPM, and collection of ambient particulates for microscopic analysis to identify instances of attachment.

2. Experimental

2.1 Study site

This study was conducted in a large-opening underground stone mine, which employees an all-diesel fleet (e.g., haul trucks, loaders, drills, light-duty vehicles). The diesel fleet consists of Tier II and III type engines as well as various diesel particulate filters (DPF). Due to the very challenging ventilation conditions, DPM concentrations in some locations can reach relatively high levels (e.g., 400 $\mu g/m^3$ or more as TC) during peak periods. Dust is generally not considered an occupational hazard in the mine; dust is dominated by carbonate minerals, silica content is negligible, and total respirable dust concentrations are generally less than 1 mg/m^3 except just adjacent to the primary crusher.

Three sampling locations were selected for the study based on prior observations of DPM and dust (Table 3.1). The goal was to sample in locations with significant DPM, but having different dust concentrations. In each location, samples were collected during a single event (i.e., on three different days). Each sampling event was for a period of about 5 hours, which coincided with a regular production shift to ensure typical DPM and dust conditions. Particulate samples were also collected in each location for subsequent microscopy analysis. Sample collection and analytical procedures are described in detail below.

Table 3.1 Description and summary of monitoring locations in study mine.

Location	Description
1	Near primary production zone (moderate dust, high DPM).
2	Near main mine exhaust and primary crusher (high dust, high DPM).
3	Remote location with respect to production, but near stationary diesel pumps (low dust, moderate DPM).

During sample collection, a TSI 3330 Optical Particle Sizer (OPS) (TSI Inc., Shoreview, MN) was used to measure dust particle number concentration and size distribution. The OPS reports particle number concentrations in 16 size bins between 0.3-10 μm; but only the 11 bins between 1-10 μm were considered here, such that any influence of DPM could be excluded. The average number concentration of particles per bin during each of the three sampling events can be seen in Table B.1, Appendix B. Assuming spherical calcite particles with diameters corresponding to the mean size of each bin, the mass concentration of dust could be estimated.

2.2 5040 sample collection and analysis

Three sampling trains were used to collect particulate samples for TC and EC assessment (Figure 3.1). Similar to other studies (e.g., Vermeulen et al., 2010; Noll et al., 2003), one train was used for total particulates, one was used for respirable particulates, and one was used for "submicron" particulates. For sampling total particulates, a closed face three-piece filter cassette was used with no size selector. For respirable particulates, a two-piece cassette was used with a 10 mm Dorr-Oliver cyclone. For submicron particulates, a DPMI (0.8 μm cut size) and 10 mm Dorr-Oliver cyclone was used.

In each sampling location, triplicate samples were collected with each sampling train (i.e., to yield a total of nine samples). Each setup used an Escort ELF pump (Zefon International Inc., Ocala, FL) calibrated to 1.7 LPM, and flow rates were checked before and after sample collection. All samples were collected on pre-burned Tissuequartz^{TM} filters (2500 QAT-UP, 37 mm; Pall Corporation, Port Washington, NY) as required by the 5040 standard method. Both primary (i.e., particulates) and secondary (i.e., adsorbed OC) filters were collected such that OC results – and hence TC results – could be corrected to represent particulate OC only (Birch, 2016).

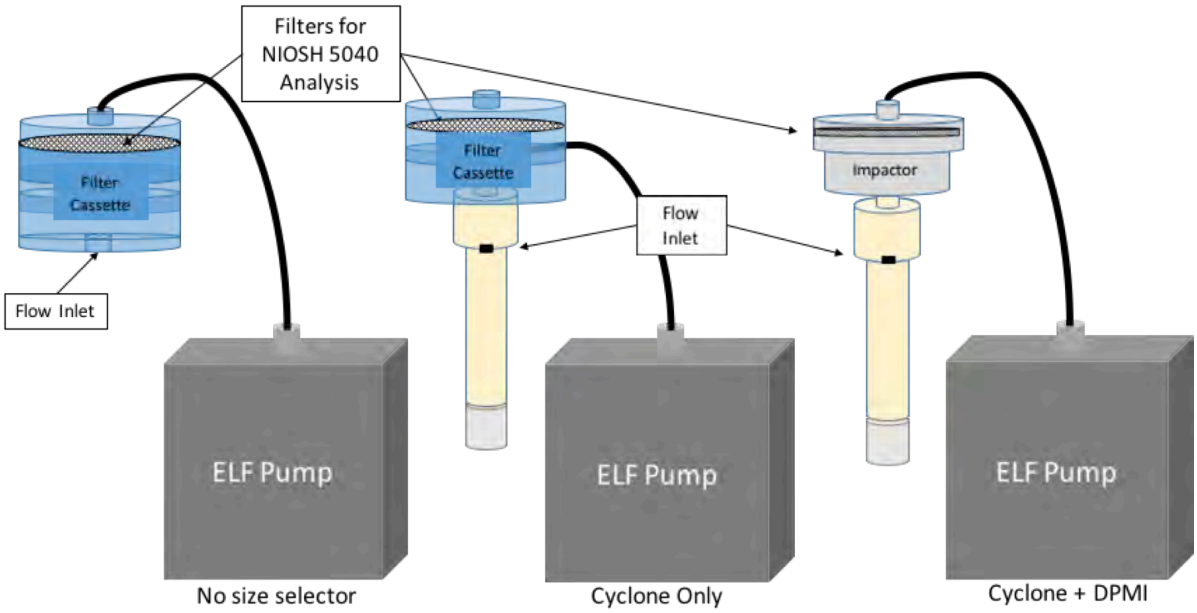

Figure 3.1 Three sampling trains to collect particulates in different size ranges.

The samples were analyzed using the NIOSH 5040 method. To prepare samples for the analysis, two punches (1.5 cm^2) were taken from each primary filter and a single punch was taken from each secondary filter. One of the primary filter punches and the secondary filter punches were analyzed directly using a Sunset Laboratory Inc. Lab OC-EC Aerosol Analyzer (Tigard, OR). The other primary filter punches were acidified prior to 5040 analysis in order to remove carbonate carbon per the method described by Birch (2016). Briefly, approximately 25 mL of 37% HCl was placed into a glass petri dish and placed in the bottom of a desiccator equipped with a ceramic tray and lid – all of which was located in a fume hood for proper ventilation. Wetted pH paper (i.e., using deionized water) indicated when the dessicator environment had sufficient acid vapor (i.e., pH of about 2), and then the filter punches were put into the dessicator on the ceramic tray. They remained there for about 1 hour, and then they were removed and placed under the fume hood for 1 hour to allow any remaining acid to volatilize. Care was taken to carefully transfer the punches onto and off of the tray with clean tweezers, in order to minimize disturbance of the particulates and avoid contamination between filters.

The 5040 analyzer outputs the amount of OC, EC and TC in each sample as $\mu g/cm^2$. On the primary filter punches that were not acidified, the OC (and hence TC) results were not

corrected for carbonate carbon (i.e., using its thermogram peak) such that results reported here include this carbon and therefore appear relatively high. On the acidified punches, the carbonate carbon was removed by the acid prior to 5040 analysis, so reported OC and TC have been corrected. As mentioned above, all OC results were corrected using their corresponding secondary filter such that only particulate OC is reported. In order to calculate the concentration of each constituent (OC, EC or TC) in the sampled environment (i.e., as $\mu g/m^3$), these mass per filter punch area results were converted using the total filter area (i.e., 8.5 cm^2), the sampling flow rate, and the sampling time.

2.3 TEM sample collection and analysis

In each sampling location, ambient particulates were sampled for later analysis by transmission electron microscopy (TEM). For this, the ESPnano electrostatic precipitator mentioned above was used. This device operates at a very low flow rate of 100 cc/min and the sampling time is programed by the user depending on expected particulate concentrations in the sampling environment (Miller et al., 2010). Preliminary tests indicated that sampling for several minutes (i.e., about 200s) was sufficient for collecting enough particles for TEM analysis, but not overloading the TEM grid. Samples were collected onto 400 mesh copper grids with an ultrathin carbon film on lacey carbon support (Ted Pella Inc., Redding, CA). Figure 3.2 shows the ESPNano's sample collection "key" with a TEM grid mounted.

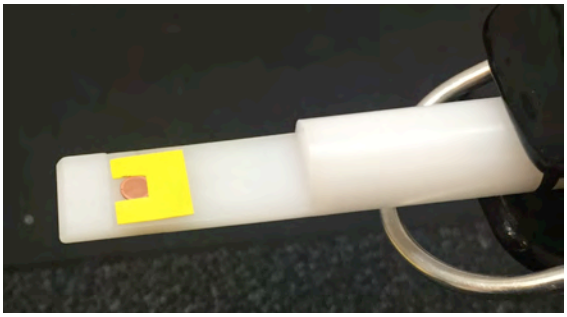

Figure 3.2 ESPnano key with an affixed TEM grid for sample collection.

TEM analysis was conducted on a JEOL 2100 instrument, which is a thermionic emission microscope with a high resolution pole piece (JEOL Ltd., Akishima, Tokyo, Japan). It is equipped with a large solid angle EDS detector, manufactured by JEOL. For each sampling location, the aim was to qualitatively assess the grid samples for particle loading and variety and then to identify 15-20 particles. Following initial analysis on particles from Location 2, it was clear that the opportunity to observe DPM and dust attachment was most likely in this location (i.e., near the crusher) so additional grids – again collected during regular mine production activities – were analyzed from there. In total, 10 samples were analyzed and TEM work was limited to about 2 hours on each.

To select particles for identification, the strategy was to begin analysis in the upper left quadrant of a grid at about 50,000x magnification, and gradually move from left to right and top to bottom of the sample (Figure 3.3). Then, about three particles were selected for identification and analysis at higher magnification before moving to another low-magnification frame of view. Since the objective of this work was to assess the possibility of DPM and dust attachment, particles suspected to be dust were prioritized for analysis over

those that were suspected to be DPM (based on characteristic morphology). For heavily loaded samples (i.e., four of the ten), this strategy worked well. For lightly loaded samples, some initial frames of view did not contain any particles so attention was focused on the grid areas where particles could be found. For most particles suspected to be or contain DPM, images were collected at two magnifications (e.g., Figure 3.4). This allowed sizing of the entire agglomerate, and verification of its characteristic graphitic layers (i.e., as reported by Ishiguro et al., 1997). Elemental mapping or spectral analysis was also conducted by energy dispersive spectroscopy (EDS) to allow identification of dust particles.

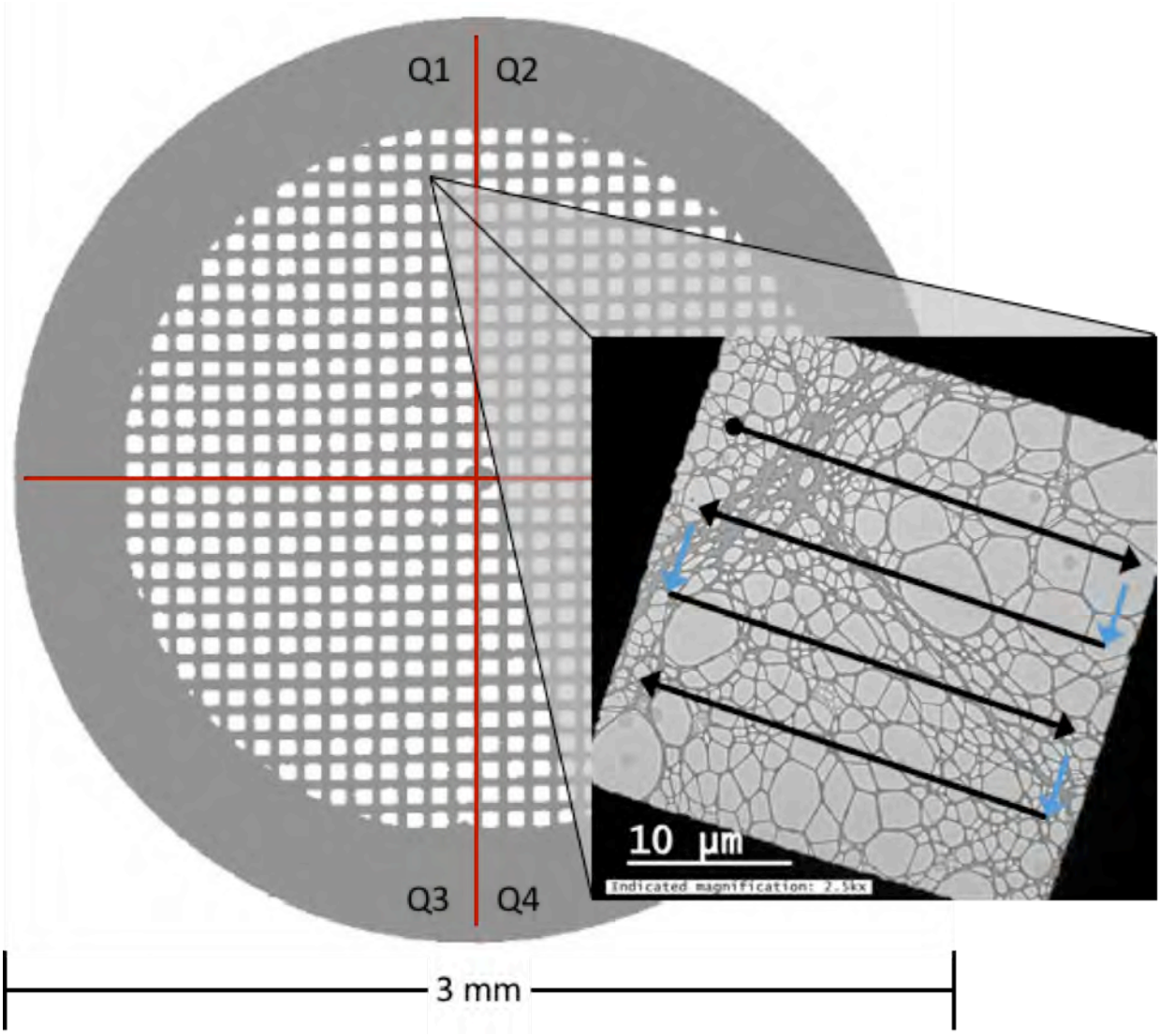

Figure 3.3 Schematic of process for locating and identifying particles on TEM grid.

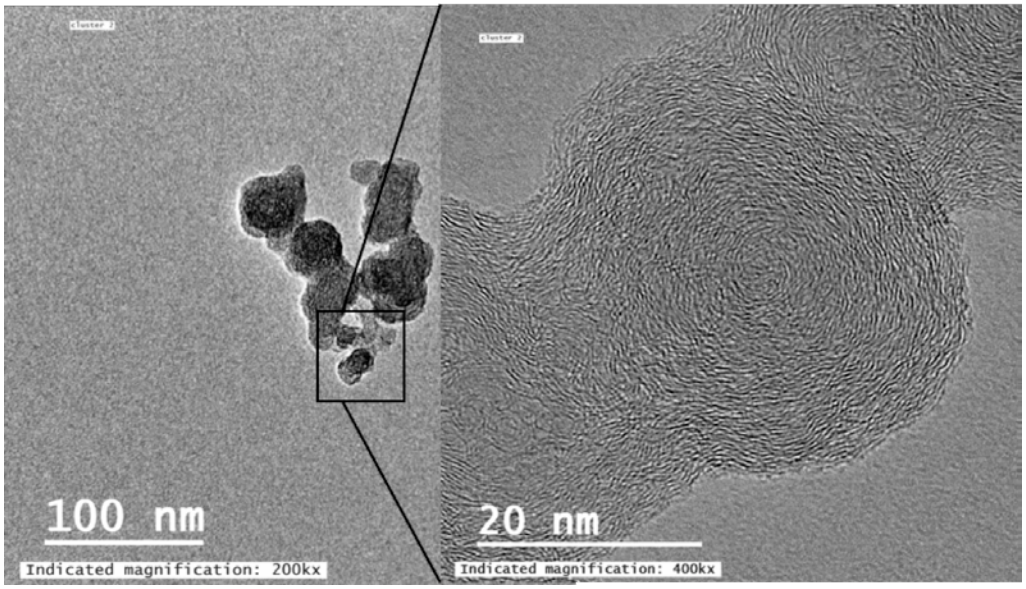

Figure 3.4 Figure to show the verification of a particle being DPM. A point on the agglomerate chain on the right is analyzed closer to see the carbon layers of a DPM particle.

3. Results and discussion

Using the OPS data, supramicron dust concentrations were estimated in each sampling location (Table 3.2). As expected, the highest dust concentration was in Location 2, which was adjacent to the primary crusher and main mine exhaust. Location 1 had a moderate dust concentration near the active production area (i.e., where mined material was being actively loaded into haul trucks). Location 3 was only affected by intermittent light duty traffic and stationary diesel pumps, and thus had a very low dust concentration. It should be reiterated that the OPS-derived values are only estimates, based on very cursory assumptions used to transform number concentrations into mass concentrations. But the observed trend is supported by the 5040 results from the total particulate samples. To explain, since dust in the mine should be dominated by carbonate minerals, the difference between acidified and non-acidified TC concentrations in a particular location should provide another measure of the dust concentration (see Figures 3.5 and 3.6, and tabulated data in Appendix B, Tables B.2 and B.3).

Table 3.2 Estimated dust mass concentration in the range of approx. 1 to 10 μm based on OPS number concentration data.

Location of Sampling	**Particle size range 1- 10 μm (mg/m^3)***
1	0.78
2	3.86
3	0.08

*Density assumption of calcite 2.7 g/cm^3 (NIOSH, 2016)

With respect to DPM, the highest 5040 EC concentrations were observed in Location 1, followed by Location 2 and then Location 3 (results from acidified samples shown in Figure 3.5). This is consistent with expectations considering the mine activities in the vicinity of each sampling location. Significant differences could generally not be observed between 5040 EC in the three size ranges sampled. There was substantial variability between the triplicate results. As this occurred across all size ranges and on both acidified and non-acidified samples (Figures 3.5 and 3.6), it is most likely related to spatial variability in the sampled environments rather than factors associated with sampling equipment (e.g., cassette types, specific pumps) or mine dust interference. Spatial variability is indeed a well-known issue for collection of airborne particulate samples in mine environments (e.g., see Kissell and Sacks, 2002 and Vinson et al., 2007).

The fact that total, respirable and submicron EC concentrations were observed to be similar for all sampling locations indicates that, on a mass basis, the study mine simply does not have considerable DPM that occurs in the supramicron range. This finding is contrary to most field reports by others (e.g., Vermeulen et al., 2010), which have shown significant supramicron DPM in mines (i.e., using EC as a surrogate) – though some other reports have also shown that most DPM resides in the submicron range (e.g., Maximilien et al., 2017). Variability in the ratio between submicron and respirable EC (or TC) in different mines is likely related to specific equipment or operating conditions. Exhaust after-treatment technologies like DPFs, for instance, are known to effectively change the particle size distribution of DPM (Lee et al., 2002 and Burgarski, et al., 2009).

Regardless, the results presented here could support respirable (instead of submicron) TC as a surrogate for DPM in mine environments where the primary mineral dust interference of concern is from carbonates. In this case, carbonate removal by acidification or analytially by integration of the carbonate peak on the 5040 thermogram would be necessary. But such an approach would allow for both removal of carbonate dust interference and accounting for the DPM that would otherwise be missed by submicron sampling. Furthermore, the results presented here add to a number of others that suggest use of EC (rather than TC) as a DPM surrogate in mines, based on the ability to more easily measure EC and the possibility of TC interferences from non-DPM sourced OC (e.g., see Noll et al., 2007; Noll et al., 2006, Noll et al,. 2014).

For diesel exhaust exposure assessments in non-metal mines, Vermeulen et al. (2010) also concluded that respirable EC is an appropriate analytical surrogate. They noted that, due to a strong observed correlation between respirable and submicron EC in their study mines (i.e., median submicron EC to respirable EC ratio of 0.77 with Pearson coefficient of 0.94), either quantity could be a suitable surrogate. However, the fact that submicron and respirable EC have a much different ratio in the current study (i.e., they are about equal, but still well correlated) highlights the favorability of respirable EC – or the need to determine a mine-specific submicron to respirable ratio if the submicron surrogate is to be used. This way, supramicron DPM is not missed by sampling efforts, or can at least be accounted for using a mine-specific correction factor.

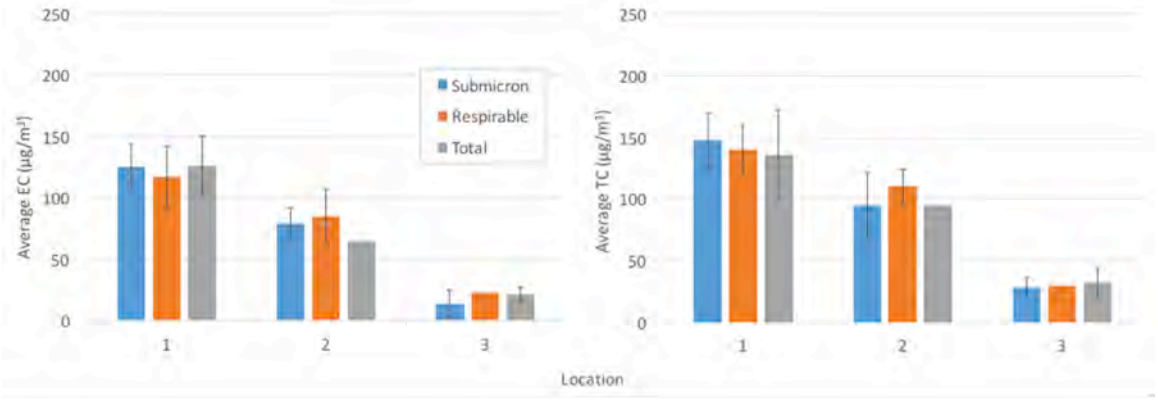

Figure 3.5 Average EC (left) and TC (right) in acidified samples in each monitoring location. Error bars represent 95% confidence intervals. (Note that confidence intervals could not be determined for total particulate results in Location 2 and respirable results in Location 3 due to a missing triplicate sample result in both of these sets.)

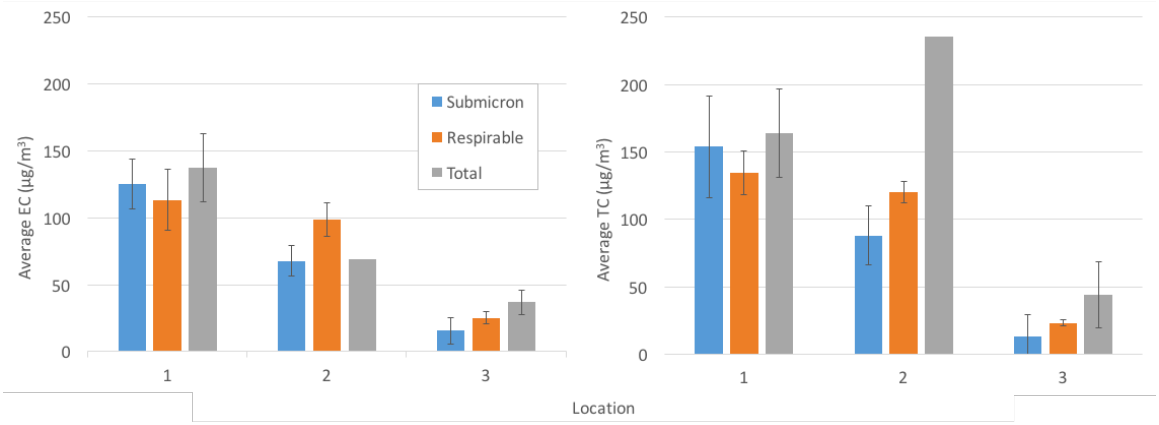

Figure 3.6 Average EC (left) and TC (right) samples in each location, non-acidified. Error bars represent 95% confidence intervals. (Note that confidence intervals could not be determined for total particulates in Location 2 due to a missing triplicate sample result).

Although the 5040 results in this study did not yield new insights about the possibility of DPM and respirable dust attachment in the mine atmosphere, the TEM results did. Table 3.3 summarizes the particles identified on each of the TEM sample grids analyzed for this study. (In Appendix B, the size and identity of each individual particle are shown in Table B.4, and images of all particles and EDS spectra, if collected, are also provided). In Location 1 near the production activities, the majority of particles on the grid were DPM agglomerates (e.g., Figure 3.6). These ranged in size from about 0.05 µm to 0.5 µm in the longest dimension viewable, and occurred in a variety of shapes from long chains to large clusters.

Table 3.3 Summary of particles analyzed by TEM in each sampling location.

Location	Sample No.	Sample Time (seconds)	Particle Loading	Total Particles Analyzed	DPM	DPM on Dust	Dust
1	1.1	200	High	19	14	0	5
2	2.1	200	High	25	16	9	0
	2.2	2	Low	1	1	0	0
	2.3	10	Low	3	2	1	0
	2.4	100	High	10	3	7	0
	2.5	200	Low	0	0	0	0
	2.6	200	Low	1	1	0	0
	2.7	200	Low	2	2	0	0
	2.8	200	Low	1	0	1	0
3	3.1	200	High	17	17	0	0

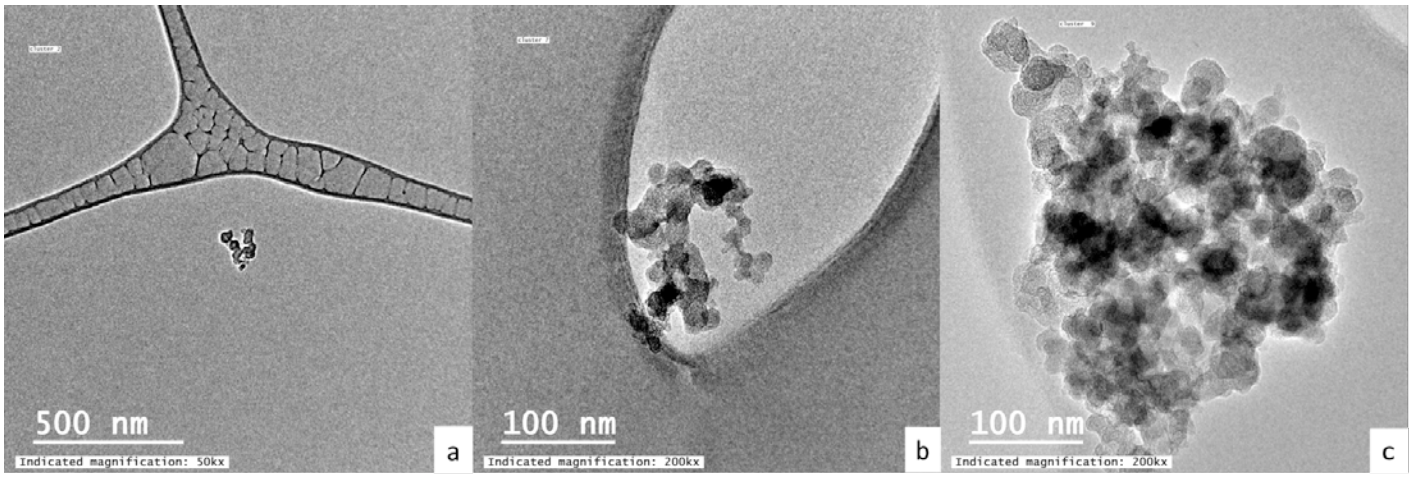

Figure 3.7 TEM images of DPM agglomerates collected in Location 1 (a - Image 1; b – Image 6; c – Image 10, ref. Table B.4, Appendix B).

Dust particles were also observed on the TEM grid (e.g., Figure 3.7). Five of these particles were selected for analysis using EDS, which revealed that two were carbonate, two were Ti-rich, and one appeared to be silica. No dust particles were found having attached DPM in Location 1. Additional TEM images from Location 1 can be found in Figures B.1 – B.15, Appendix B.

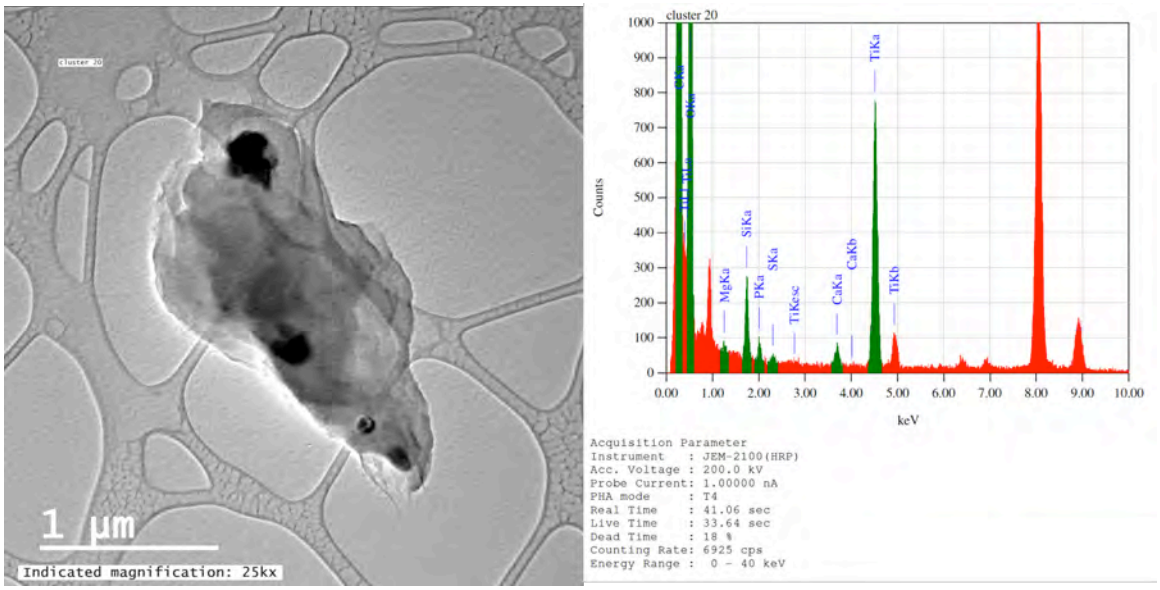

Figure 3.8 TEM image and EDS spectra of a Ti-rich dust particle collected in Location 1 (Image 18, ref. Table B.4, Appendix B).

In the remote Location 3, no dust particles could be found on the TEM sample. However, many DPM agglomerates were observed (e.g., Figure 3.8). While the DPM again ranged in size, qualitatively it appeared to be larger in this location than in Location 1 (see Table B.4 in Appendix B). This may be related to the specific source(s) of DPM. While Location 3 is expected to be influenced to some extent by emissions from the production area, a diesel water pump was also running near the sampling location. Some evidence of the high humidity in this area was also seen during the TEM work. In some cases, very small spots indicative of evaporated water drops were observed around the DPM clusters (e.g., Figure 3.9). In two instances, Cu-rich particles were observed with DPM surrounding them (e.g., Figure 3.10). Given that significant copper content is not expected in dust generated in the mine, these particles are suspected to be copper salts precipitated following deposition of DPM agglomerates with condensed water on the copper TEM grid. Additional TEM images from Location 3 can be found in Figures B.57 – B.69, Appendix B.

In Location 2 near the primary crusher and main exhaust, both DPM and dust particles were found on the TEM samples. On the samples with the lightest particle loading, only DPM particles could generally be observed – and one sample, no particles were found, which may mean that something went wrong during sample collection. Two samples were considered densely loaded, and most of the dust particles were found in these. Like in Location 3, some very large DPM clusters were found; and relatively fewer very small DPM particles were found here versus the other locations. Notably, all dust particles selected for analysis were observed to have attached DPM. The DPM appeared to completely surround the dust particle in some cases (e.g., Figure 3.11, but it was only observed on particle edges in others (e.g., Figures 3.12). EDS spectra indicated that the dust particles were of several different mineral types, including carbonates and alumino-silicates. Some of the particles were in the submicron range, but others were not. Due to the lower limits on magnification in the TEM,

larger particles could not be measured. Additional TEM images from Location 2 can be found in Figures B.16 – B.56, Appendix B.

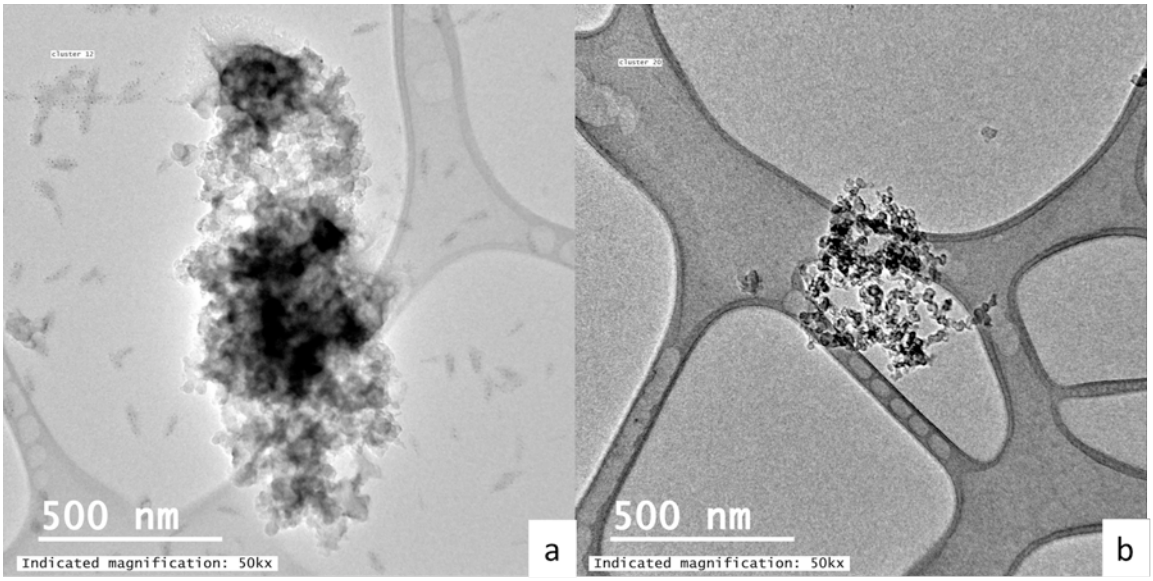

Figure 3.9 TEM images of DPM agglomerates collected in Location 3 (a - Image 63; b – Image 65, ref. Table B.4, Appendix B).

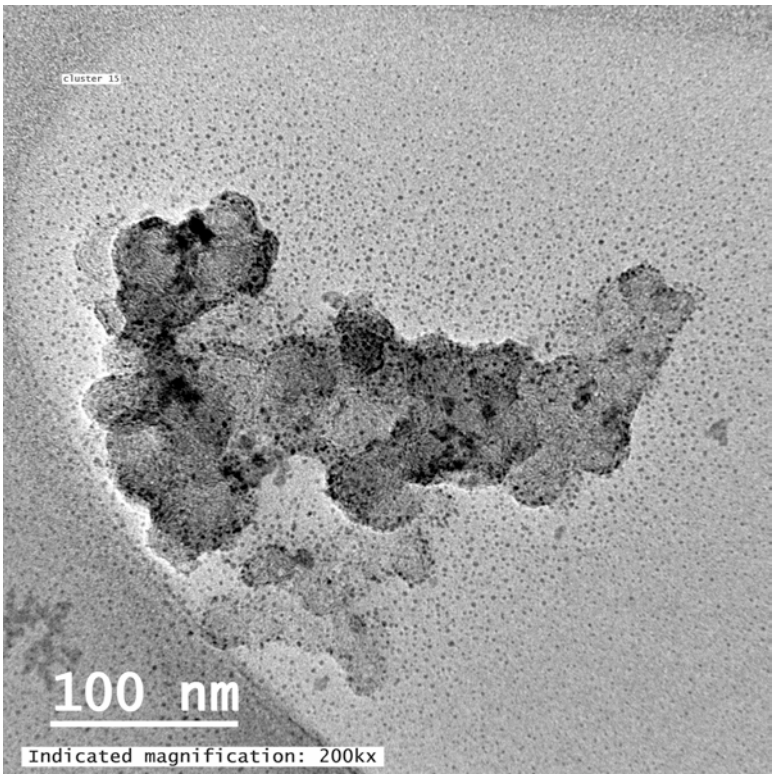

Figure 3.10 TEM image of DPM from Location 3 (Image 70, ref. Table B.4, Appendix B). The small dark spots are interpreted as evaporated water droplets containing precipitated Cu.

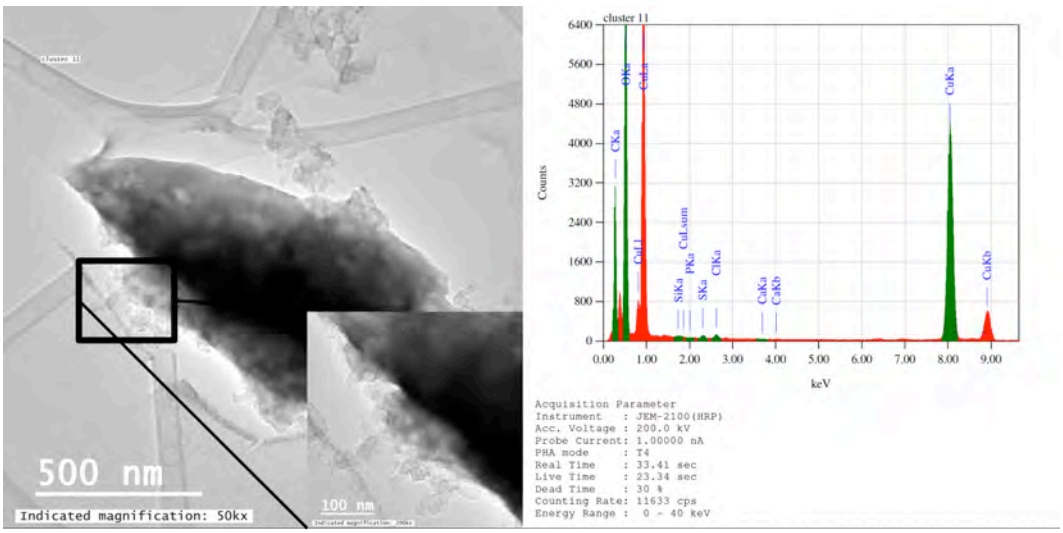

Figure 3.11 TEM image and EDS spectra of a Cu-rich particle with DPM surrounding it from Location 3 (Image 79, ref. Table B.4, Appendix B).

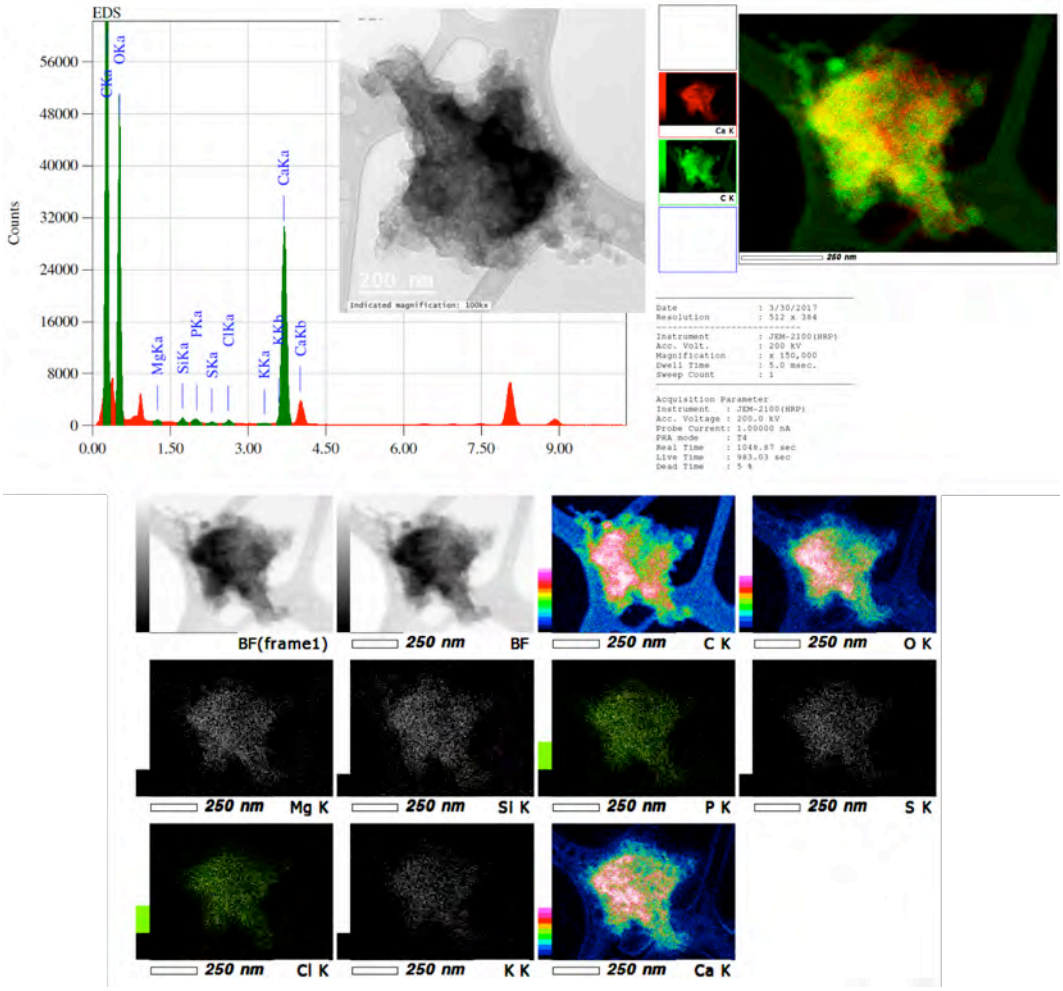

Figure 3.12 TEM image, EDS spectra and element map of DPM surrounding a carbonate dust particle from Location 2 (Image 58, ref. Table B.4, Appendix B).

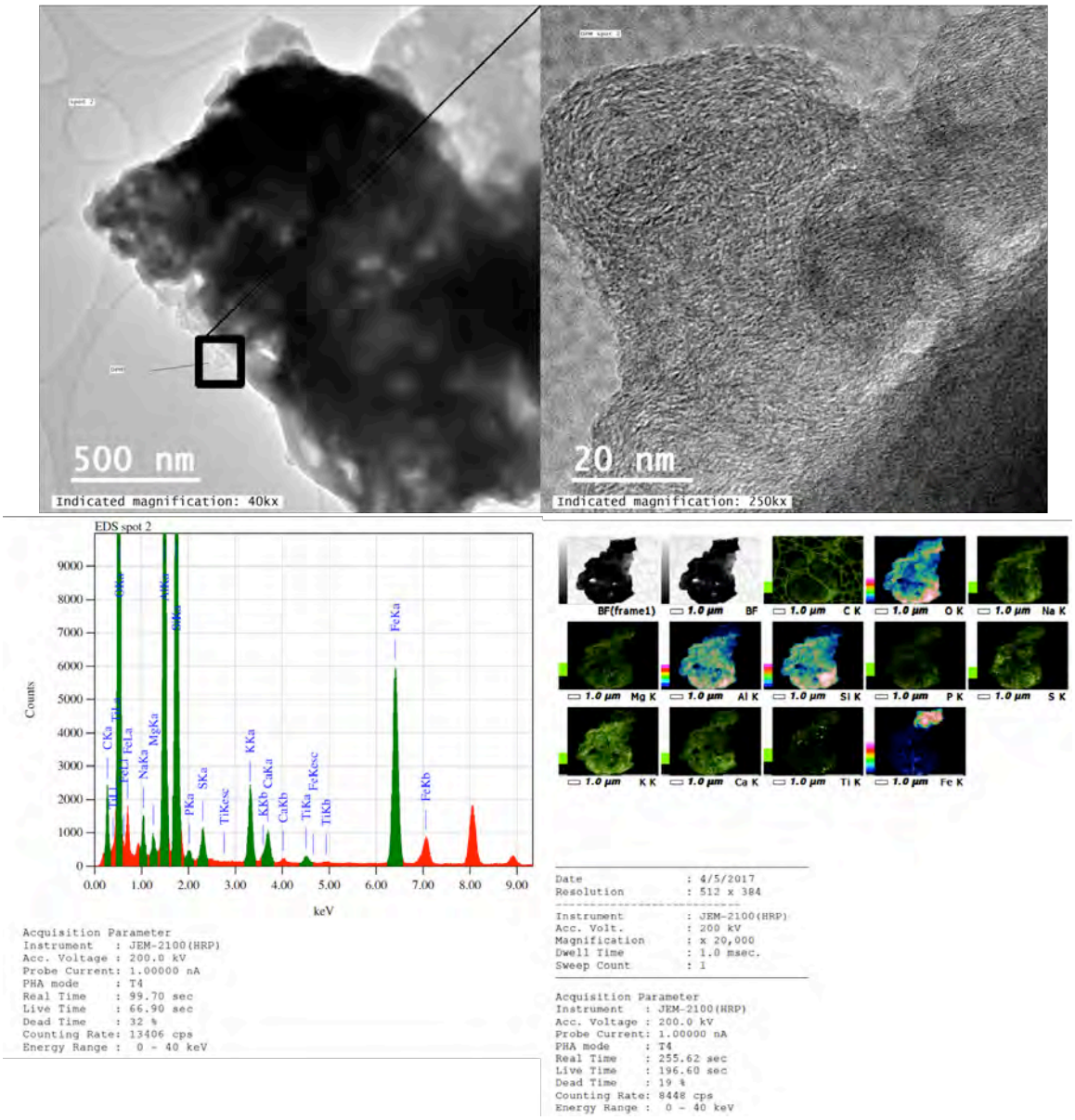

Figure 3.13 TEM image, EDS spectra and element map of DPM on the edges of a large alumino-silicate dust particle from Location 2 (Image 62, ref. Table B.4, Appendix B).

4. Conclusions

Pairing mass measurements of EC in different size fractions with microscopy analysis, this study sought to investigate the possibility of DPM and dust attachment in an underground stone mine. Such attachment may have implications for both DPM sampling and exposure outcomes. Based on the 5040 sample results, a significant fraction of EC was not observed to occur in the supramicron range, but the TEM results did confirm that DPM and dust can attach to some extent in the mine atmosphere. It is important to note that the TEM work

undertaken here was exploratory in that the aim was to see if attachment could be observed, rather than an attempt to quantify its frequency. However, the strategy employed for the current study could be adapted for future investigations.

While not a primary focus of this study, the findings presented here also suggest that respirable EC, as opposed to submicron EC or TC, may be an appropriate surrogate for DPM monitoring in mines where mineral dust interferences should be dominated by carbonates. This could allow for accurate accounting of DPM that may otherwise be missed by submicron sampling, and effective removal of carbonates by sample acidification was demonstrated here.

5. Acknowledgements

The authors would like to thank CDC/NIOSH (Contract Number: 200-2014-59646) for funding the work. Sincere thanks also to Shawn Vanderslice of NIOSH for sample analysis, Chris Winkler of Virginia Tech ICTAS-NCFL for assistance with TEM work, Chelsea Barrett for helping with equipment setup, and all the personnel at the study mine for their interest and support.

6. References

Abdul-Khalek, I.S., Kittelson, D.B., Graskow, B.R., Wei, Q. and Brear, F. (1998). Diesel Exhaust Particle Size: Measurement Issues and Trends. *SAE Technical Paper Series*.

Birch, M. E. (2016). Monitoring of Diesel Particulate Exhaust in the Workplace. *NIOSH Manual of Analytical Methods (NMAM)*, 5th Edition.

Bukowiecki, N., Kittelson, D.B., Watts, W.F., Burtscher, H., Weingartner, E., Baltensperger, U. (2002). Real-time characterization of ultrafine and accumulation mode particles in ambient combustion aerosols. *Journal of Aerosol Science*, 33, 1139-1154.

Bugarski, Aleksandar D., Janisko, Samuel J., Cauda, Emanuele G., Noll, James D. and Mischler, Steven E. (2011). Diesel Aerosols and Gases in Underground Mines: Guide to Exposure Assessment and Control. *Report of Investigations*. Publication No. 2012-101.

Bugarski, A., Schnakenberg, G., Hummer, J., Cauda, E., Janisko, S., & Patts, L. (2009). Effects of diesel exhaust aftertreatment devices on concentrations and size distribution of aerosols in underground mine air. *Environmental Science & Technology*, 43(17), 6737-6743. doi:10.1021/es9006355

Burtscher, H. (2005). Physical characterization of particulate emissions from diesel engines: A review. *Journal of Aerosol Science*, 36(7), 896-932. doi:10.1016/j.jaerosci.2004.12.001

Cantrell, B. K., & Rubow, K. L. (1991) Development of personal diesel aerosol sampler design and performance criteria. *Mining Engineering*, 43(2), 232-236.

Cantrell, B. K., & Rubow, K. L. (1992). Diesel exhaust aerosol measurements in underground metal and nonmetal mines. USBM Diesels in Underground Mines Information and Technology Transfer Seminar, Minneapolis, MN, 18-18.

Cantrell, B. K., & Watts, W. F. (1997). Diesel exhaust aerosol: Review of occupational exposure. Applied Occupational and Environmental Hygiene, 12(12), 1019-1019.

Cauda, Emanuele, Miller, Art, Stabile, Luca and Buonanno, Giorgio. (2014) Characterizing the exposure of miners to mixed aerosols. *Proceedings of the International Conference on Atmospheric Dust*. Taranto, Italy, June 1-6, 2014.

Cauda, Emanuele, Sheehan, Maura, Gussman, Robert, Kenny, Lee and Volkwein, Jon. (2014). An Evaluation of Sharp Cut Cyclones for Sampling Diesel Particulate Matter Aerosol in the Presence of Respirable Dust. *Annals of Occupational Hygiene,* Vol 58., No. 8, 995-1005.

Chou, Charles C.-K., Chen, TZE-Kuang, Huang, Shu-Hui, Liu, Shaw C. (2003). Radiative Absorption Capability of Asian Dust with Black Carbon Contamination. *Geophysical Research Letters*, 30(12), 1616.

Haney, Robert A. (2000). Sampling and Inferences For Diesel Particulate Matter in Underground Metal and Nonmetal Mines. Retrieved from http://www.msha.gov/S&HINFO/TECHRPT/diesel/haneyimvc7.pdf

Ishiguro, T., Takatori, Y., & Akihama, K. (1997). Microstructure of diesel soot particles probed by electron microscopy: First observation of inner core and outer shell. *Combustion and Flame*, 108(1), 231-234.

Kittelson, D. (1998). Engines and nanoparticles: A review. Journal of Aerosol Science, 29(5-6), 575-588.

Kissell, F., & Sacks, H. (2002). Inaccuracy of area sampling for measuring the dust exposure of mining machine operators in coal mines. *Mining Engineering*, 54(2), 33-39.

Karagianes, M., palmer, R., & Busch, R. (1981). effects of inhaled diesel emissions and coal-dust in rats. *American Industrial Hygiene Association Journal*, 42(5), 382-391.

Lee, J., Goto, Y., and Odaka, M., (2002) Measurement of the Diesel Exhaust Particle Reduction Effect and Particle Size Distribution in a Transient Cycle Mode with an Installed Diesel Particulate Filter (DPF), *SAE Technical Paper 2002-01-1005*, doi:10.4271/2002-01-1005.

Maricq, Matti M. (2007). Chemical characterization of particulate emissions from diesel engines: A review. *Journal of Aerosol Science*, 38(11), 1079-1118. doi:10.1016/j.jaerosci.2007.08.001

Maximilien, Debia, Couture, Caroline, Njanga, Pierre-Eric, Neesham-Grenon, Eve, Lachapelle, Guillaume, Coulombe, Hugo, Hallé, Stéphane, Aubin, Simon (2017). Diesel engine exhaust exposures in two underground mines, *International Journal of Mining Science and Technology*, 267(4), 641-645, ISSN 2095-2686, http://dx.doi.org/10.1016/j.ijmst.2017.05.011.

Miller, A., Frey, G., King, G., & Sunderman, C. (2010). A handheld electrostatic precipitator for sampling airborne particles and nanoparticles. *Aerosol Science and Technology*, 44(6), 417-427.

National Institute of Occupational Safety and Health (NIOSH). (2016). Limestone. *NIOSH Pocket Guide to Chemical Hazards.* Retrieved from: https://www.cdc.gov/niosh/npg/npgd0369.html.

Noll, J.D., Bugarski, A.D., Patts, L.D., Mischler, S.E. and McWilliams, L. (2007). Relationship between elemental carbon, total carbon, and diesel particulate matter in several underground Metal/Non-metal mines. *Environmental Science & Technology*, 41(3), 710-716. doi:10.1021/es061556a

Noll J.D., Janisko S., Mischler S.E. (2013). Real-time diesel particulate monitor for underground mines. *Analytical Methods*; 5(12), 2954–63.

Noll J.D., Mischler S.E., Schnakenberg Jr., G.H., Bugarski, A.D. (2006). Measuring Diesel Particulate Matter in Underground Mines Using Sub Micron Elemental Carbon as a Surrogate. *Proceedings for the 11th US North American Mine Ventilation Symposium*. State College, Pennsylvania: Vol. 2006, pp. 105–110.

Noll, J.D., Timko, R. J., McWilliams, L., Hall, P., & Haney, R. (2005). Sampling results of the improved SKC diesel particulate matter cassette. *Journal of Occupational and Environmental Hygiene*, 2(1), 29-37. doi:10.1080/15459620590900320

Noll, J., Gilles, S., Wu, H. W., & Rubinstein, E. (2015). The relationship between elemental carbon and diesel particulate matter in underground Metal/Nonmetal mines in the United States and coal mines in Australia. *Journal of Occupational and Environmental Hygiene*, 12(3), 205-211. doi:10.1080/15459624.2014.960577

Pietikainen, Mari, Oravisjarvi, Kati, Rautio, Arja, Voutilainen, Arto, Ruuskanen, Juhani, and Keiski, Riitta L. (2009). Exposure assessment of particulates of diesel and natural gas fueled buses *in silico*. *Science of the Total Environment*. 408, 163-168.

U.S. Department of Labor Mine Safety and Health Administration (MSHA). (2008). Diesel Particulate Matter Exposure of Underground Metal and Nonmetal Miners. Rules and Regulations, Federal Register 30 CFR Part 57. 73(98), 29058-29060. Retrieved from: https://arlweb.msha.gov/REGS/FEDREG/NOTICES/2008Misc/E8-11329.asp

Vermeulen, Roel, Coble, Joseph B., Yereb, Daniel, Lubin, Jay H. Blair, Aaron, Portengen, Lutzen, Stewart, Patricia A., Attfield, Michael, Silverman, Debra T. (2010). The Diesel Exhaust in Miners Study: III. Interrelations between Respirable Elemental Carbon and Gaseous and Particulate Components of Diesel Exhaust derived from Area Sampling in Underground Non-metal Mining Facilities. *Annals of Occupational Hygiene.* Vol. 54, No. 7, pp. 762-773.

Vinson, R., Volkwein, J., & McWilliams, L. (2007). Determining the spatial variability of personal sampler inlet locations. *Journal of Occupational and Environmental Hygiene*, 4(9), 708-714. doi:10.1080/15459620701540618.

Appendix A. Chapter 2 Supplemental Data

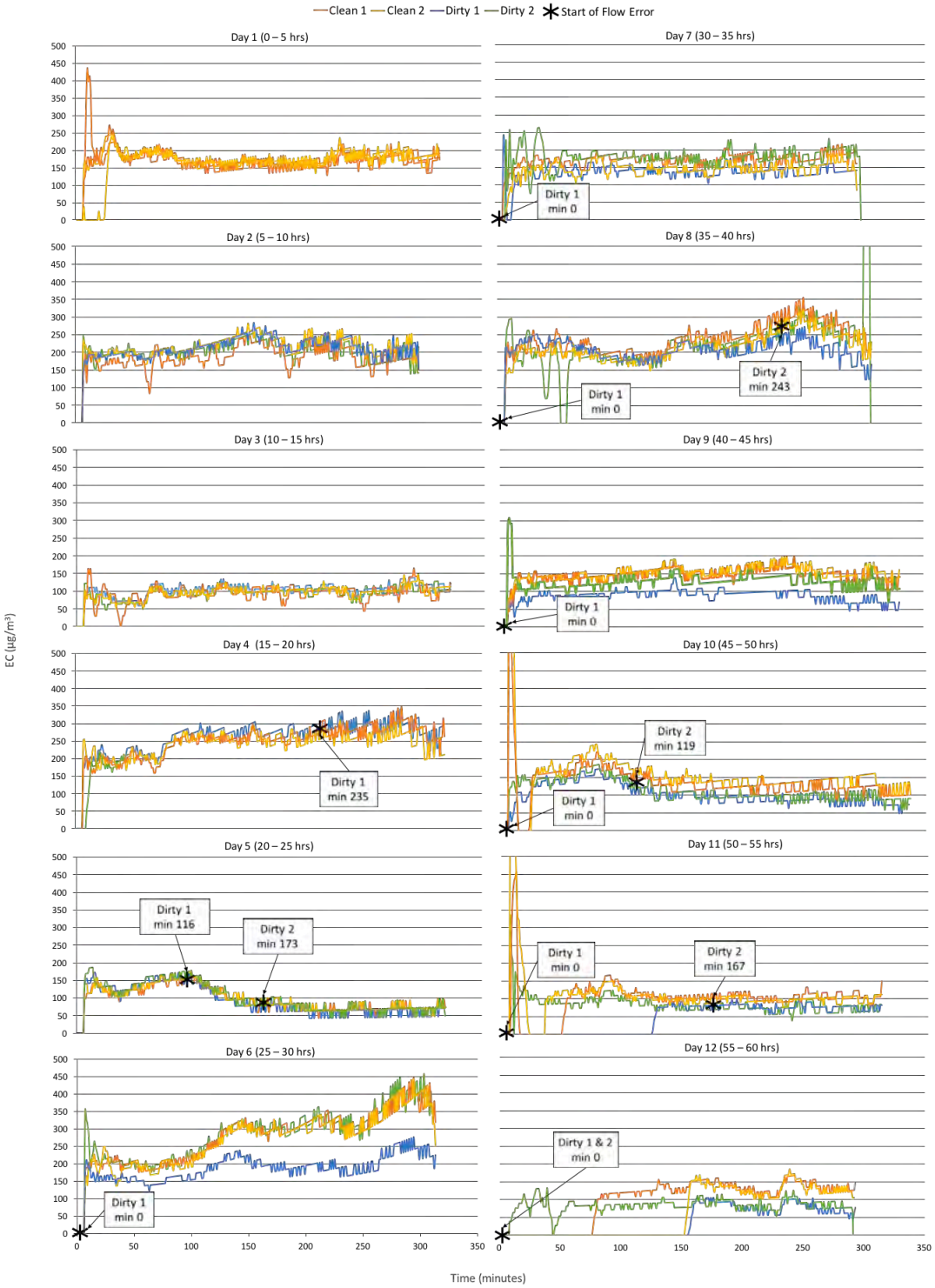

Figure A.2 Time series data showing mass EC concentration values (as 5 minute rolling average) measured by the Airtecs. These data have not been corrected for the standard Airtec flow rate of 1.7 LPM. Times when flow errors were registered on the Airtecs are denoted on each plot.

Appendix B. Chapter 3 Supplemental Data

Table B.1 Number of particles per bin between 1 and 10μm as measured by OPS in each monitoring location.

Location	1	2	3
Midpoint Bin Diameter (μm)	**Average No./Bin**		
1.007	5.334	10.400	1.406
1.254	2.089	4.732	0.479
1.562	2.059	5.096	0.444
1.944	2.589	7.695	0.399
2.421	1.965	7.138	0.206
3.014	1.245	5.120	0.103
3.752	0.867	3.820	0.063
4.672	0.633	2.971	0.043
5.816	0.419	2.083	0.031
7.241	0.300	1.590	0.028
9.015	0.199	1.182	0.027

Table B.2 Average EC before and after acidification from each sample location with a 95% confidence interval (CI) and relative standard deviation (RSD).

		EC Before Acidification			EC After Acidification		
Location	**Size Fraction**	**AVG (μg/m3)**	**95% CI**	**RSD (%)**	**AVG (μg/m3)**	**95% CI**	**RSD (%)**
1	Submicron	125.01	18.47	13.05	125.79	18.69	13.13
	Respirable	113.41	22.82	17.78	117.36	25.05	18.87
	Total	137.17	25.39	16.36	126.63	23.86	16.65
2	Submicron	67.84	11.41	14.86	79.66	12.63	14.01
	Respirable	98.57	12.26	10.99	85.26	22.48	23.30
	Total	70.23	N/A	N/A	66.17	N/A	N/A
3	Submicron	15.61	9.65	54.63	14.38	11.08	68.09
	Respirable	25.22	4.63	16.23	24.57	N/A	N/A
	Total	36.73	9.35	22.49	21.36	6.51	26.93

N/A = one sample out of the triplicate samples was damaged or unusable.

Table B.3 Average TC before and after acidification from each sample location with a 95% confidence interval (CI) and relative standard deviation (RSD).

		TC Before Acidification			TC After Acidification		
Location	**Size Fraction**	**AVG (µg/m3)**	**95% CI**	**RSD (%)**	**AVG (µg/m3)**	**95% CI**	**RSD (%)**
1	Submicron	153.73	37.95	21.81	147.29	22.28	13.37
	Respirable	134.62	16.18	10.62	140.03	19.94	12.58
	Total	164.01	32.72	17.63	136.50	36.46	23.60
2	Submicron	88.00	21.84	21.93	94.73	27.25	25.42
	Respirable	120.33	7.99	5.87	110.23	13.67	10.96
	Total	235.88	N/A	N/A	95.63	N/A	N/A
3	Submicron	13.08	16.14	109.06	28.25	7.97	24.93
	Respirable	23.27	2.02	7.68	30.37	N/A	N/A
	Total	43.97	24.22	48.68	32.08	11.99	33.04

N/A = one sample out of the triplicate samples was damaged or unusable.

Table B.4. Individual particle information from TEM images and EDS spectra analysis. Size of each particle is measured at its longest observable length.

Location	Image No.	Classification	Size	Histogram of DPM Size
1	1	DPM	0.125	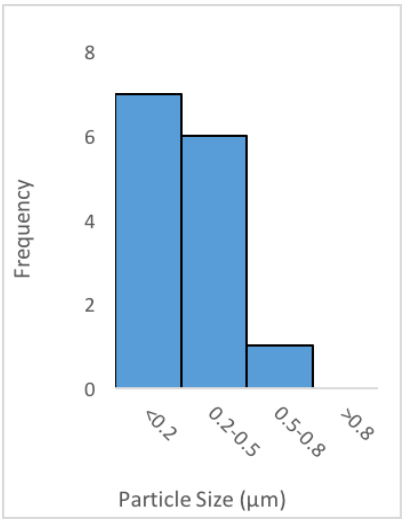
	2	DPM	0.525	
	3	DPM	0.5	
	4	DPM	0.1	
	5	DPM	0.2	
	6	DPM	0.15	
	7	DPM	0.1	
	8	DPM	0.2	
	9	DPM	0.125	
	10	DPM	0.05	
	11	DPM	0.4	
	12	DPM	0.4	
	13	DPM	0.3	
	14	DPM	0.1	
	15	Dust (Ca/Mg carbonate)	0.1	
	16	Dust (Ca/Mg carbonate)	0.1	
	17	Dust (possibly silica)	4.0	
	18	Dust (Ti rich)	2.0	
	19	Dust (Ti rich)	0.1	

Table B.4. Individual particle information from TEM images and EDS spectra analysis. Size of each particle is measured at its longest observable length.

Location	Image No.	Classification	Size	Histogram of DPM Size
2	20	multiple DPM clusters	0.5	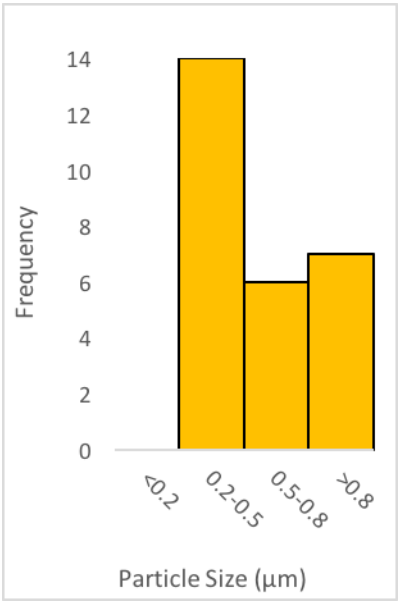
	21	DPM on dust (unidentified)	1.5	
	22	multiple DPM clusters	0.5	
	23	DPM on dust (Ca carbonate)	1.0	
	24	DPM on dust (unidentified)	1.0	
	25	multiple DPM clusters	0.5	
	26	DPM on dust (unidentified)	0.05	
	27	DPM on dust (Ca carbonate)	4	
	28	DPM on dust (Ca/Mg Carbonate)	1.5	
	29	DPM on dust (Al Silicate)	0.6	
	30	DPM on dust (Na rich)	1.5	
	31	multiple DPM clusters	1.0	
	32	DPM	1.5	
	33	DPM	1.25	
	34	DPM	0.6	
	35	DPM	1.75	
	36	DPM	1.5	
	37	DPM	1.0	
	38	DPM	0.4	
	39	DPM	0.8	
	40	DPM	0.3	
	41	DPM	0.8	
	42	DPM	0.5	
	43	DPM	0.25	
	44	DPM	0.4	
	45	DPM	0.4	
	46	DPM	0.6	
	47	DPM	0.6	
	48	DPM	0.2	
	49	DPM	0.2	
	50	DPM	0.2	
	51	DPM	0.3	
	52	DPM	0.3	
	53	DPM on dust (unidentified)	0.6	
	54	DPM on dust (unidentified)	0.4	
	55	DPM on dust (Ca carbonate)	0.4	
	56	DPM on dust (unidentified)	0.6	
	57	DPM on dust (Ca carbonate)	0.8	
	58	DPM on dust (Ca carbonate)	0.7	
	59	DPM on dust (Ca carbonate)	0.4	
	60	DPM	0.6	
	61	DPM	1.25	
	62	DPM on dust (Al/Fe silicate)	6.0	

Table B.4. Individual particle information from TEM images and EDS spectra analysis. Size of each particle is measured at its longest observable length.

Location	Image No.	Classification	Size	Histogram of DPM Size
3	63	DPM	1.25	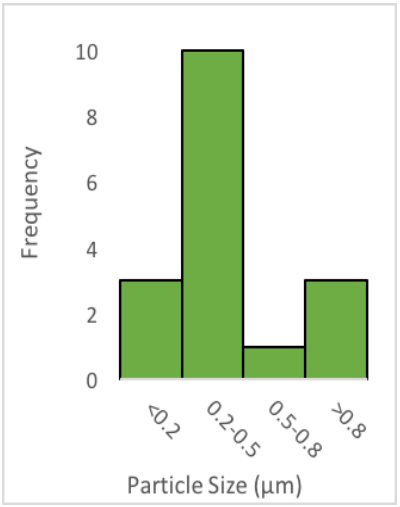
	64	DPM	1.5	
	65	DPM	0.5	
	66	DPM	0.5	
	67	DPM	1.0	
	68	DPM	0.5	
	69	DPM	0.2	
	70	DPM	0.3	
	71	DPM	0.3	
	72	DPM	0.4	
	73	DPM	0.25	
	74	DPM	0.1	
	75	DPM	0.1	
	76	DPM	0.1	
	77	DPM	0.2	
	78	DPM	0.525	
	79	DPM	0.2	

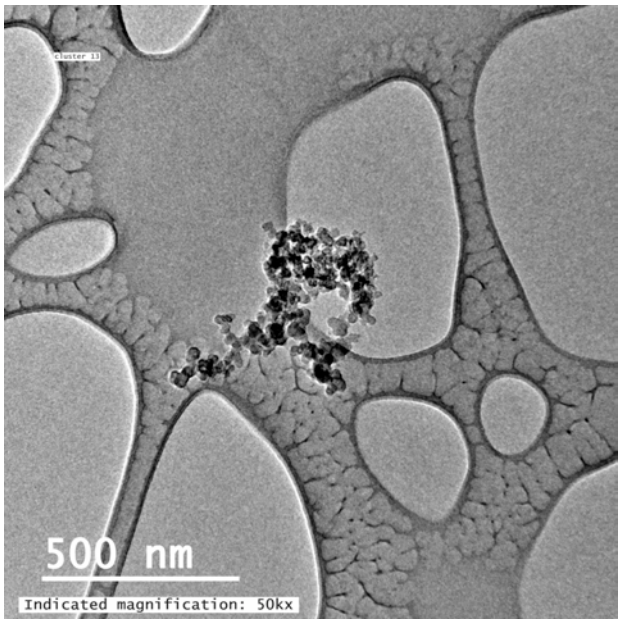

Figure B.1 TEM image of DPM from Location 1 (Image 2, ref. Table B.4).

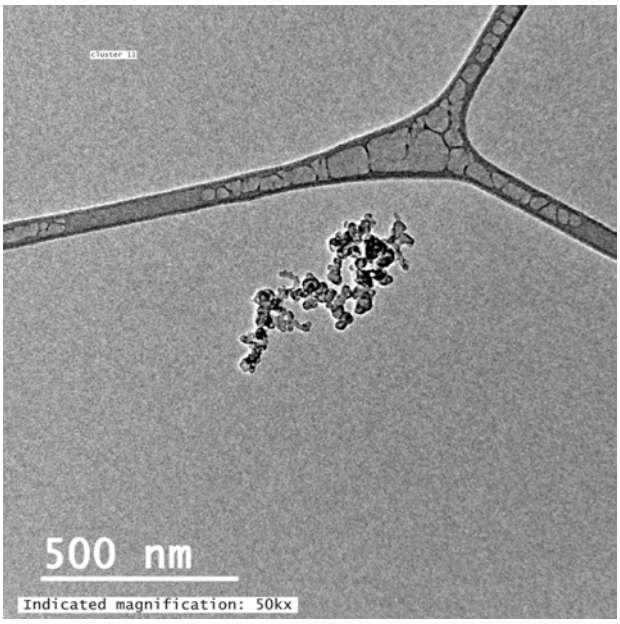

Figure B.2 TEM image of DPM from Location 1 (Image 3, ref. Table B.4).

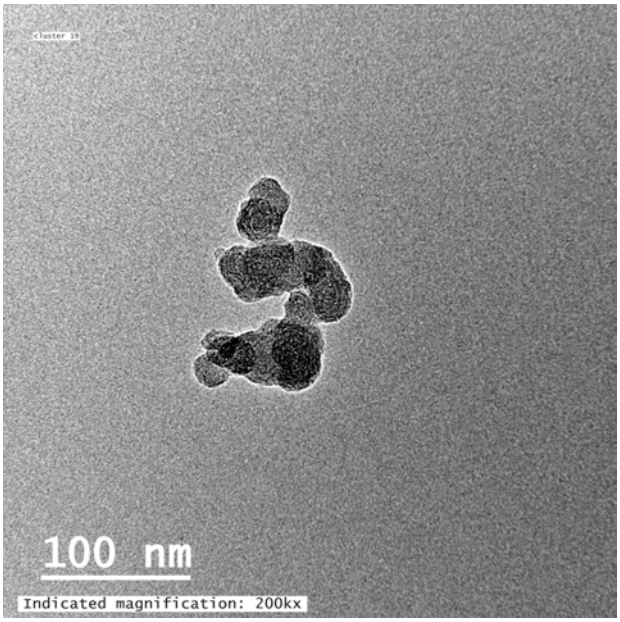

Figure B.3 TEM image of DPM from Location 1 (Image 4, ref. Table B.4).

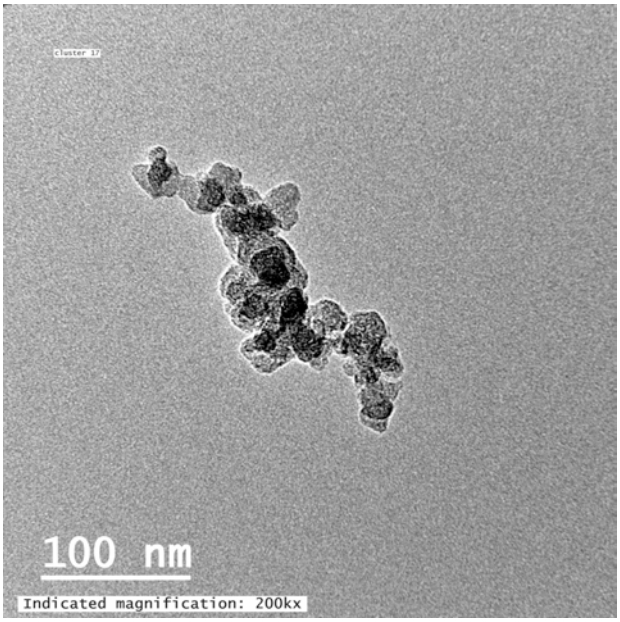

Figure B.4 TEM image of DPM from Location 1 (Image 5, ref. Table B.4).

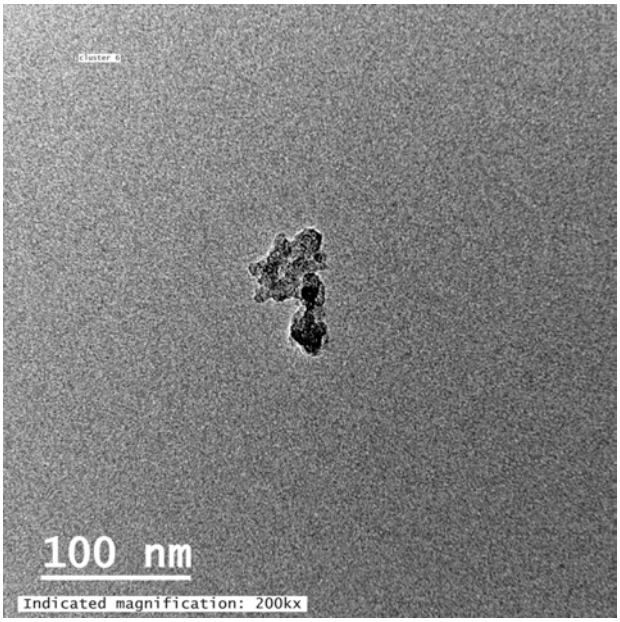

Figure B.5 TEM image of DPM from Location 1 (Image 7, ref. Table B.4).

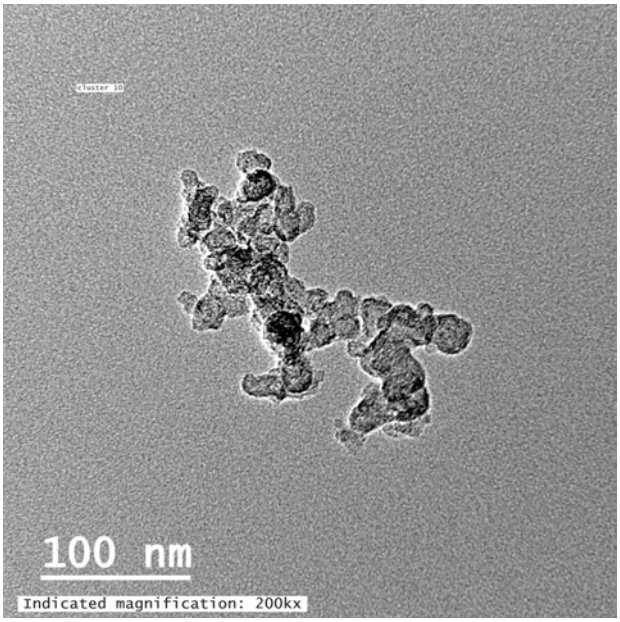

Figure B.6 TEM image of DPM from Location 1 (Image 8, ref. Table B.4).

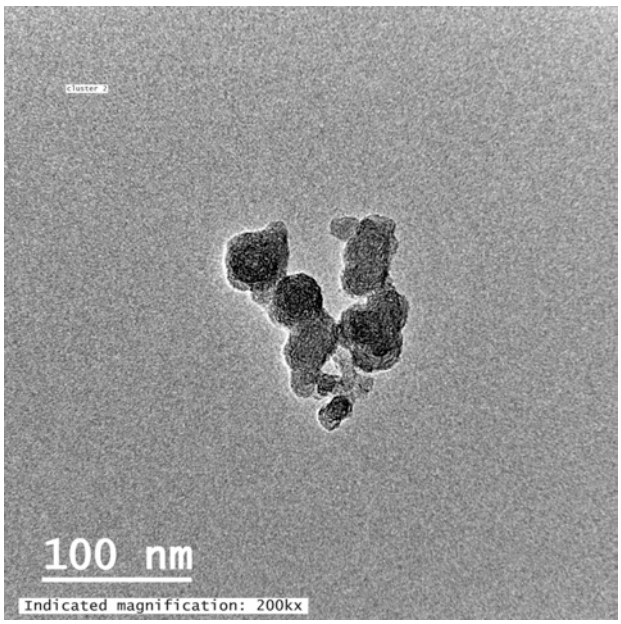

Figure B.7 TEM image of DPM from Location 1 (Image 9, ref. Table B.4).

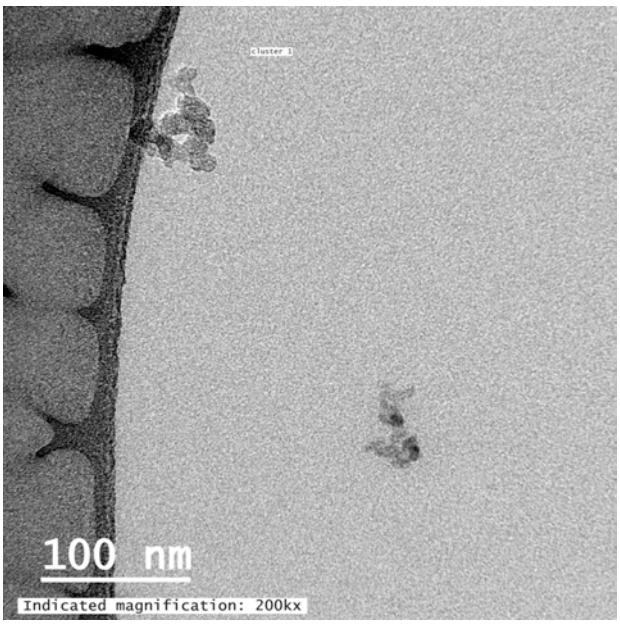

Figure B.8 TEM image of two DPM clusters from Location 1 (Image 11, ref. Table B.4).

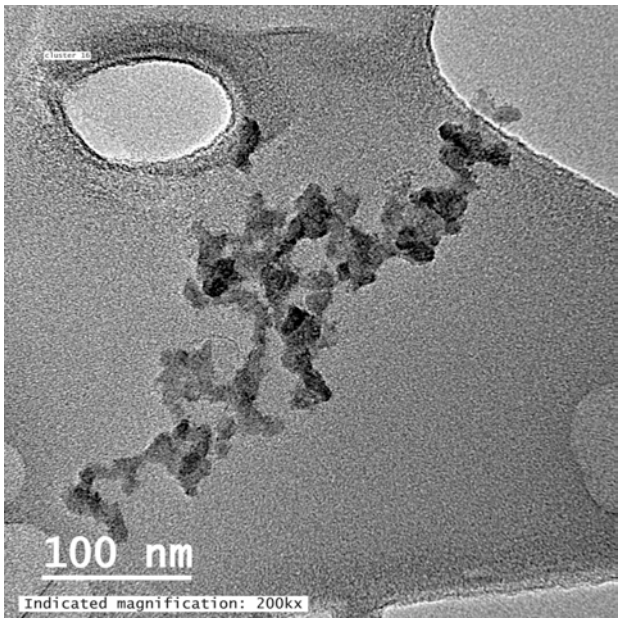

Figure B.9 TEM image of DPM from Location 1 (Image 12, ref. Table B.4).

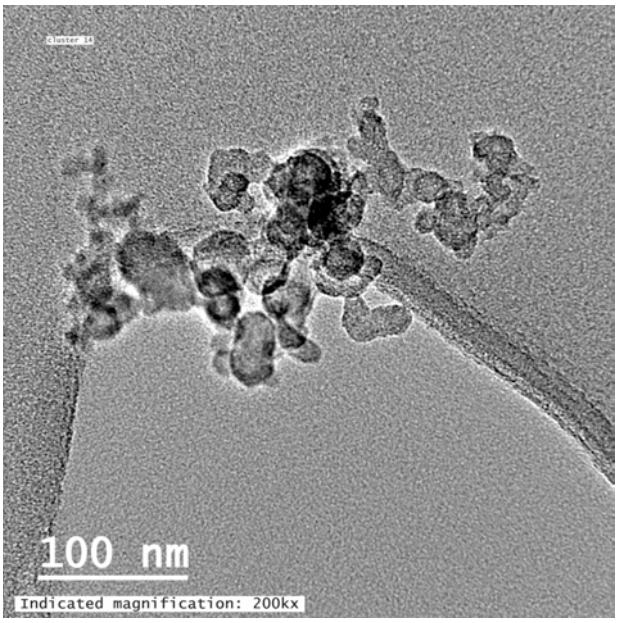

Figure B.10 TEM image of DPM from Location 1 (Image 13, ref. Table B.4).

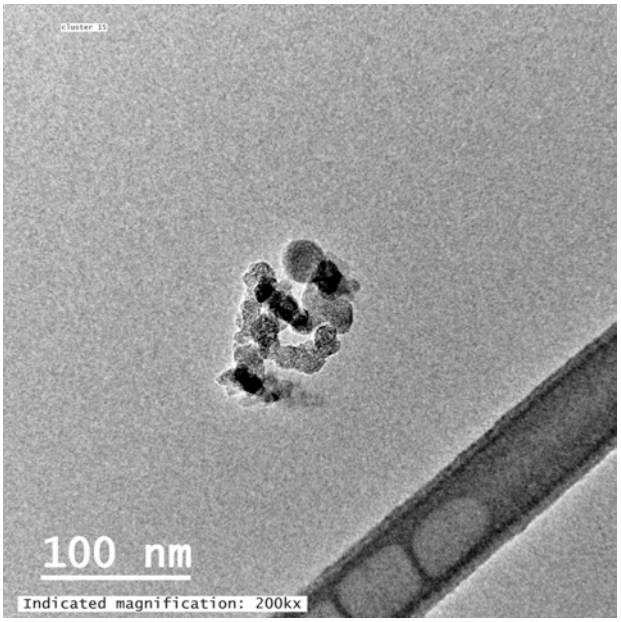

Figure B.11 TEM image of DPM from Location 1 (Image 14, ref. Table B.4).

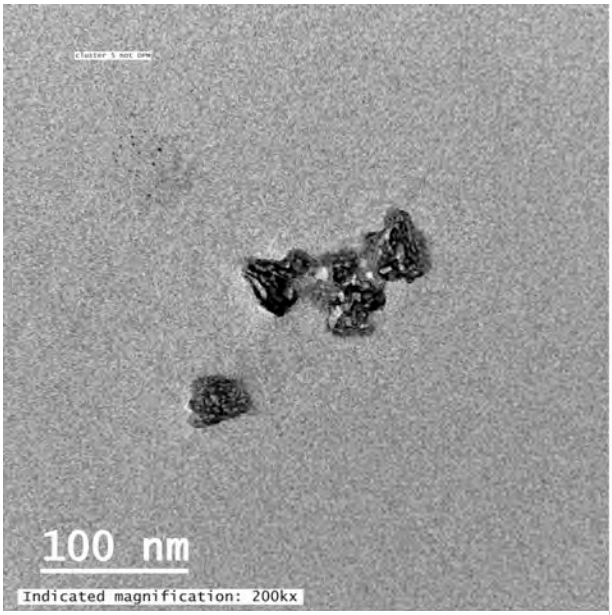

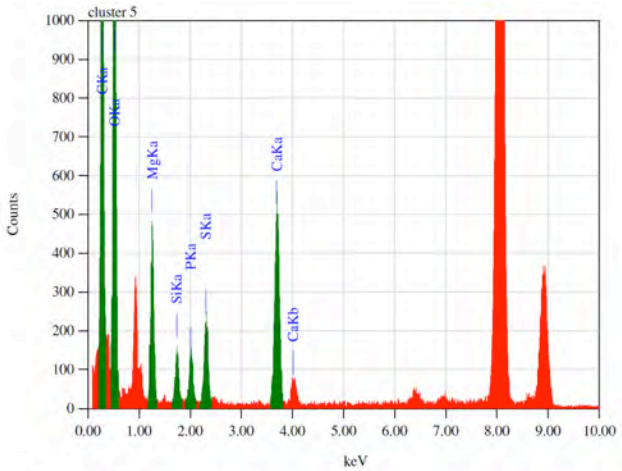


```
Acquisition Parameter
Instrument    : JEM-2100(HRP)
Acc. Voltage  : 200.0 kV
Probe Current: 1.00000 nA
PHA mode      : T4
Real Time     : 82.33 sec
Live Time     : 78.42 sec
Dead Time     : 4 %
Counting Rate: 1441 cps
Energy Range :  0 - 40 keV
```

Figure B.12 TEM image of Ca/Mg carbonate dust particle and EDS spectra from Location 1 (Image 15, ref. Table B.4).

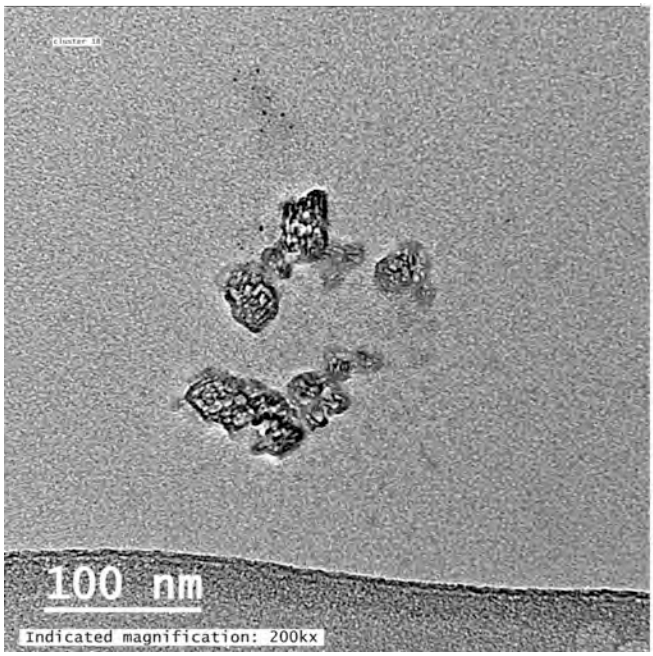

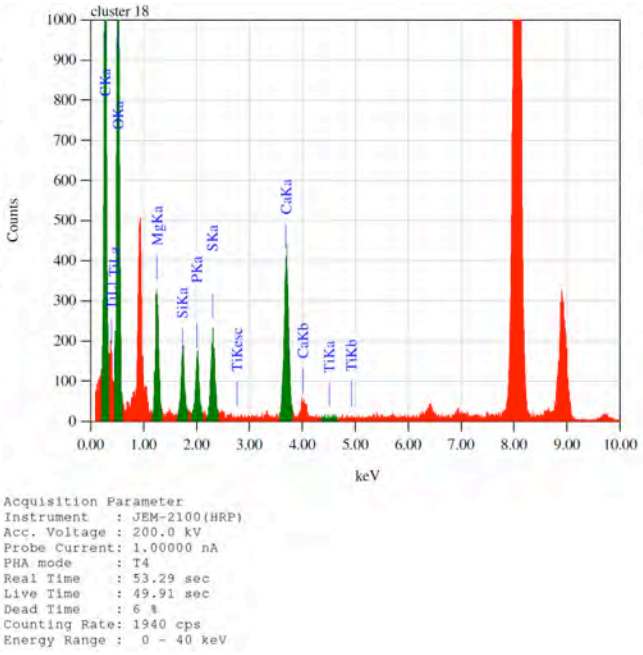

Figure B.13 TEM image of Ca/Mg carbonate dust particle and EDS spectra from Location 1 (Image 16, ref. Table B.4).

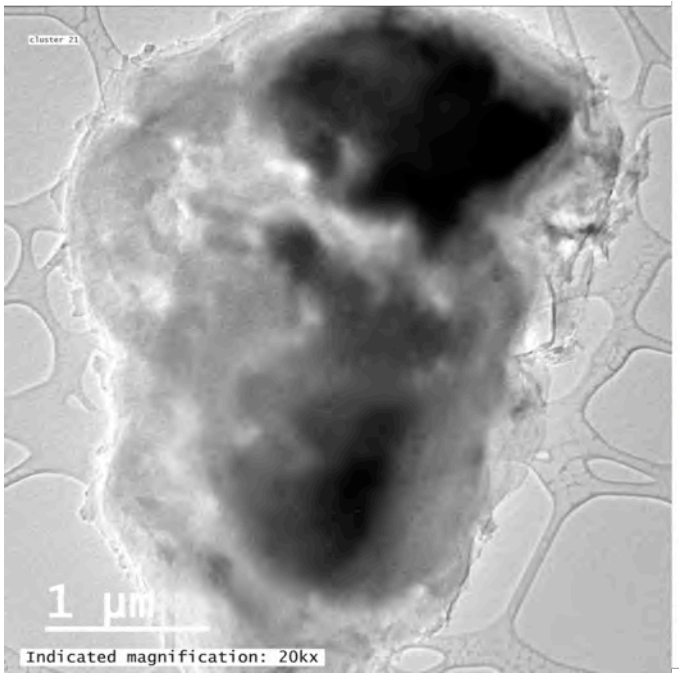

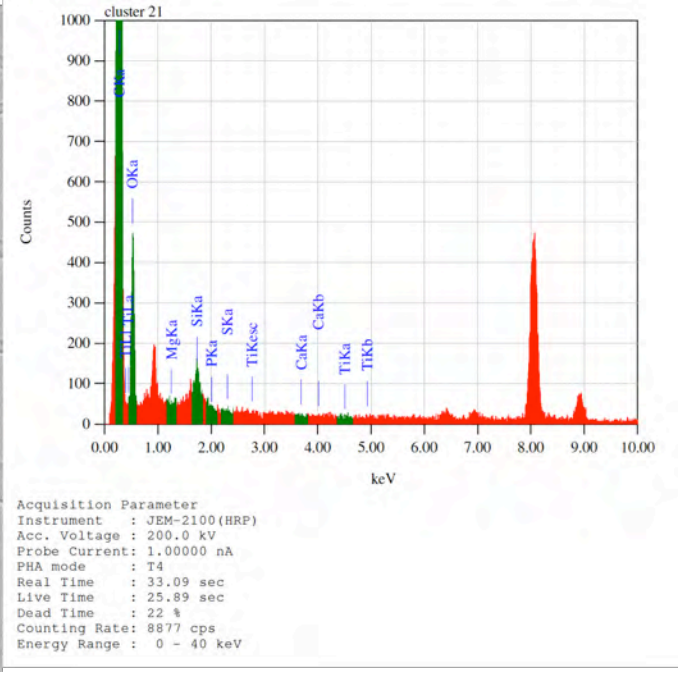

Figure B.14 TEM image of possibly silica dust particle and EDS spectra from Location 1 (Image 17, ref. Table B.4).

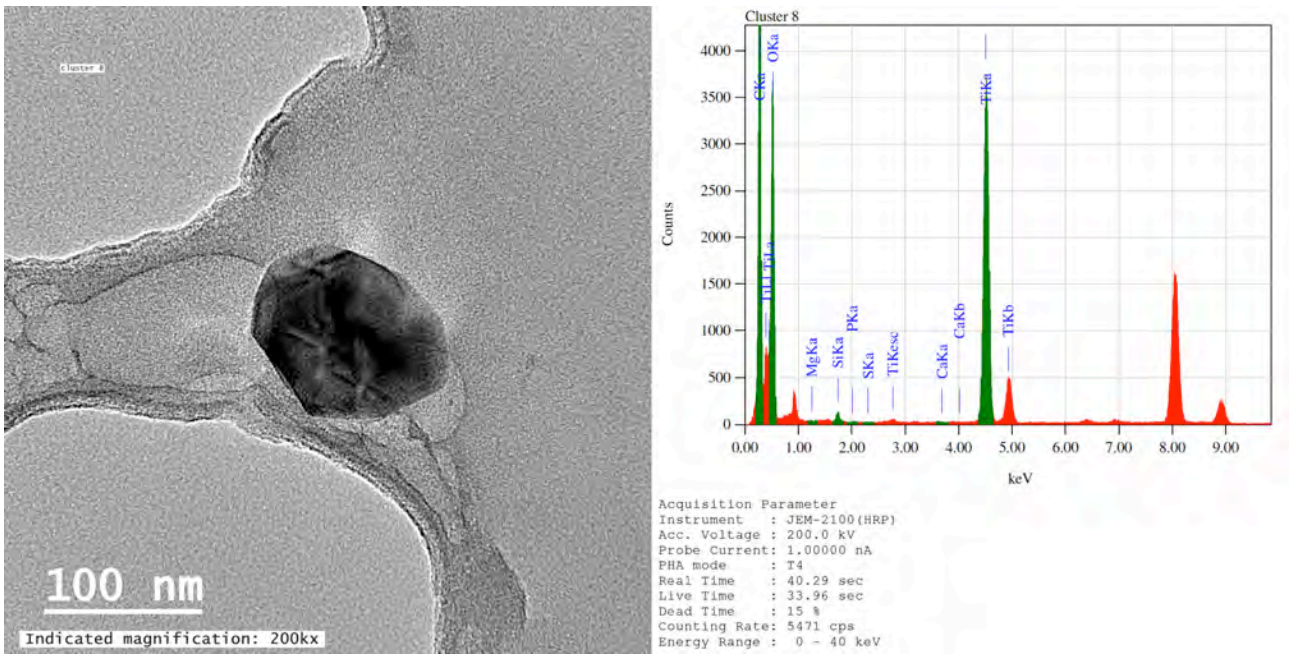

Figure B.15 TEM image of Ti-rich dust particle and EDS spectra from Location 1 (Image 19, ref. Table B.4).

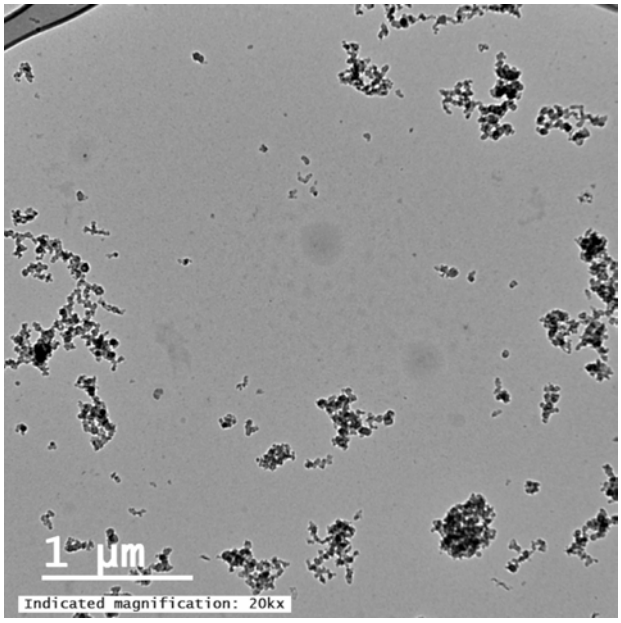

Figure B.16 TEM image of multiple DPM clusters from Location 2 (Image 20, ref. Table B.4).

Figure B.17 TEM image of DPM and unidentified dust co-occurring from Location 2 (Image 21, ref. Table B.4). EDX was not completed on this sample.

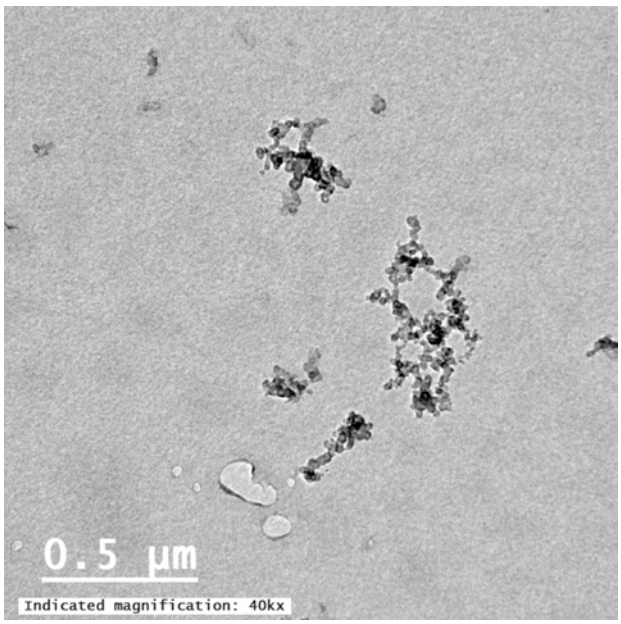

Figure B.18 TEM image of multiple DPM clusters from Location 2 (Image 22, ref. Table B.4).

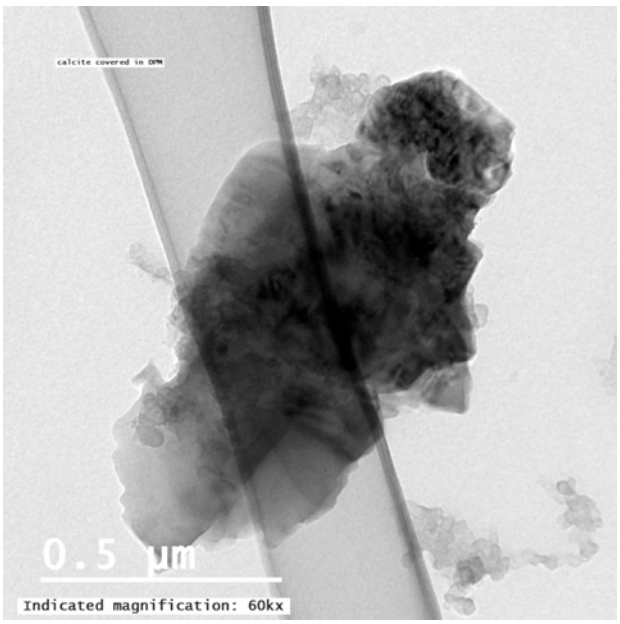

Figure B.19 TEM image of DPM and unidentified dust co-occurring from Location 2 (Image 23, ref. Table B.4). EDX was not completed on this sample.

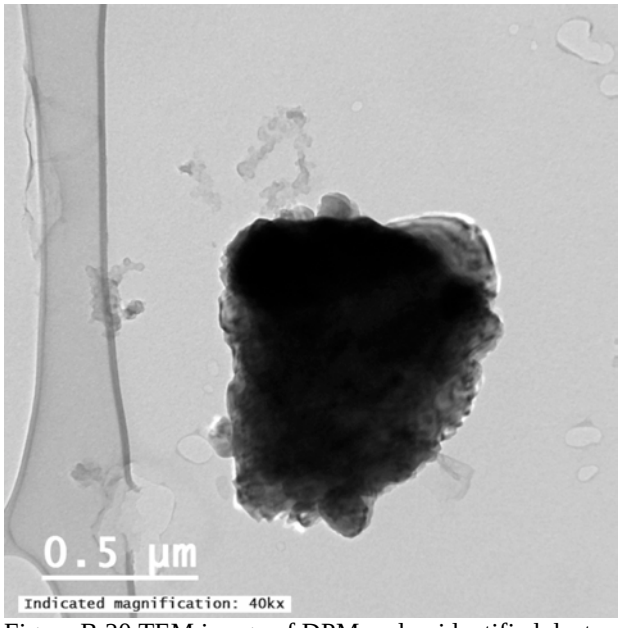

Figure B.20 TEM image of DPM and unidentified dust co-occurring from Location 2 (Image 24, ref. Table B.4). EDX was not completed on this sample.

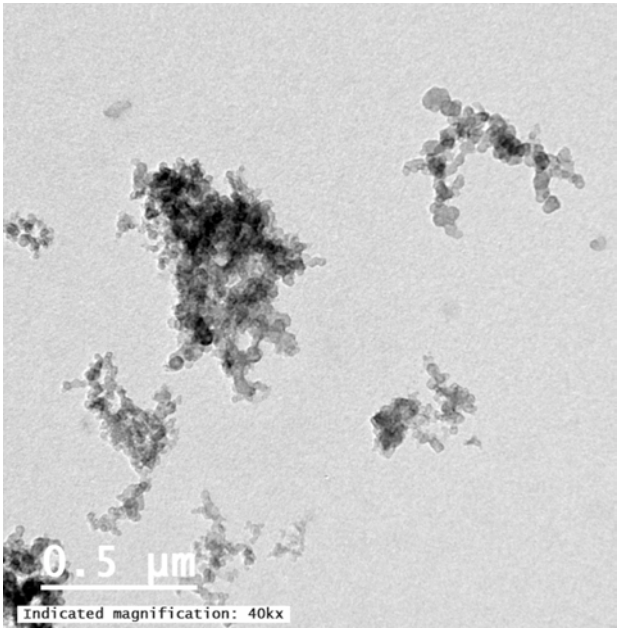

Figure B.21 TEM image of multiple DPM clusters from Location 2 (Image 25, ref. Table B.4).

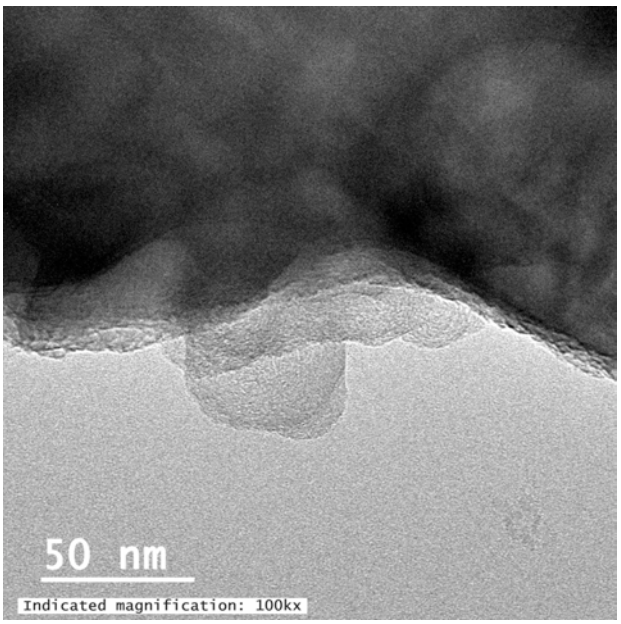

Figure B.22 TEM image of DPM attached to an unidentified large dust particle from Location 2 (Image 26, ref. Table B.4). EDS was not completed on this sample.

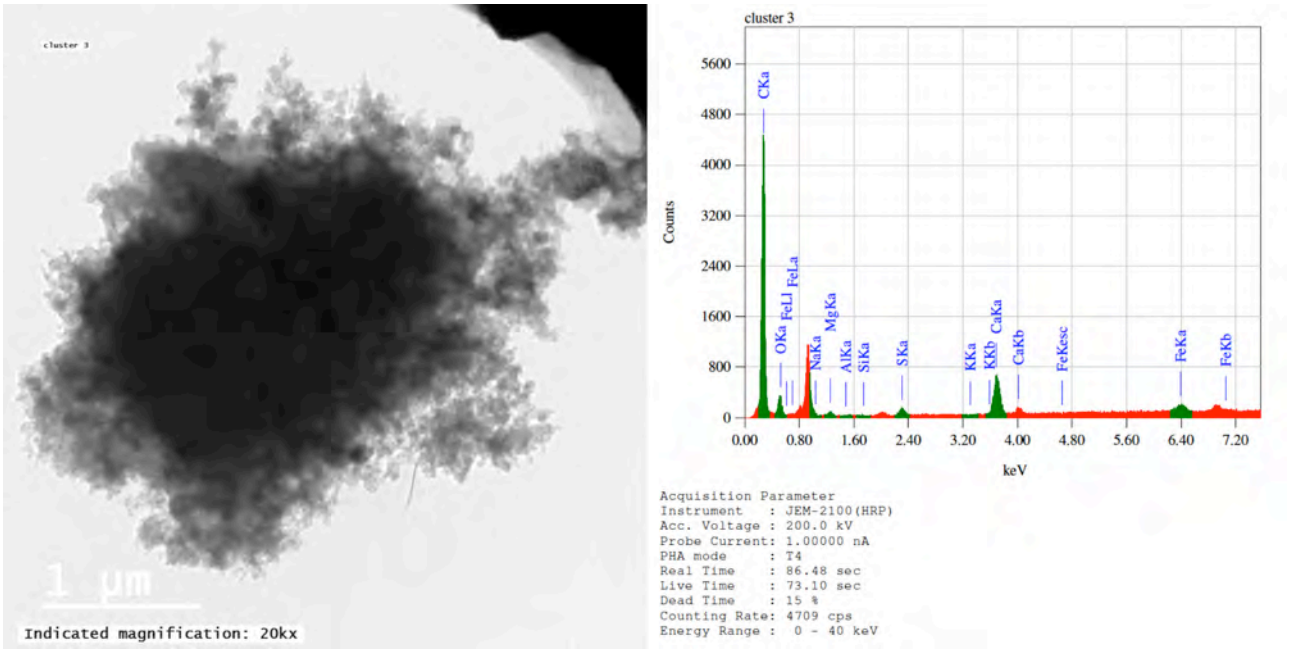

Figure B.23 TEM image and EDS spectra of DPM and Ca carbonate dust co-occurring from Location 2 (Image 27, ref. Table B.4). The DPM seems to be completely surrounding the dust particle.

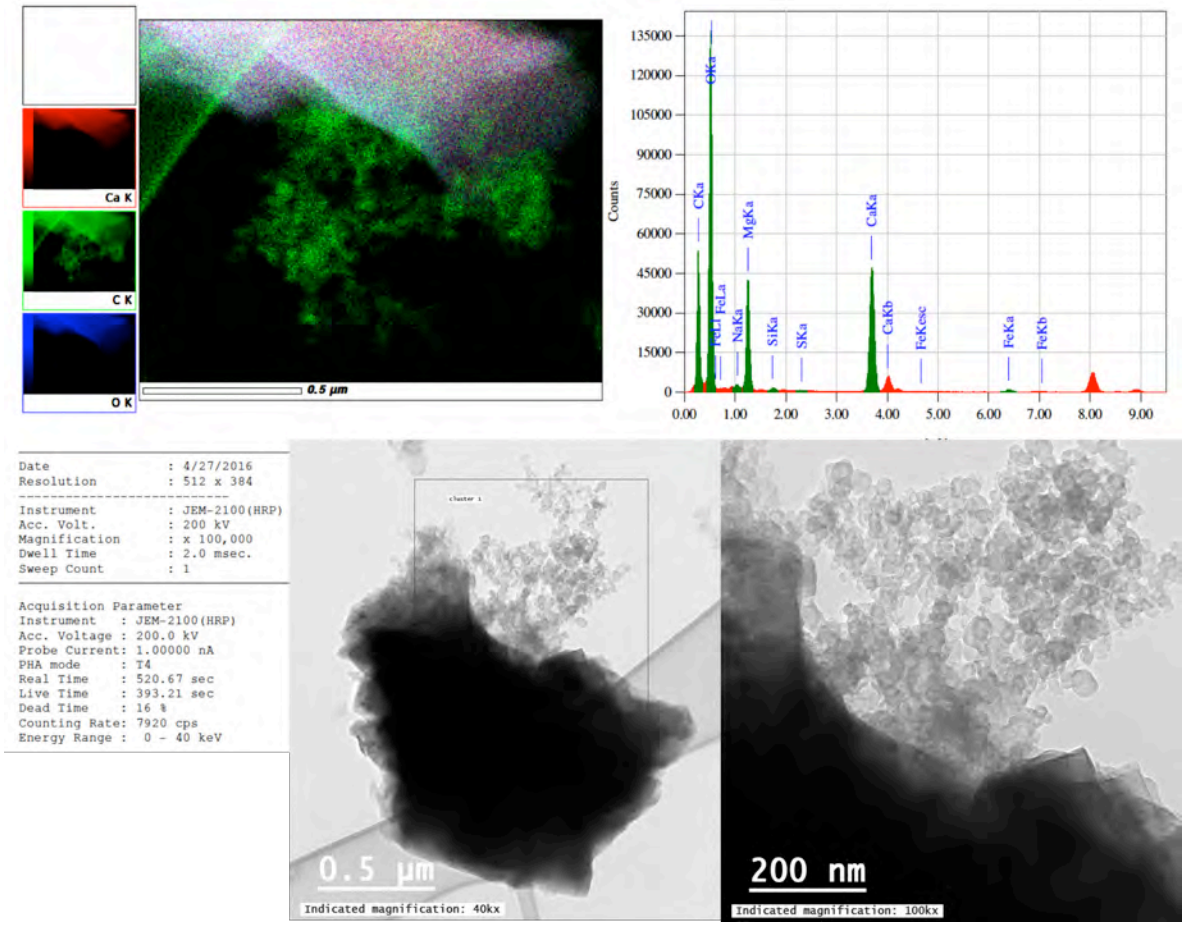

Figure B.24 TEM image, EDS spectra and element map of DPM and Ca/Mg carbonate dust co-occurring from Location 2 (Image 28, ref. Table B.4).

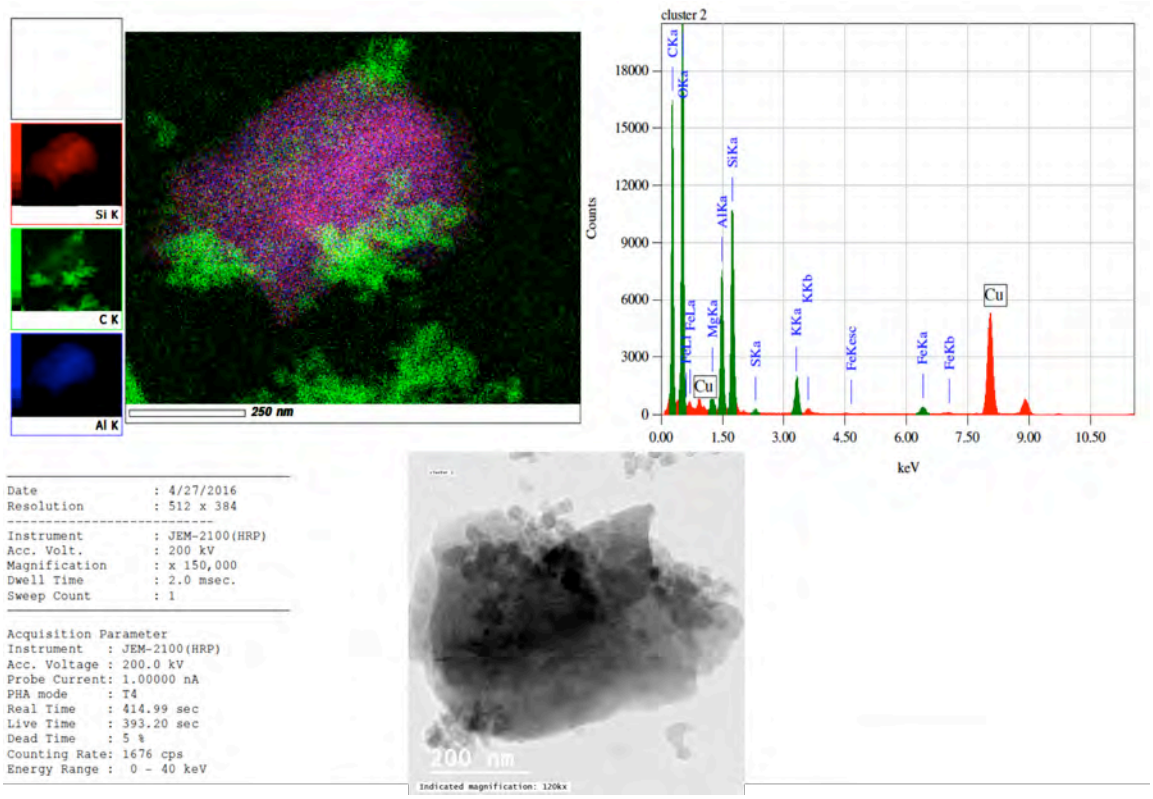

Figure B.25 TEM image, EDS spectra and element map of DPM and Al-silicate dust co-occurring from Location 2 (Image 29, ref. Table B.4).

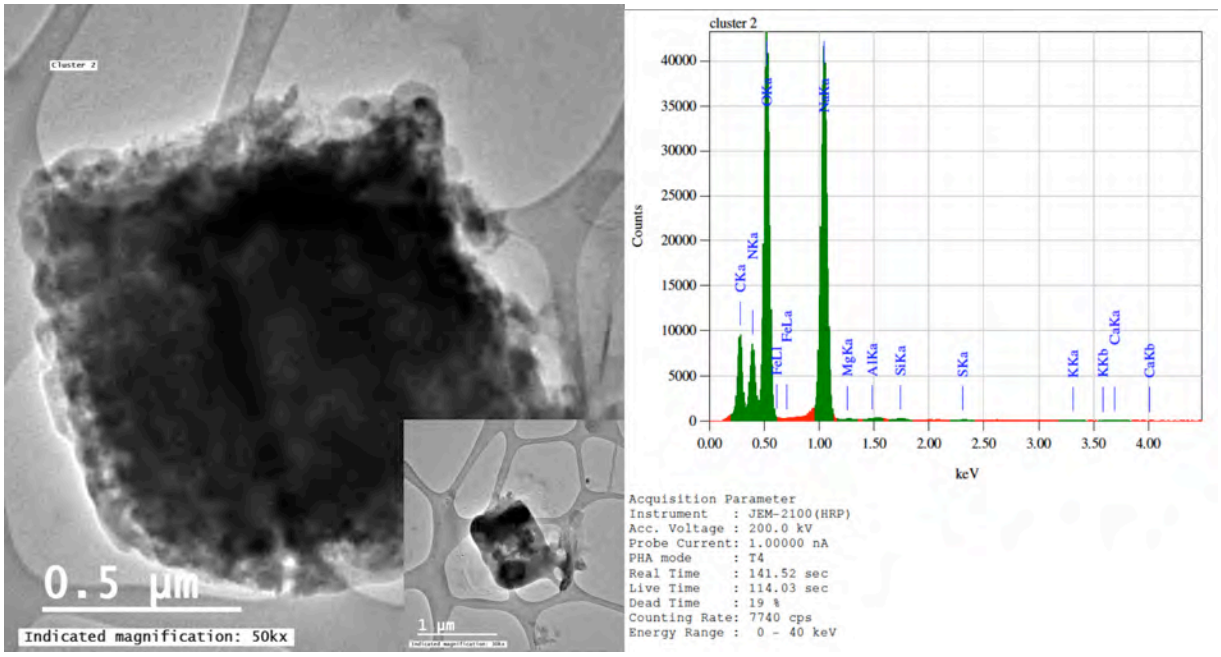

Figure B.26 TEM image and EDS spectra of DPM and Na-rich dust co-occurring from Location 2 (Image 30, ref. Table B.4).

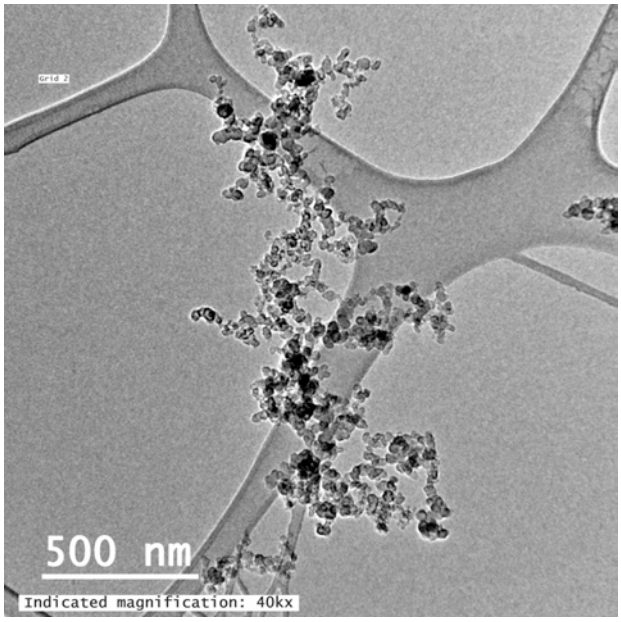

Figure B.27 TEM image of DPM from Location 2 (Image 35, ref. Table B.4).

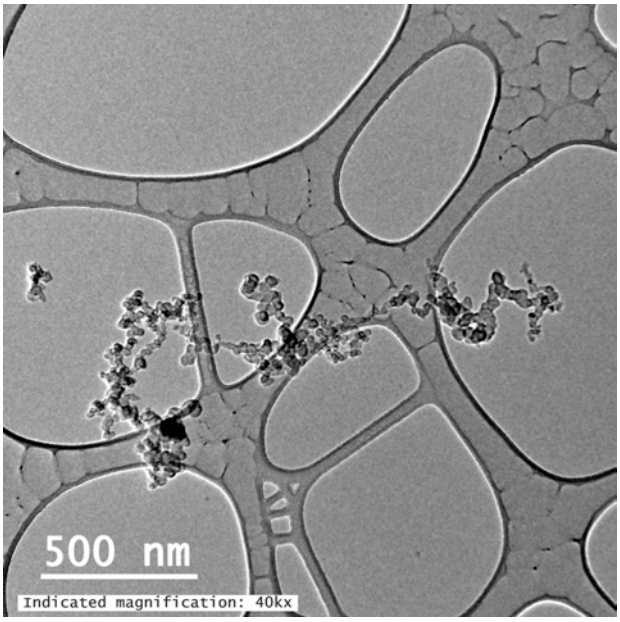

Figure B.28 TEM image of DPM from Location 2 (Image 36, ref. Table B.4).

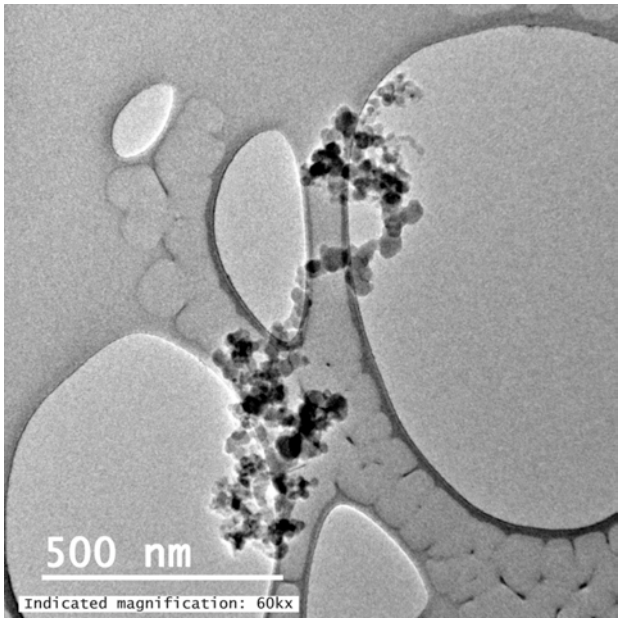

Figure B.29 TEM image of DPM from Location 2 (Image 37, ref. Table B.4).

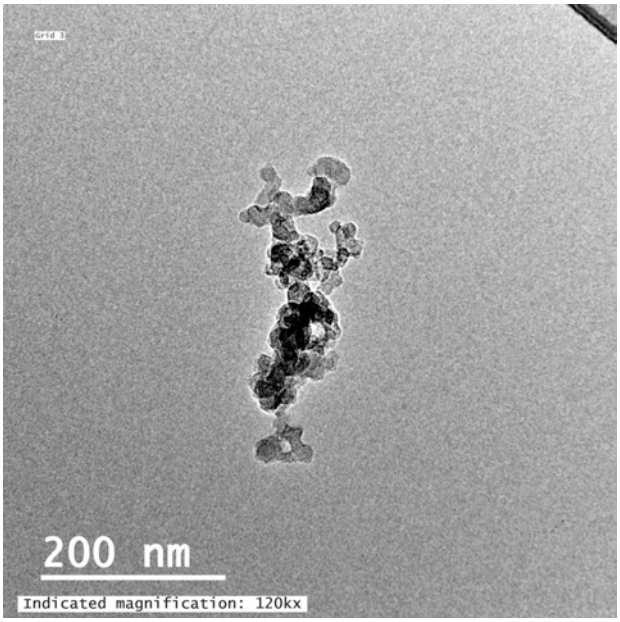

Figure B.30 TEM image of DPM from Location 2 (Image 38, ref. Table B.4).

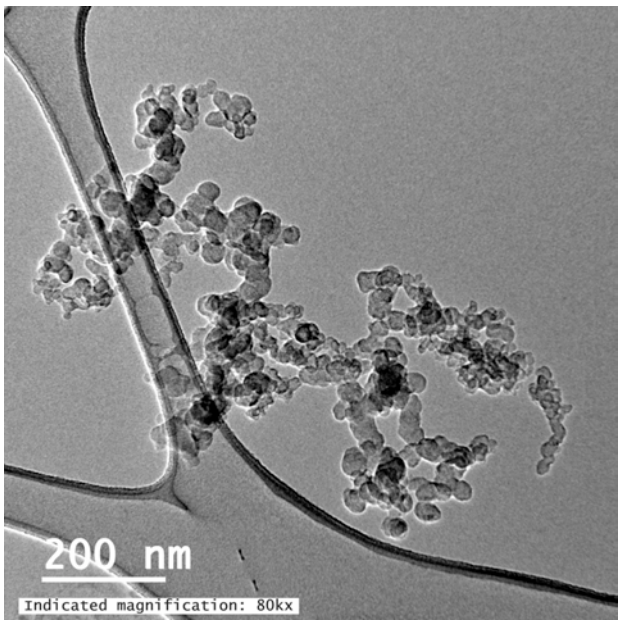

Figure B.31 TEM image of DPM from Location 2 (Image 39, ref. Table B.4).

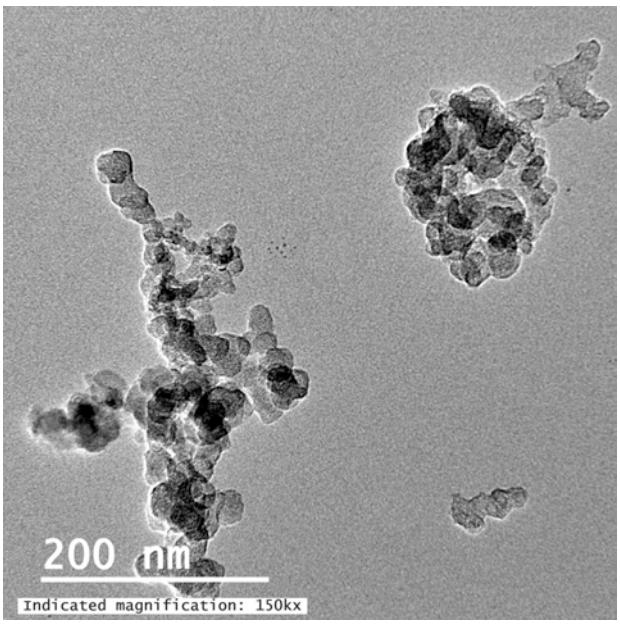

Figure B.32 TEM image of DPM from Location 2 (Image 40, ref. Table B.4).

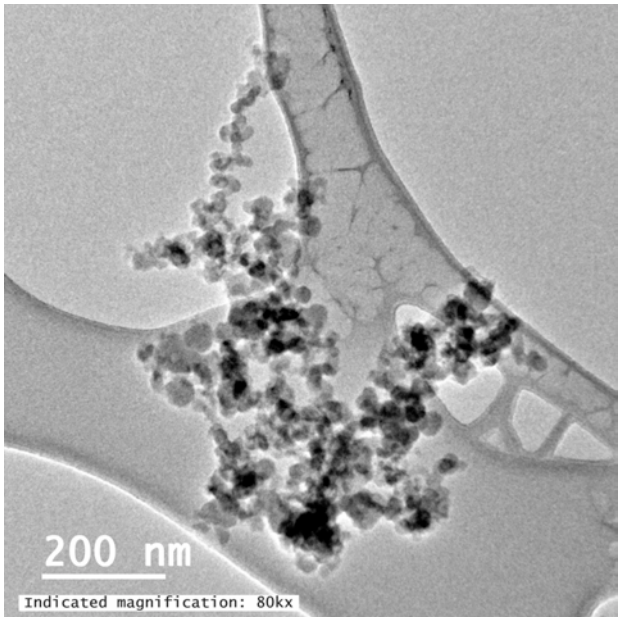

Figure B.33 TEM image of DPM from Location 2 (Image 41, ref. Table B.4).

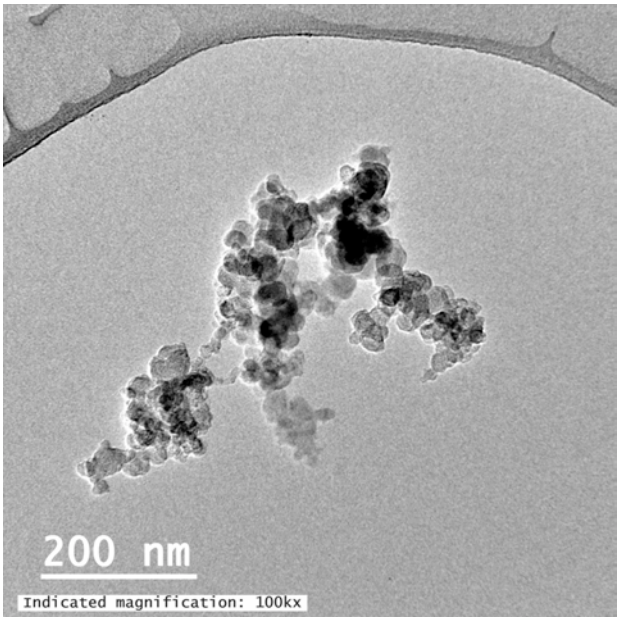

Figure B.34 TEM image of DPM from Location 2 (Image 42, ref. Table B.4).

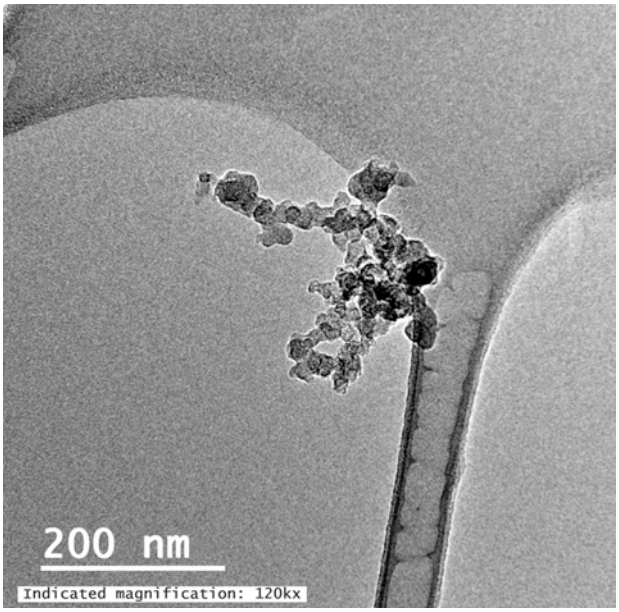

Figure B.35 TEM image of DPM from Location 2 (Image 43, ref. Table B.4).

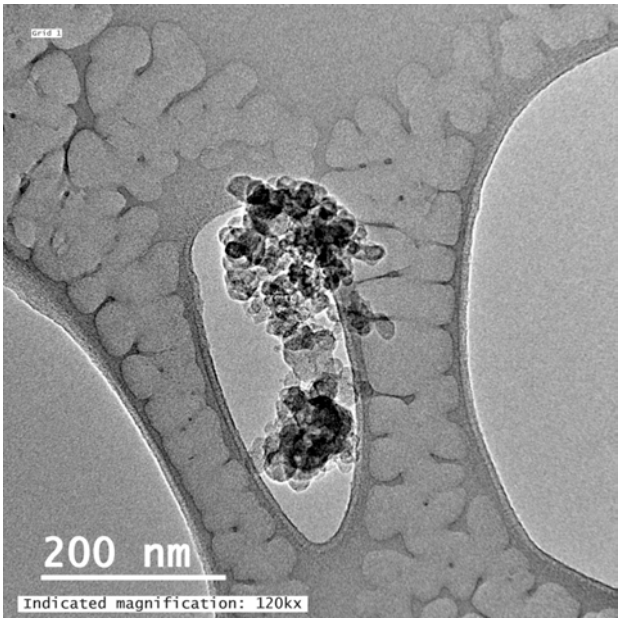

Figure B.36 TEM image of DPM from Location 2 (Image 44, ref. Table B.4).

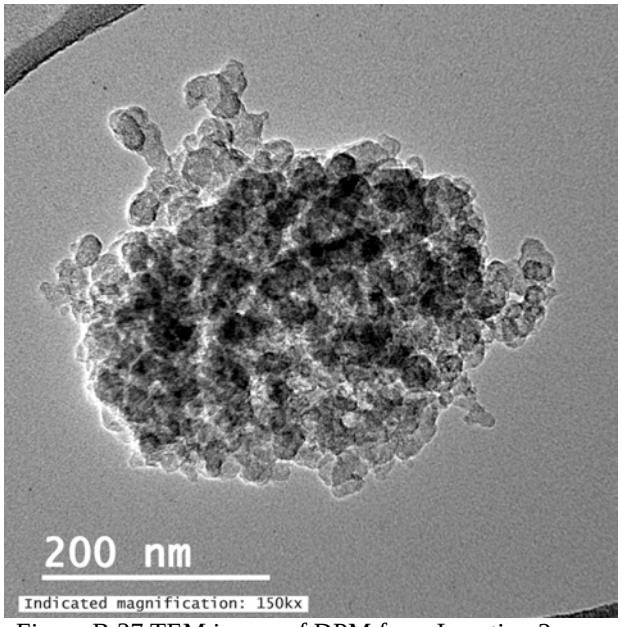

Figure B.37 TEM image of DPM from Location 2 (Image 45, ref. Table B.4).

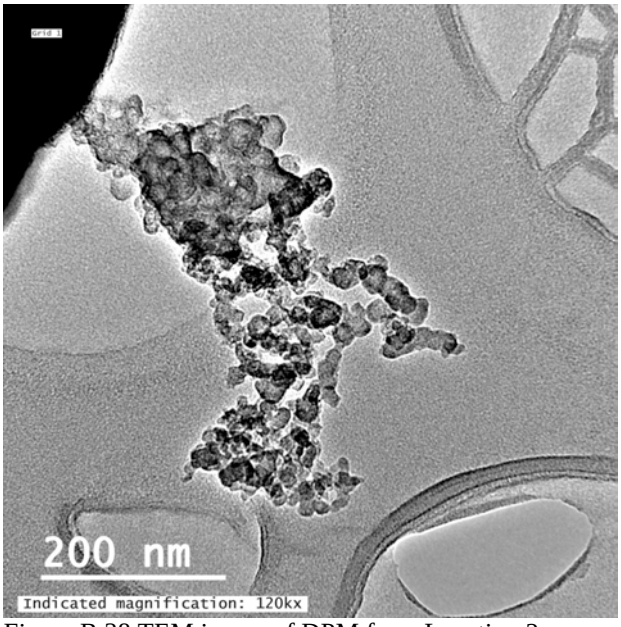

Figure B.38 TEM image of DPM from Location 2 (Image 46, ref. Table B.4).

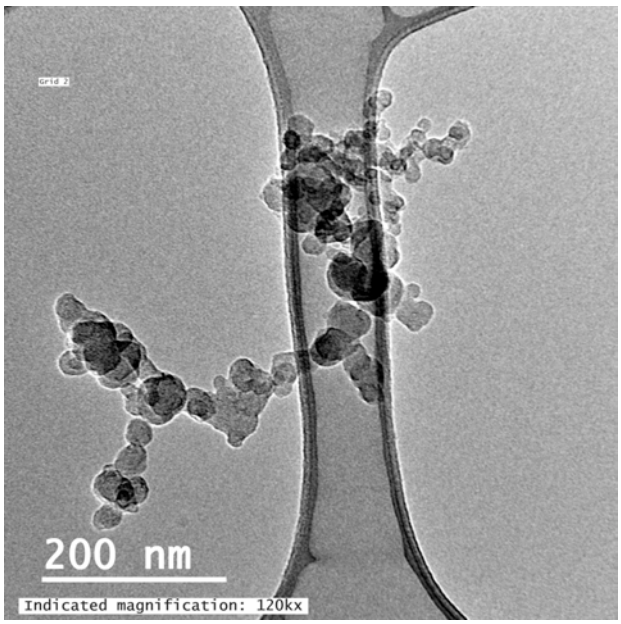

Figure B.39 TEM image of DPM from Location 2 (Image 47, ref. Table B.4).

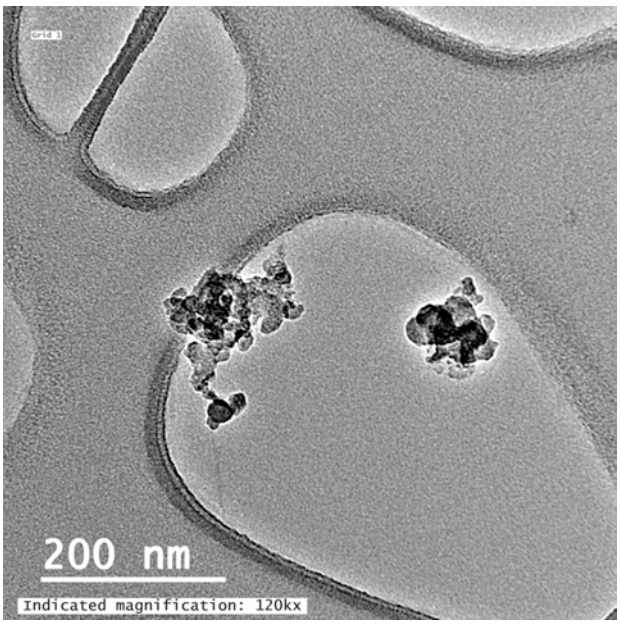

Figure B.40 TEM image of DPM from Location 2 (Image 48, ref. Table B.4).

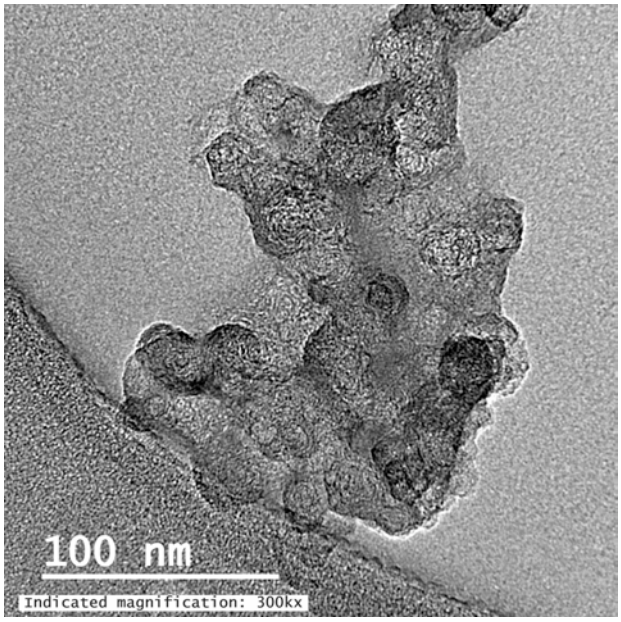

Figure B.41 TEM image of DPM from Location 2 (Image 49, ref. Table B.4).

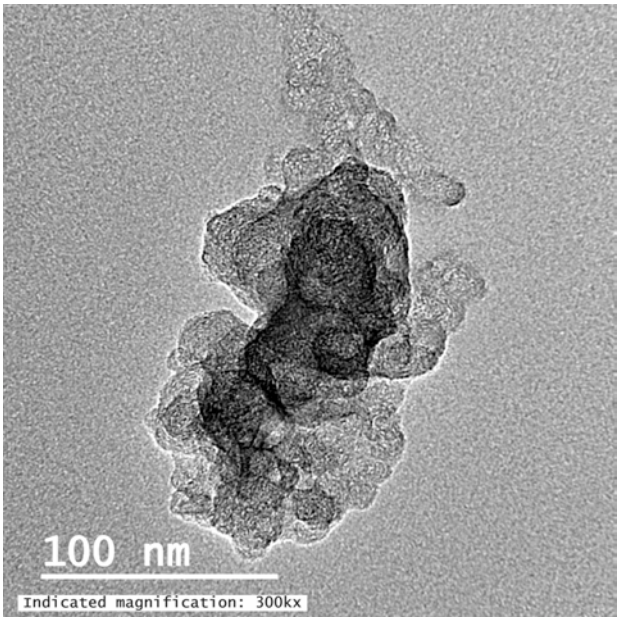

Figure B.42 TEM image of DPM from Location 2 (Image 50, ref. Table B.4).

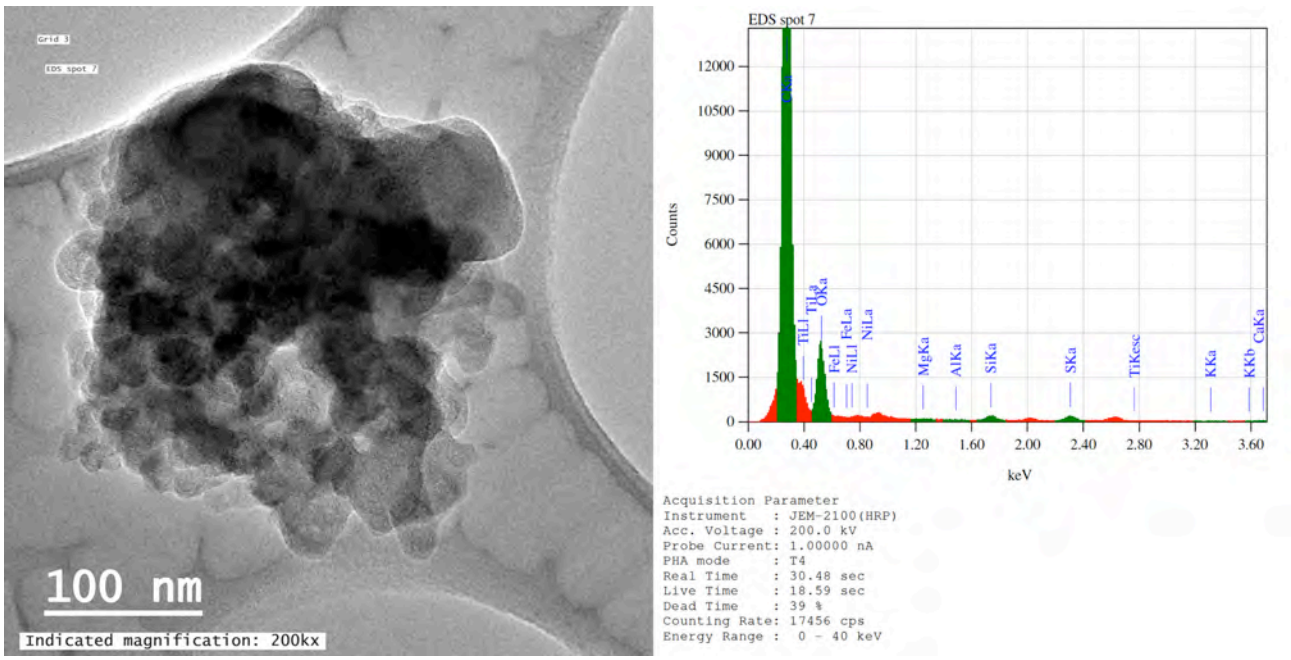

Figure B.43 TEM image and EDS spectra of DPM from Location 2 (Image 51, ref. Table B.4).

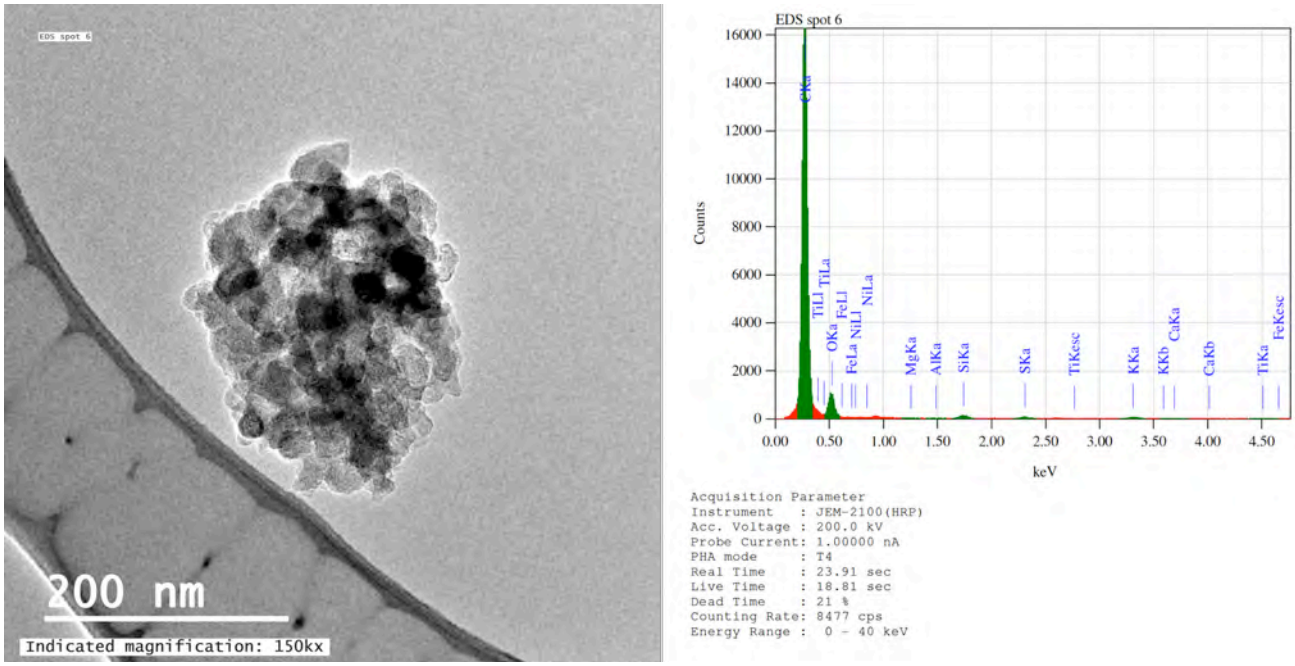

Figure B.44 TEM image and EDS spectra of DPM from Location 2 (Image 52, ref. Table B.4).

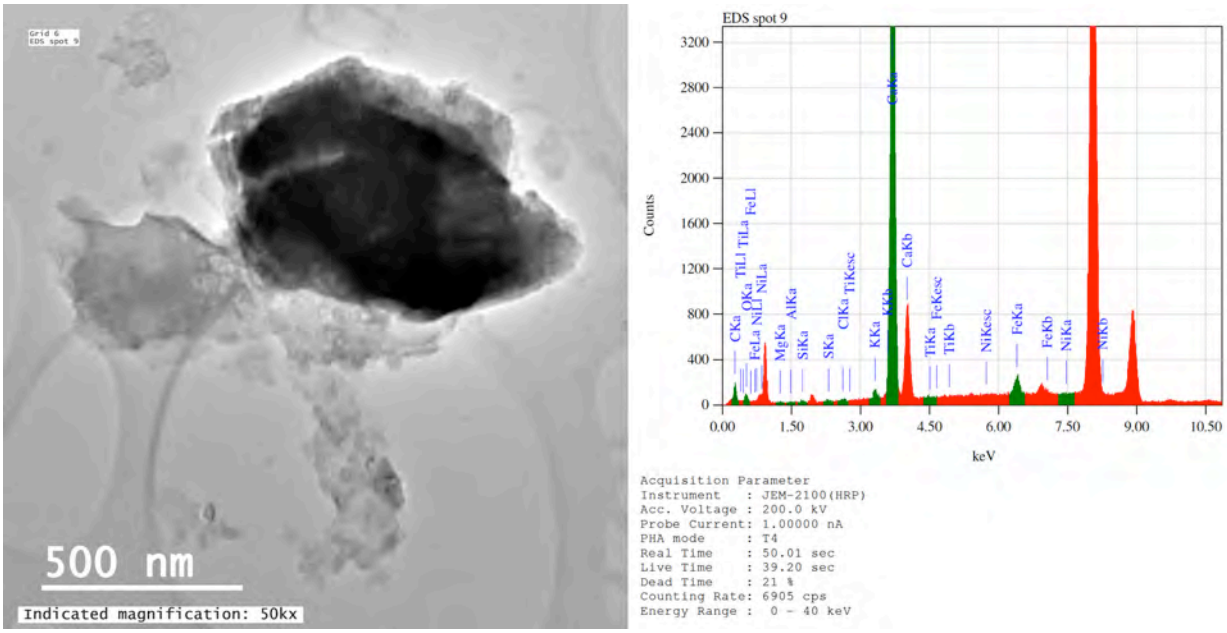

Figure B.45 TEM image and EDS spectra of DPM and unidentified dust co-occurring from Location 2 (Image 53, ref. Table B.4).

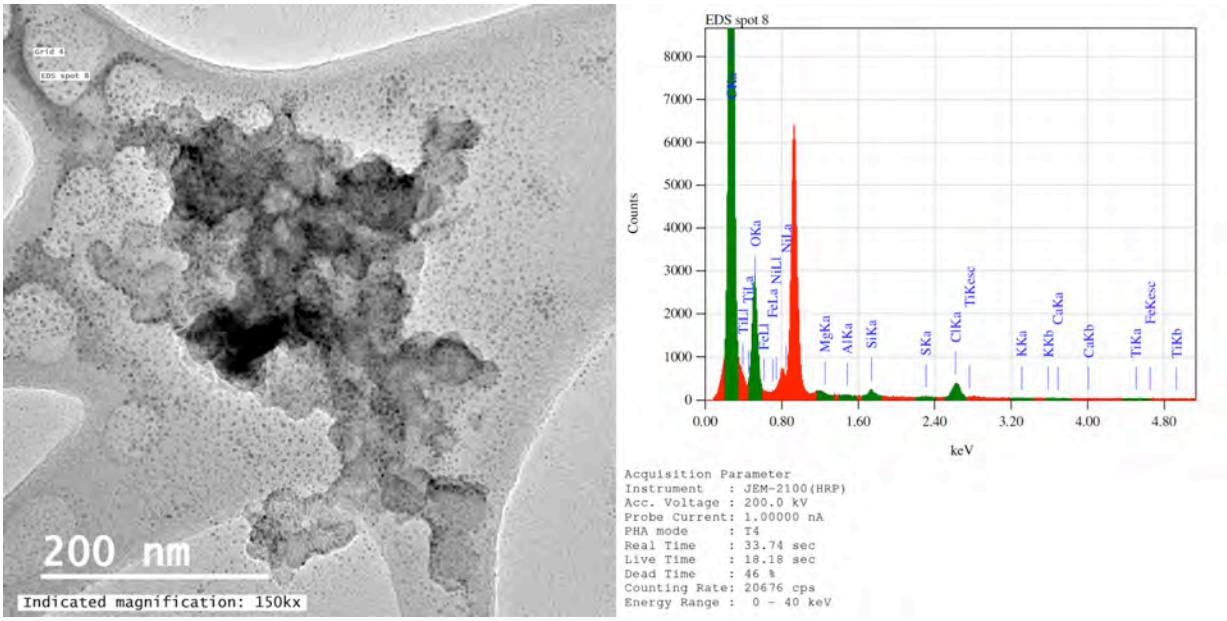

Figure B.46 TEM image and EDS spectra of DPM and unidentified dust co-occurring from Location 2 (Image 54, ref. Table B.4). Note the Cu precipitate surrounding the DPM. Note the Cu precipitate surrounding the DPM.

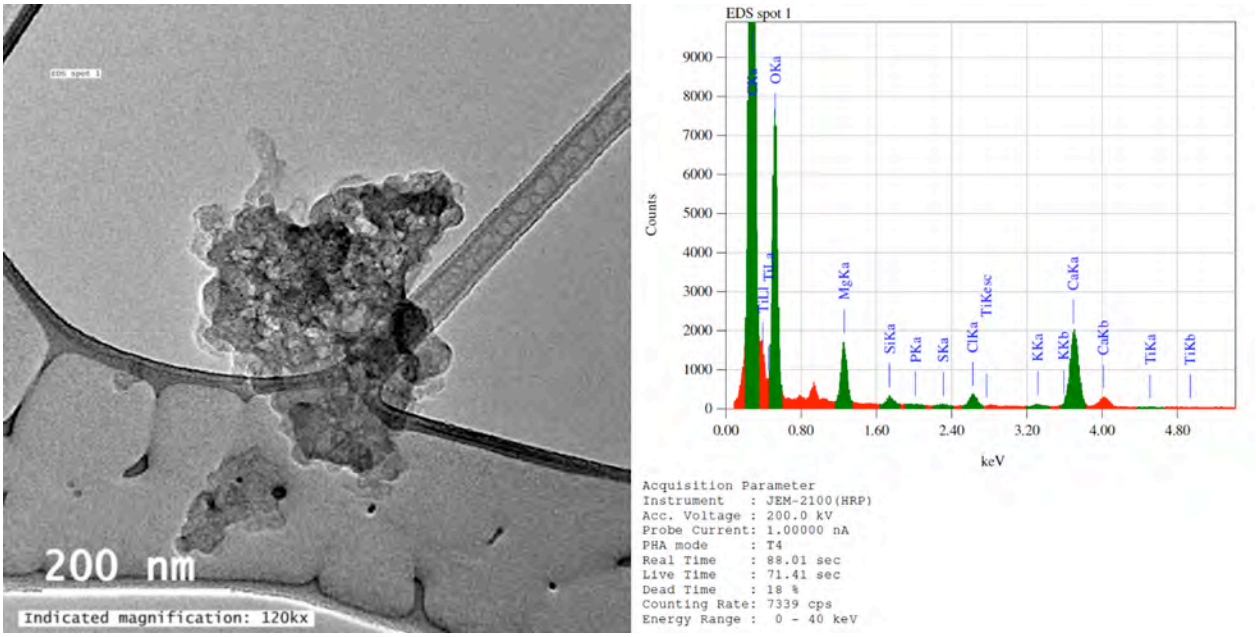

Figure B.47 TEM image and EDS spectra of DPM and Ca carbonate dust co-occurring from Location 2 (Image 55, ref. Table B.4).

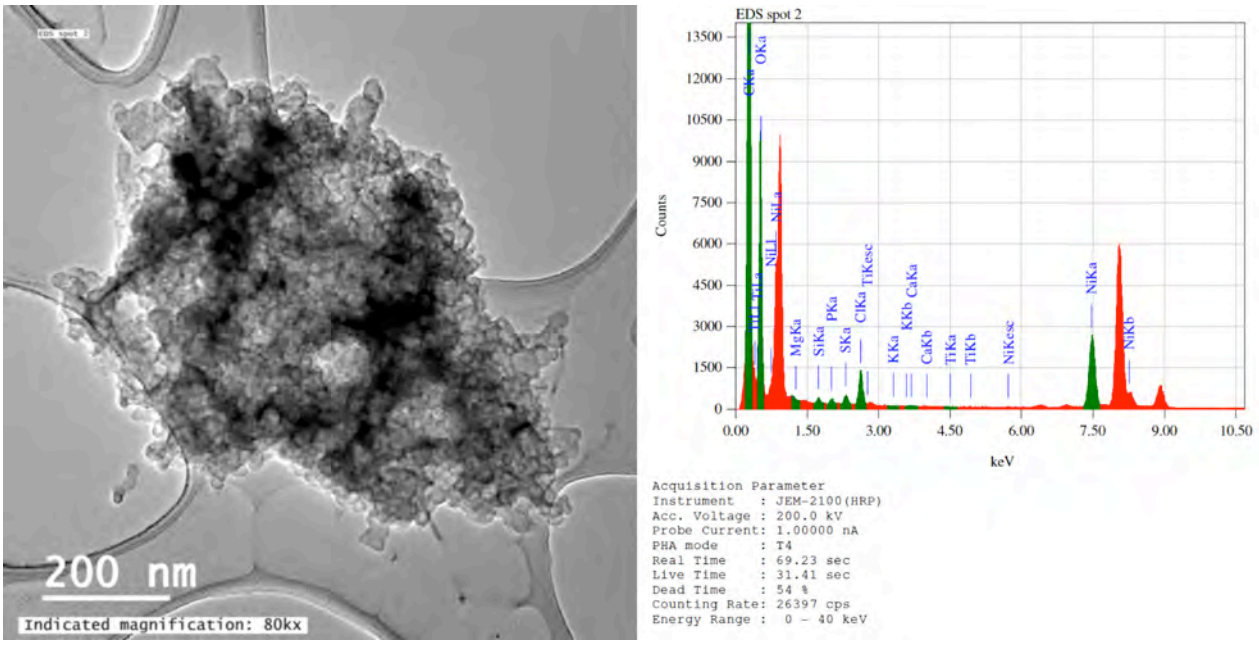

Figure B.48 TEM image and EDS spectra of DPM and unidentified dust co-occurring from Location 2 (Image 56, ref. Table B.4).

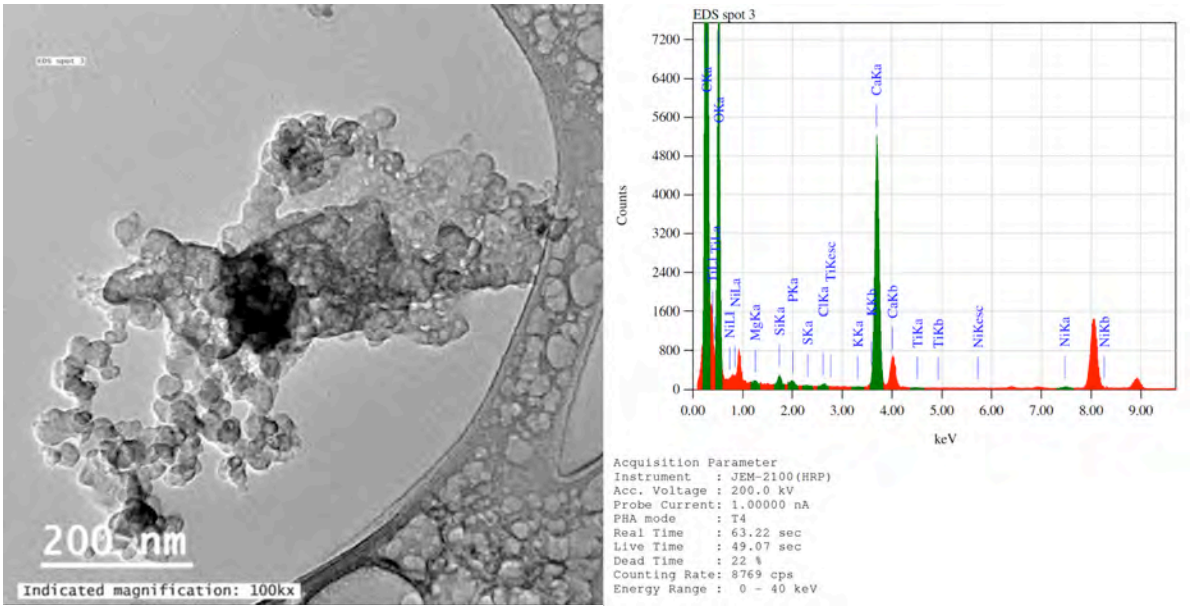

Figure B.49 TEM image and EDS spectra of DPM and Ca carbonate dust co-occurring from Location 2 (Image 57, ref. Table B.4).

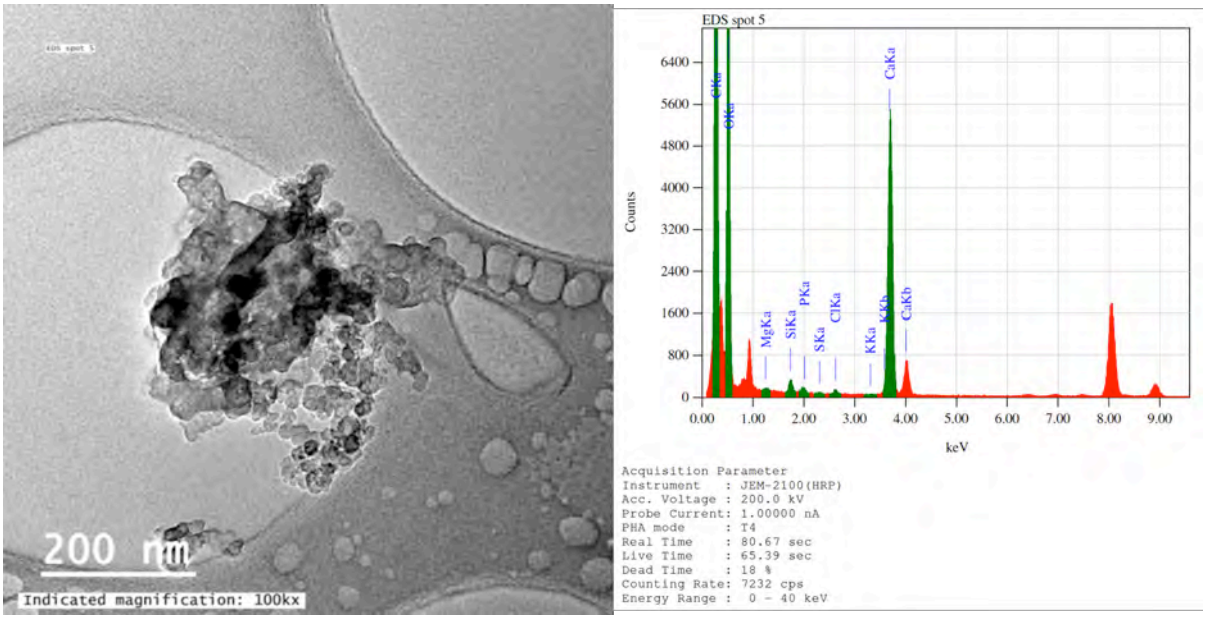

Figure B.50 TEM image and EDS spectra of DPM and Ca carbonate dust co-occurring from Location 2 (Image 59, ref. Table B.4).

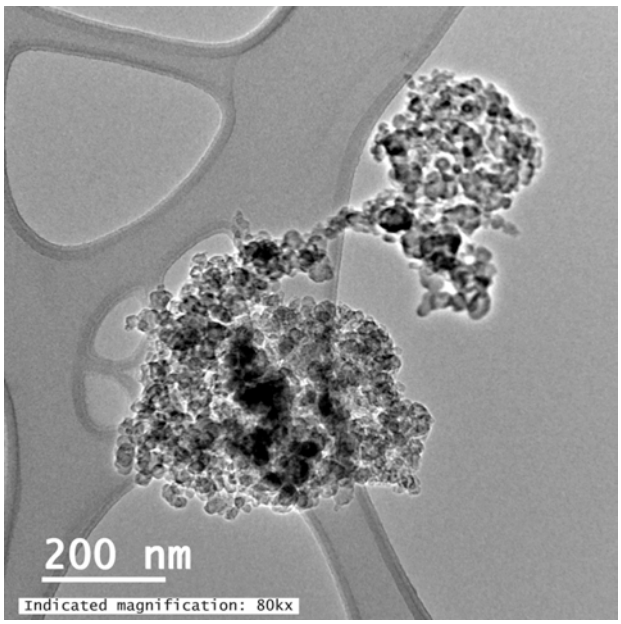

Figure B.51 TEM image of DPM from Location 2 (Image 60, ref. Table B.4).

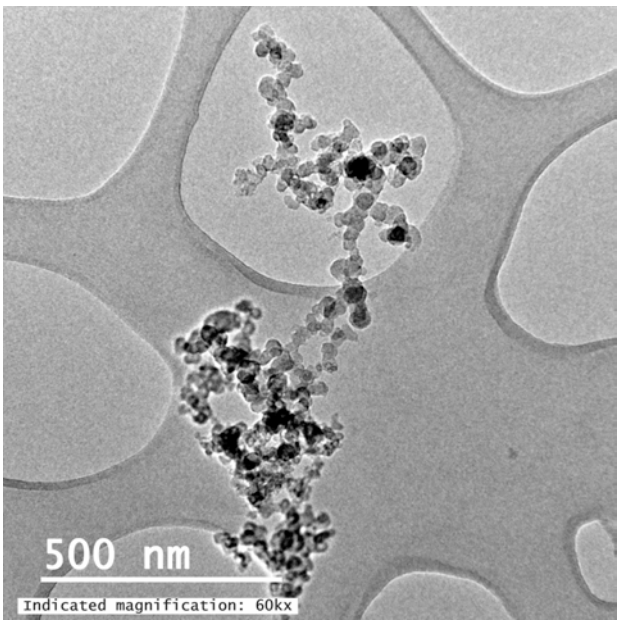

Figure B.52 TEM image of DPM from Location 2 (Image 61, ref. Table B.4).

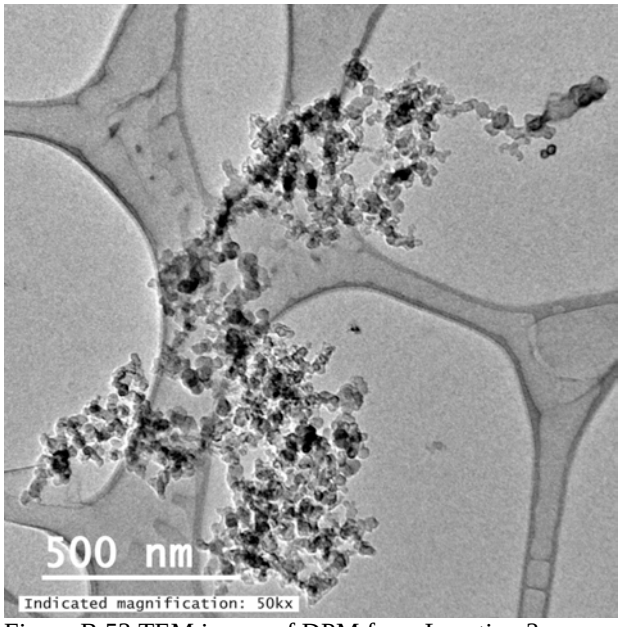

Figure B.53 TEM image of DPM from Location 3 (Image 64, ref. Table B.4).

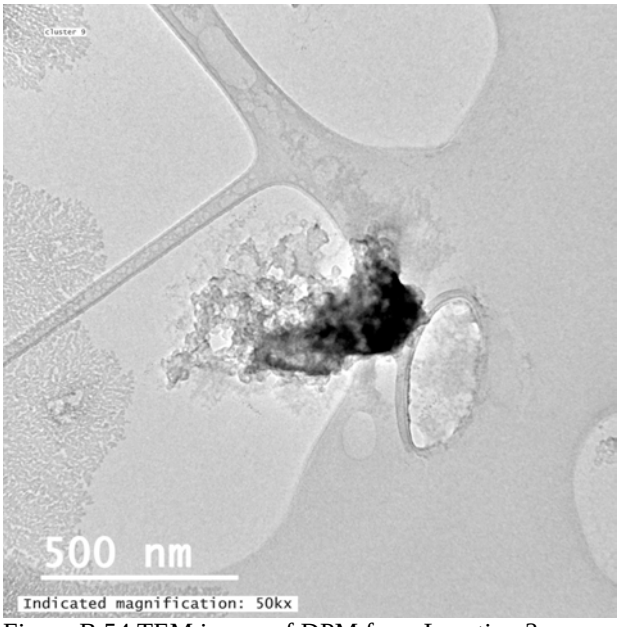

Figure B.54 TEM image of DPM from Location 3 (Image 66, ref. Table B.4). Note the Cu precipitate in a dendritic pattern.

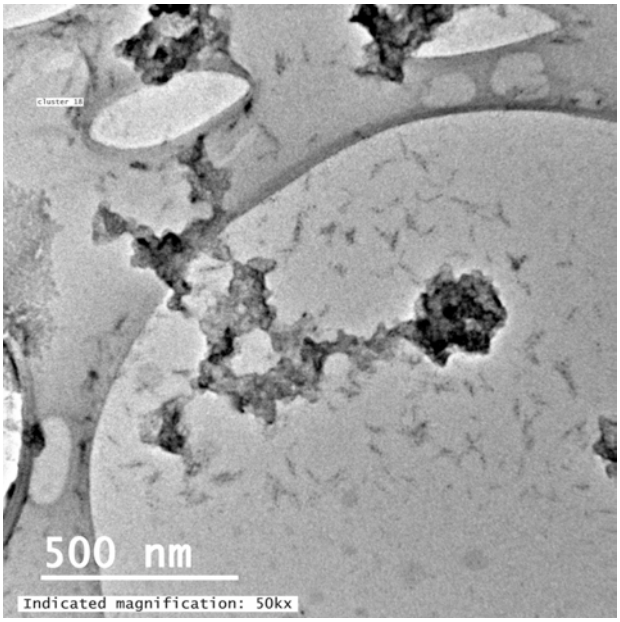

Figure B.55 TEM image of DPM from Location 3 (Image 67, ref. Table B.4). Note the Cu precipitate in the background.

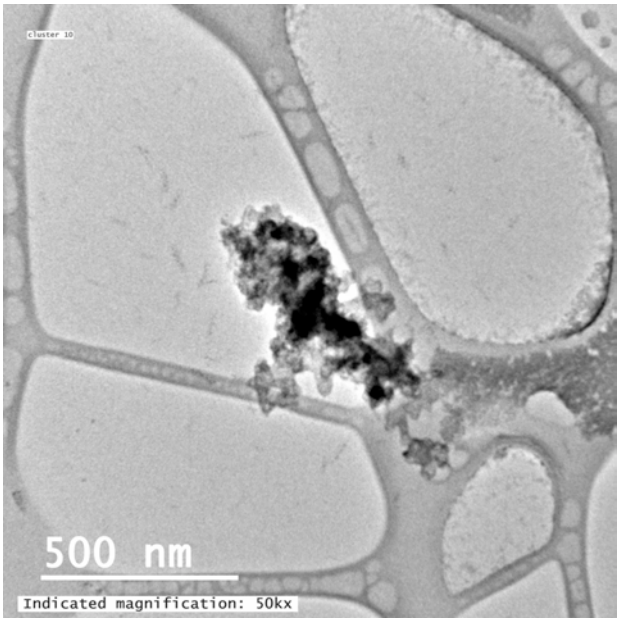

Figure B.56 TEM image of DPM from Location 3 (Image 68, ref. Table B.4). Note the Cu precipitate in the background.

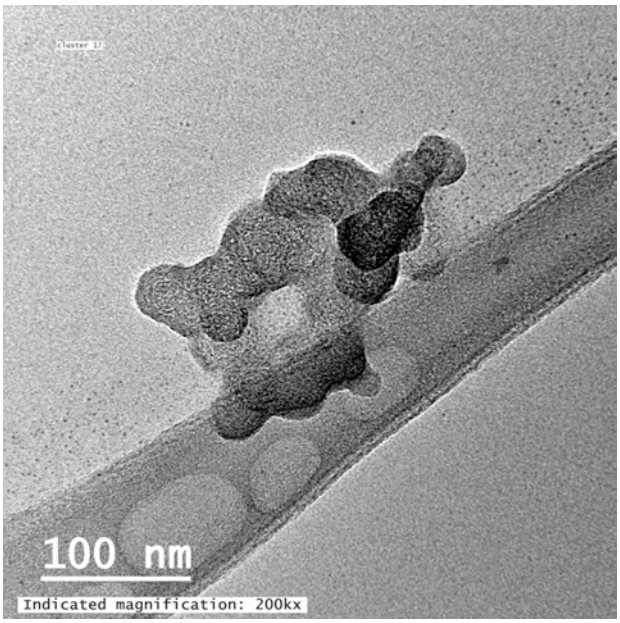

Figure B.57 TEM image of DPM from Location 3 (Image 69, ref. Table B.4). Note the Cu precipitate surrounding the DPM.

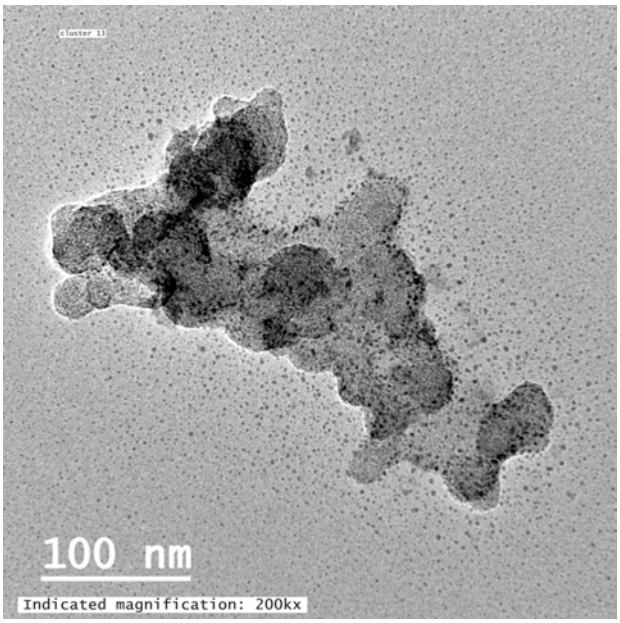

Figure B.58 TEM image of DPM from Location 3 (Image 71, ref. Table B.4). Note the Cu precipitate surrounding the DPM.

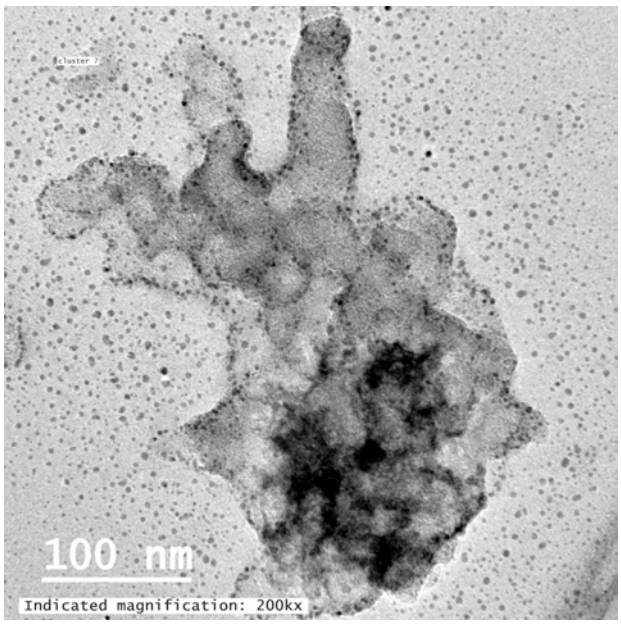

Figure B.59 TEM image of DPM from Location 3 (Image 72, ref. Table B.4). Note the Cu precipitate surrounding the DPM.

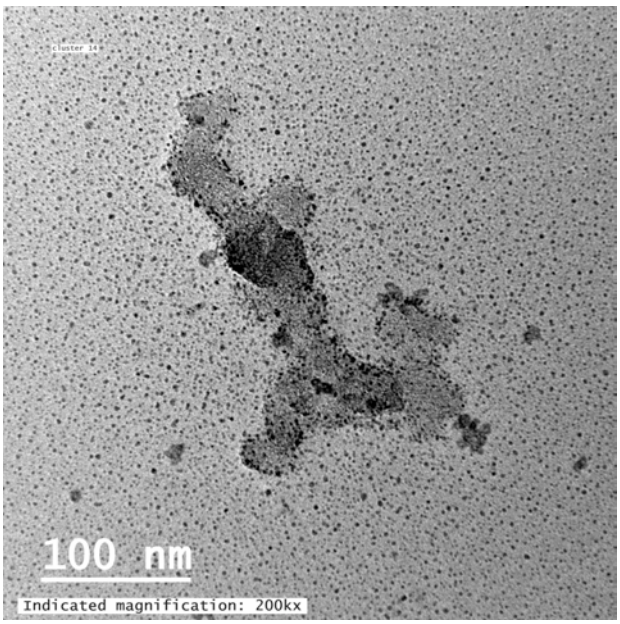

Figure B.60 TEM image of DPM from Location 3 (Image 73, ref. Table B.4). Note the Cu precipitate surrounding the DPM.

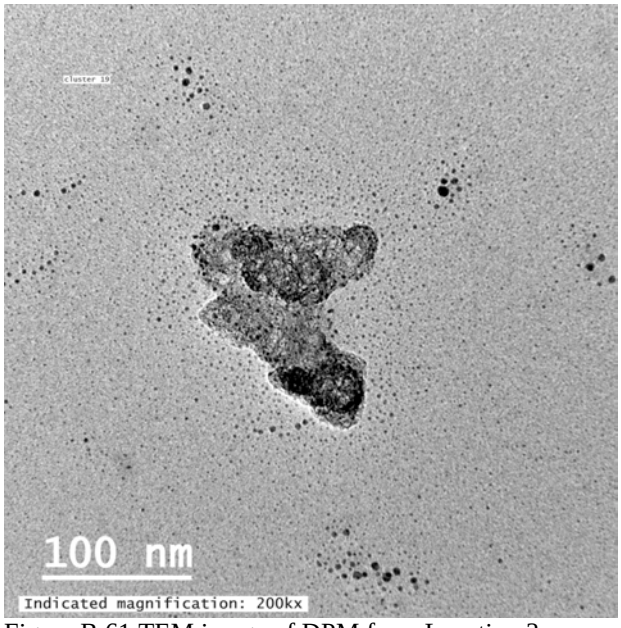

Figure B.61 TEM image of DPM from Location 3 (Image 74, ref. Table B.4). Note the Cu precipitate surrounding the DPM.

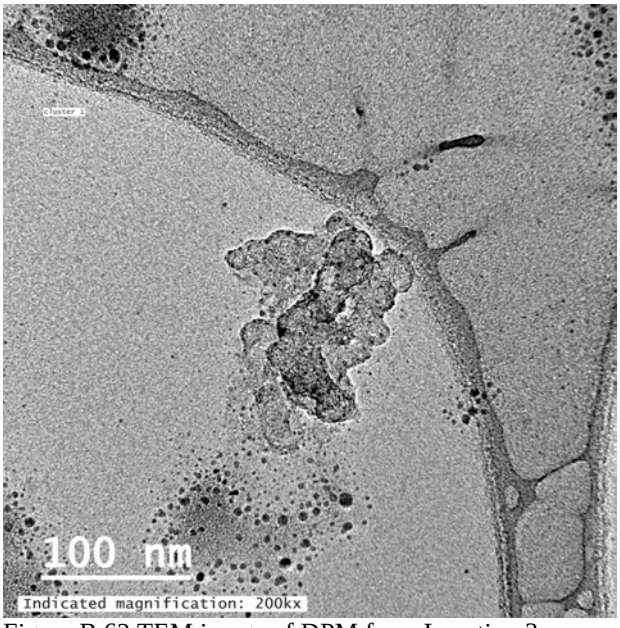

Figure B.62 TEM image of DPM from Location 3 (Image 75, ref. Table B.4). Note the Cu precipitate surrounding the DPM.

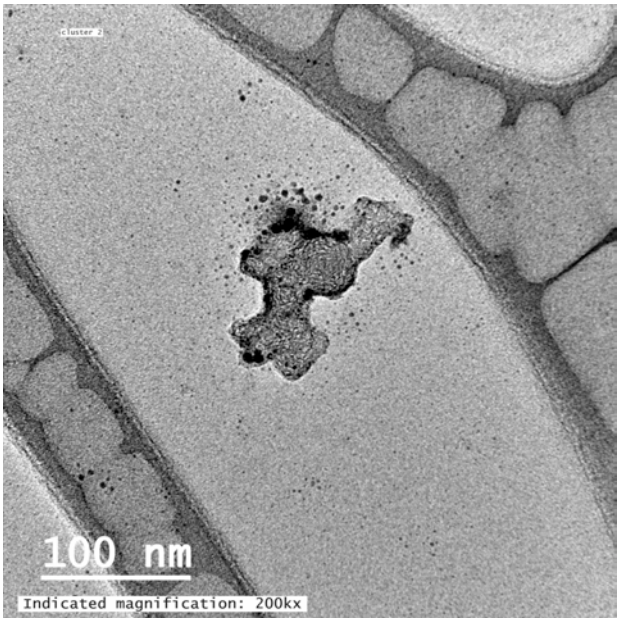

Figure B.63 TEM image of DPM from Location 3 (Image 76, ref. Table B.4). Note the Cu precipitate surrounding the DPM.

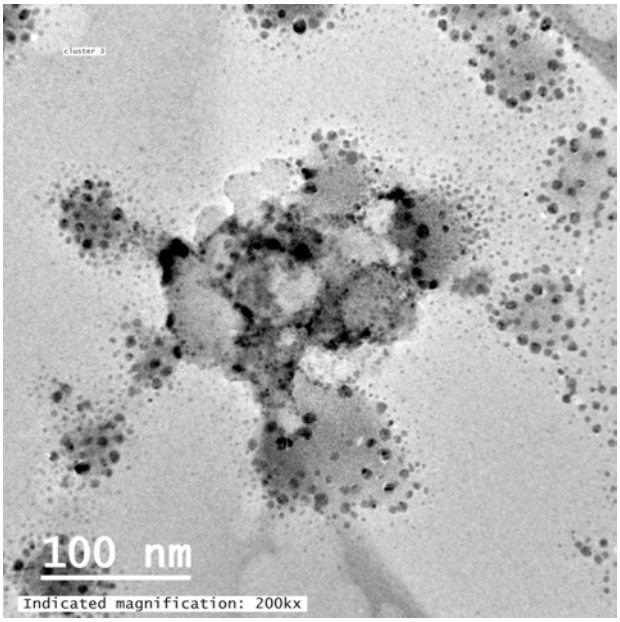

Figure B.64 TEM image of DPM from Location 3 (Image 77, ref. Table B.4). Note the Cu precipitate surrounding the DPM.

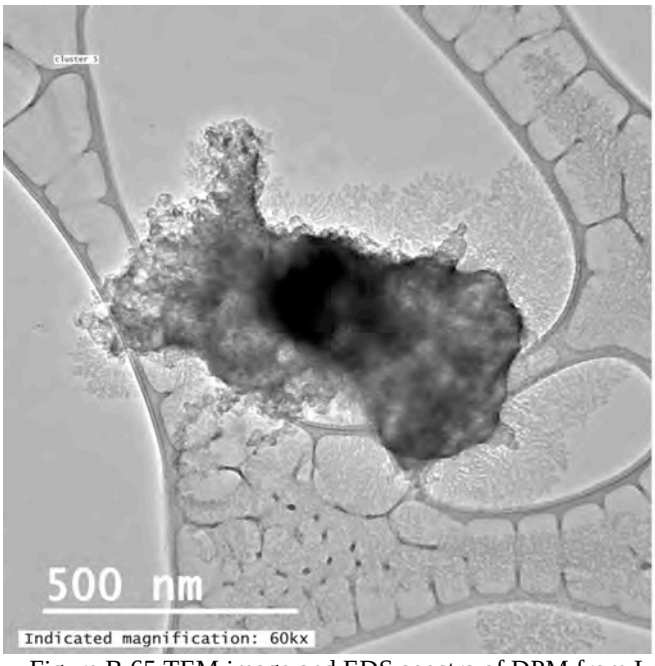

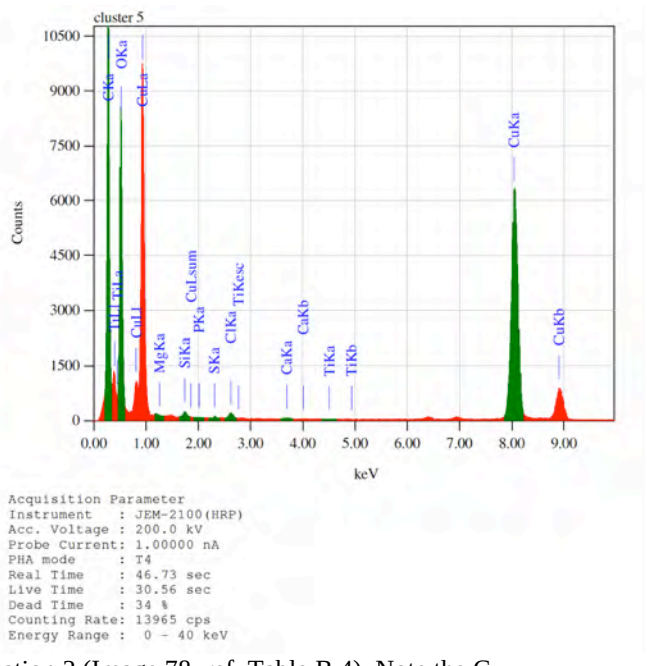

Figure B.65 TEM image and EDS spectra of DPM from Location 2 (Image 78, ref. Table B.4). Note the Cu precipitate surrounding the DPM in a dendritic pattern, as well as the large Cu peak in the spectra.